Conversion of *Ortho* Aminomethyl Substituted Nitrogen Heterocycles to Bis(carbonyl)amides and Some Transition Metal Chemistry of Thus Derived Bis(carbonyl)amides

A Dissertation Submitted to
Indian Institute of Technology Guwahati
As Partial Fulfillment for the Degree of
Doctor of Philosophy

Submitted by

Rojalin Sahu
Roll No. 06612220

Department of Chemistry
Indian Institute of Technology Guwahati
Guwahati – 781 039

April 2011

Department of Chemistry
Indian Institute of Technology Guwahati
Guwahati – 781039

DECLARATION

I hereby declare that the work embodied in this Dissertation entitled "**Conversion of *Ortho* Aminomethyl Substituted Nitrogen Heterocycles to Bis(carbonyl)amides and Some Transition Metal Chemistry of Thus Derived Bis(carbonyl)amides**" has been carried out by me in the Department of Chemistry, Indian Institute of Technology Guwahati, under the supervision of Dr. V. Manivannan.

In keeping with the scientific tradition, due acknowledgement has been made, wherever the work described is based on the findings of other investigators.

(Rojalin Sahu)
Date Roll. No. 06612220

Department of Chemistry
Indian Institute of Technology Guwahati
Guwahati–781039

Dr. V. Manivannan
Associate Professor

CERTIFICATE

It is certified that the work contained in the Dissertation entitled "**Conversion of *Ortho* Aminomethyl Substituted Nitrogen Heterocycles to Bis(carbonyl)amides and Some Transition Metal Chemistry of Thus Derived Bis(carbonyl)amides**" submitted by **Rojalin Sahu** to the Indian Institute of Technology Guwahati for the award of the degree of Doctor of Philosophy has been carried out under my supervision in the Department of Chemistry, Indian Institute of Technology Guwahati. This work has not been submitted elsewhere for the award of any other degree.

(Dr. V. Manivannan)
Supervisor

Date

Dedication

"I would like to dedicate this thesis to my divine parents who has been supporting me through all thick and thin of my life. And also to my beloved husband who is a powerful source of inspiration and energy.**"**

ACKNOWLEDGEMENT

It is now and only after the completion of my thesis that I realize the immense necessity of writing this page, in an effort to acknowledge those who in all possible ways helped me in carrying out and completing this task. Mere mention of their names here does not serve to repay in measure the debt that I owe.

First of all, I acknowledge Indian Institute of Technology Guwahati, India for providing me an opportunity to pursue research career at Department of Chemistry.

No words would be enough to express my profound sense of gratitude to my thesis supervisor Dr. V. Manivannan for providing me a platform to start my research career. I am heartily thankful to him for his constant encouragement, guidance and support throughout my research and enabled me to develop skills to carry out the research work.

I am very much thankful to my doctoral committee members Prof. B. K. Patel, Prof. M. Ray, Prof. A. K. Saikia, for their precious and constructive suggestion for my thesis. I am thankful to all the faculty members and supporting staffs of my Department for their warmth and support. I would also like to thank all staffs of Central Instrumentation Facility (CIF) for providing ambient atmosphere of research and freedom to execute experiments.

It's my pleasure to thank my labmates specifically Vijendra and Himanshu for their all time support. I would like to acknowledge my friends Ashok, Archana, Sunita, Arpita, Anu, Maya, Mamta, Sneha, Ramkesh, Ketan, Bijoy, Bapuni, Kunu, with whom I have spent various memorable moments. I am thankful to my departmental friends. for their gesture of assistance in various ways and Babulal bhaiya for collecting X-ray data of the crystals discussed in this thesis.

I acknowledge my parents, mother in law, brother Raja, and husband for their never ending support, love and affection. I am extremely grateful to almighty for providing me the strength and energy to withstand in all critical situations.

Rojalin Sahu

Abbreviations

a	Unit cell dimension a
b	Unit cell dimension b
c	Unit cell dimension c
D	density of the crystal
α	Interfacial angle α in a unit cell
β	Interfacial angle β in a unit cell
γ	Interfacial angle γ in a unit cell
Z	Unit cell formula units
λ	Wave length
ν	Wave number
μ	Absorption coefficient
ε	Molar extinction coefficient
τ	Geometric parameter applicable for five-co-ordinate structures as an index of the degree of trigonality between trigonal bipyramidal and rectangular pyramidal.
μ_{eff}	Effective magnetic moment
H	Applied Magnetic Field
g	Lande splitting factor
A	Hyperfine splitting constant

Contents

Chapter 1

Introduction, Materials and Methods

Abstract

The aim of this Chapter is to provide an overall view on the ways by which bis(2-pyridylcarbonyl)amine (**L1H**) is being obtained and its coordination chemistry. This Chapter also highlights the role of **L1H** in the context of its impact upon design, synthesis, and structure of coordination polymers and some simple coordination complexes, based on the reports till date. Both discrete- and infinite buildups are examined as well as their potential applications are briefly explained where ever necessary. The materials used in this study, their commercial sources, method of solvent purification, specifications of the instruments used for the characterization of the compounds, procedures of crystallographic data collection and refinement etc., are also briefed in the end.

1.1 Formation and Coordination Modes of Bis(2-pyridylcarbonyl)amide

Bis(2-pyridylcarbonyl)amine (**L1H**) is a potential pentadentate ligand and bind as bis(2-pyridylcarbonyl)amide ion (**L1**).

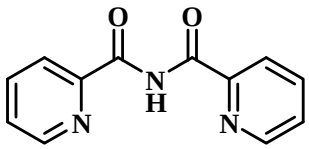

L1H

In 1976, Lerner and Lippard prepared for the first time, the copper(II) complexes of **L1** by copper(II)-assisted hydrolysis of 2,4,6-tris(2-pyridyl)-1,3,5-triazine (**tptz**) [1, 2].

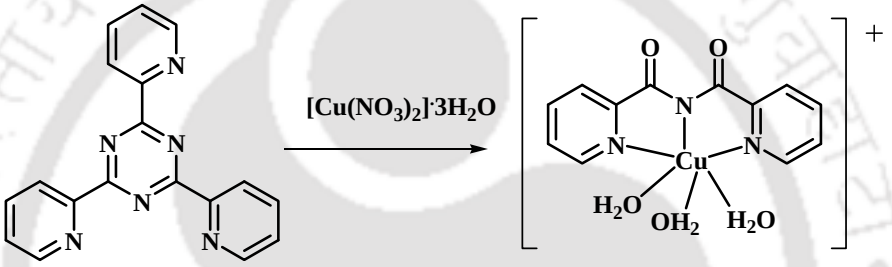

Paul *et al* reported that hydrolysis of **tptz** also occur in the presence of $RhCl_3$ [3–6]. Direct method of preparation of **L1H** is by the solid state reaction of pyridine-2-carboxylic acid with PCl_5 and NH_3 [7]. Recently an alternative method involving the oxidation of imine and methylene functions present in the Schiff base, *N*-(2-pyridylmethyl)pyridine-2-carbaldimine, using $[Cu(OAc)_2(H_2O)]$ was reported [8].

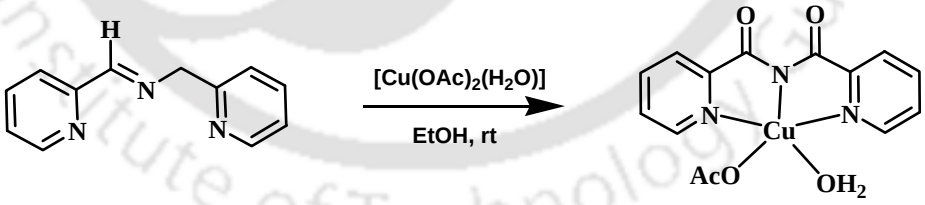

Normally, **L1** acts as a tridentate end-cap chelating ligand with its three nitrogen atoms coordinated to the metal ion. Thus chelated metal complexes can further utilize the two oxygen atoms of **L1** to bind the other metal ions to generate metallo-supramolecular assemblies. That is, $[M(\mathbf{L1})_2]$ or $[M(\mathbf{L1})_2]^+$ or $[M(\mathbf{L1})(L)_x]$ (L = monodentate ligand and *x* = 2 or 3), can act as ligand towards a second metal ion. The possible coordination modes are shown in below.

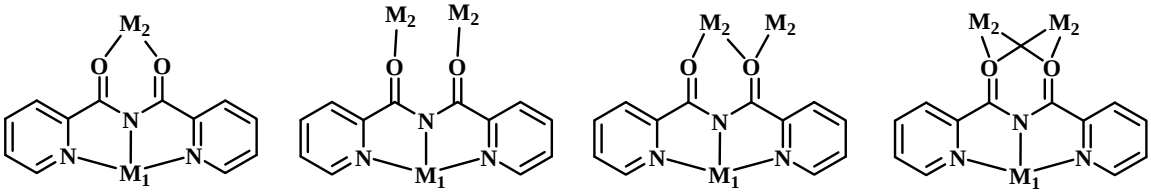

In general, metal complex assemblages like multiple helicates, grids, cages, two dimensional sheets, diamond networks, and zeolite mimics, display properties such as magnetism, conductivity and photo activity. In such assemblages observed properties are often induced by cooperative interaction between the metal ions. Hence, use of a "complex ligand" as a building component is effective not only in the construction of the desired structures but also to design the spatial arrangement of metal ions, and to tune the metal-metal interaction. In this regard, **L1** is one such ligand having the potential to form coordination polymers.

1.2 Bischelate as Building Component

Using $[M^{II}(\mathbf{L1})_2]$ (M = Mn, Fe, Ni, Cu) linear trinuclear complexes $[M(\mathbf{L1})_2\{M'(\mathbf{hfac})_2\}_2]$ (where MM'_2 = $NiMn_2$, $CuMn_2$, $FeMn_2$, $NiFe_2$, $FeFe_2$; $MnMn_2$, and $\mathbf{hfac}^-$ = hexafluoroacetylacetonate) have been synthesized (**I**) for studying their magnetic behaviors and structural characteristics [9–11].

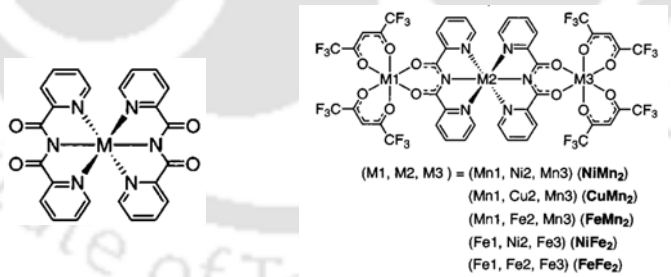

(I)

Two trinuclear complexes $[Fe^{II}(ClO_4)_2\{M^{III}(\mathbf{L1})_2\}_2](ClO_4)_2$ (M = Co, Fe) and three chain complexes *catena*-$[Fe^{II}(ClO_4)_2\{M^{III}(\mathbf{L1})_2\}]ClO_4$ (M = Co, Cr, Fe) were synthesized, structures for all complexes and magnetic properties for *catena* complexes were reported [12].

A graphite-like compound having large cavity without interpenetration (**II**) was prepared using $[Ni^{II}(\mathbf{L1})_2]$ and $Fe(ClO_4)_2{\cdot}6H_2O$ and structurally characterized [13,14].

Heterobimetallic 1D coordination polymers (**III**) of composition $[\{Ln(O_2NO)(H_2O)_3\}\text{-}\{Ni(\mathbf{L1})_2\}](NO_3)_2{\cdot}3H_2O$ (Ln = Gd, Tb, Dy) have been obtained from $[Ni(\mathbf{L1})_2]$ complex and corresponding lanthanide salts. These three compounds are isostructural and their structure consists of infinite cationic chains, with Ln^{III} ions being connected by $[Ni(\mathbf{L1})_2]$ complexes acting as bridging bis-bidentate ligands [15].

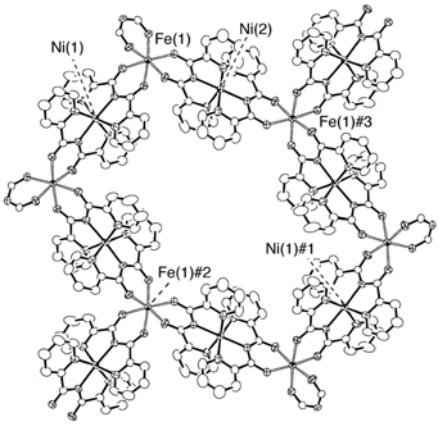

(**II**)

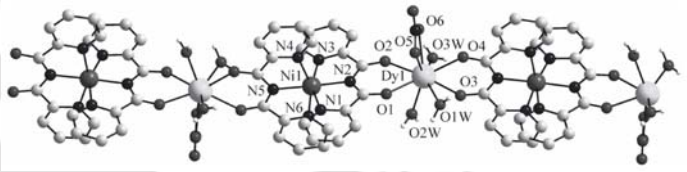

(**III**)

Molecular structures and 3d–4f magnetic exchange interactions in trinuclear complexes (**IV**), $[\{Dy(hfac)_3\}_2\{M^{II}(\mathbf{L1})_2\}]{\cdot}CHCl_3$ (M = Fe^{II} and Ni^{II}) have been reported [16]. An alternating Fe^{II} (high-spin)/Fe^{III} (low-spin) mixed valence single-chain magnet, *catena*-$[Fe^{II}(ClO_4)_2\{Fe^{III}(\mathbf{L1})_2\}]ClO_4$, prepared by using $[Fe(\mathbf{L1})_2]^+$ was structurally characterized and its magnetic properties (**V**) was evaluated [17,18].

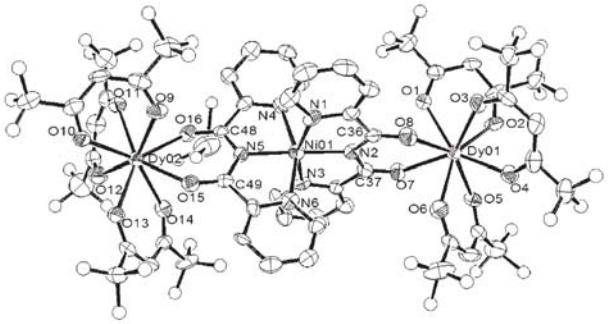

(**IV**)

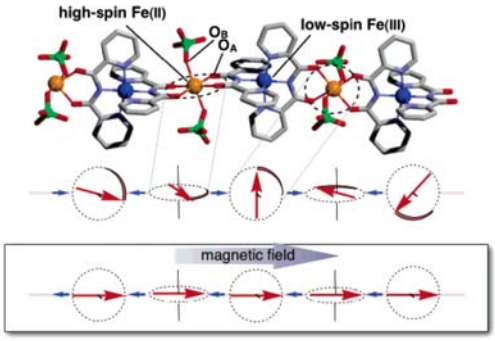

(**V**)

A short-range spin ordering was observed by Muon-Spin Relaxation method in (**VI**) *catena*-$[Fe^{II}(ClO_4)_2\{Fe^{III}(\mathbf{L1})_2\}]ClO_4$ [19] and the binuclear $Fe^{III}Dy^{III}$ compound $[Fe(\mathbf{L1})(\mu\text{-}\mathbf{L1})Dy(NO_3)_4]$ shows antiferromagnetic behavior [20]. A discrete bimetallic

complex $[Fe(\mathbf{L1})_2][Er(NO_3)_3(H_2O)_4](NO_3)$ exhibiting stacks of $[Fe(\mathbf{L1})_2]^+$ and $[Er(NO_3)_3(H_2O)_4]$ entities connected by hydrogen bonds has been reported [21,22].

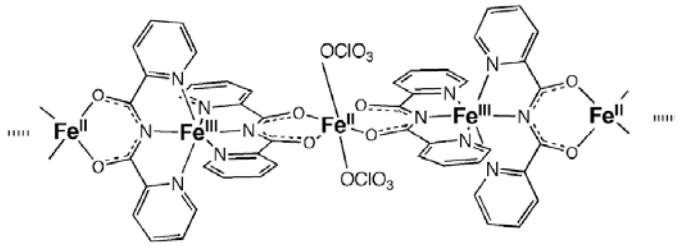

(**VI**)

1.3 Monochelate as Building Component

The mononuclear complex $[PPh_4]$-*mer*-$[Fe^{III}(\mathbf{L1})(CN)_3]\cdot H_2O$ and a ladder-like cationic chain (**VII**) compound $\{[Fe^{III}(\mathbf{L1})(\mu\text{-}CN)_3Mn^{II}(H_2O)_3]^+$ were prepared and characterized by X-ray diffraction analysis as its $[Fe^{III}(\mathbf{L1})(CN)_3]\cdot 3H_2O$ salt [23]. Cyano-bridged one-dimensional heterobimetallic coordination polymers, $[(\mathbf{L1})_2Fe^{III}{}_2(CN)_6Cu(H_2O)_2\cdot 1.5H_2O]_n$ (**VIII**) and $[(\mathbf{L1})Fe^{III}(CN)_3Cu(\mathbf{L1})(H_2O)H_2O]_n$ and trinuclear complex, $[(\mathbf{L1})_2Fe^{III}{}_2(CN)_6Mn(CH_3OH)_2(H_2O)_2]\cdot 2H_2O$ have been synthesized using tricyanometalate precursor $[Fe(\mathbf{L1})(CN)_3]^-$ ion and all are structurally characterized and their magnetic interaction were studied [24].

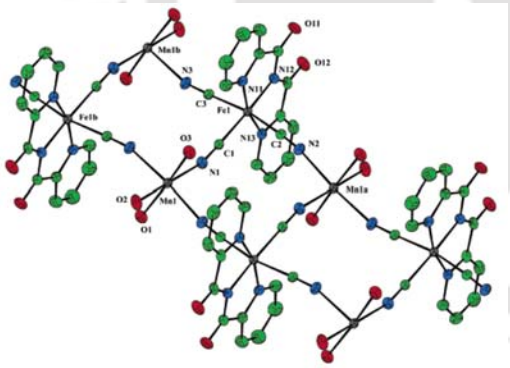

(**VII**)

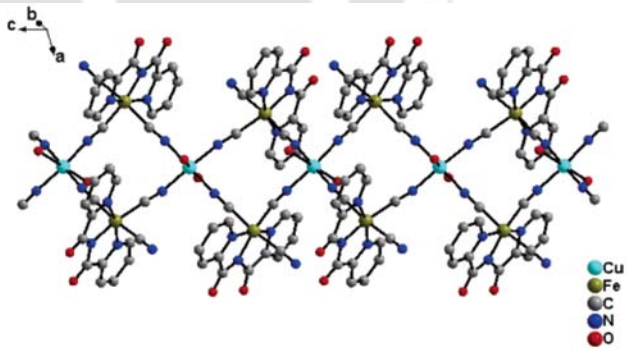

(**VIII**)

Two families of 1D polymeric complexes Cu(**L1**)(X) (X = CN^-, N_3^-) and $[Cu_{1-x}Fe_x(\mathbf{L1})](ClO_4)$ (x = 0 and 0.23) were synthesized. The structure of Cu(**L1**)(CN) was solved *ab initio* from X-ray powder diffraction data and refined by Rietveld methods. The $Cu(\mathbf{L1})^+$ complex was characterized by X-ray single crystal diffraction, in which linking by the amide oxygen atoms (**IX**) lead to a 1-D chain, exhibiting antiferromagnetic interactions [25].

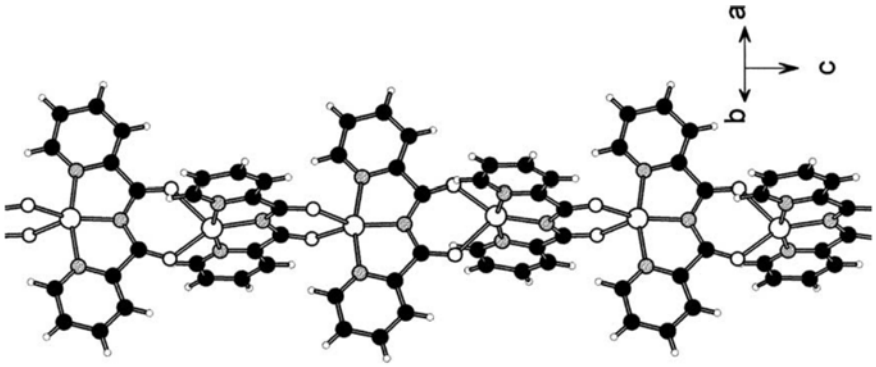

(**IX**)

Cyano-bridged heterobimetallic complexes, $[Cu_2(\mathbf{L1})_2(H_2O)_2Fe_2(5,5'\text{-dmbpy})_2(CN)_8][Cu(\mathbf{L1})Fe(5,5'\text{-dmbpy})(CN)_4]_2\cdot 4H_2O$ and $[Cu(\mathbf{L1})Fe(4,4'\text{-dmbpy})(CN)_4]_n$ (dmbpy = dimethyl-2,2′-bipyridine) have been synthesized and structurally characterized. The former complex contains two dinuclear and one tetranuclear heterobimetallic clusters (**X**) in an asymmetric unit whereas the structure of later complex features a one-dimensional heterobimetallic *zigzag* chain (**XI**). Magnetic studies show ferromagnetic coupling between Cu(II) and Fe(III) ions with g = 2.28, J_1 = 2.64 cm^{-1}, J_2 = 5.40 cm^{-1} and TIP = -2.36×10^{-3} for the former complex, and g = 2.17, J = 4.82 cm^{-1} and zJ' = 0.029 cm^{-1} for the later complex [26].

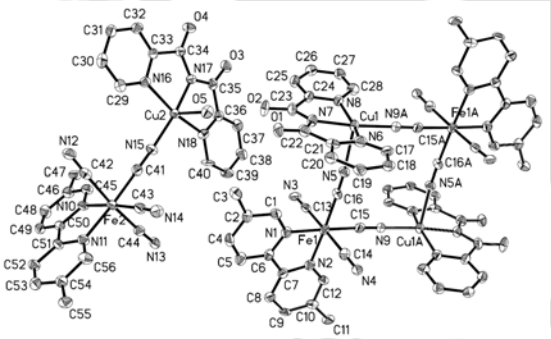

(**X**)

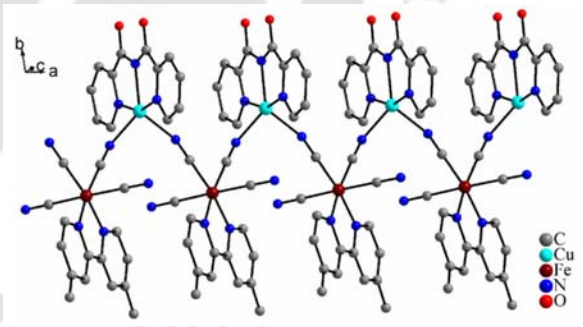

(**XI**)

A mixed valent hepta-iron complex $[Fe(EtOH)_2\{Fe_3(\mu_3\text{-}O)(\mathbf{L1})_2Cl_4(EtO)_2\}_2]$ with a ground state spin value of S = 12/2 having the molecular structure (**XII**) have been constructed from a tri-iron cluster $[Fe_3(\mu_3\text{-}O)(\mathbf{L1})_2Cl_4(EtO)_2]^-$ [27].

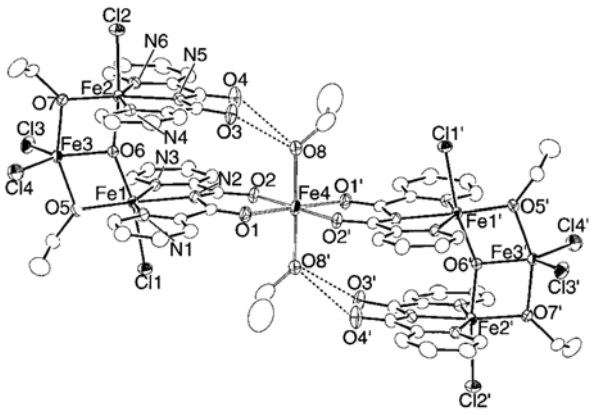

(XII)

The cyanide-bridged tetranuclear bimetallic rectangle $[AsPh_4][Fe^{III}_2Cu^{II}_2(\mu\text{-}CN)_4(CN)_8(\mathbf{L1})_2]\cdot 4H_2O$ has been prepared and its crystal structure (**XIII**) was determined by single crystal X-ray diffraction [28]. Another bimetallic rectangle (**XIV**), using a capping ligand at the Fe(III) center, $[(Tp)Fe(CN)_3Cu(\mathbf{L1})]_2\cdot 4H_2O$ (Tp = tris(pyrazolyl)hydroborate) was also structurally characterized [29].

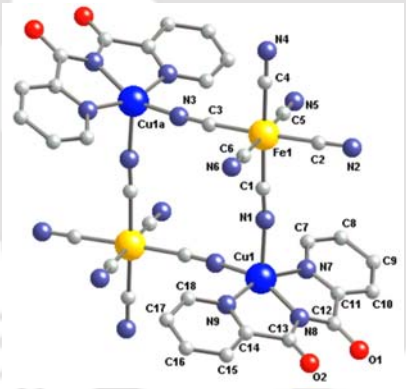

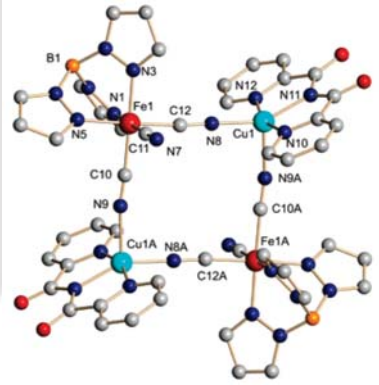

(XIII) **(XIV)**

One sulfur from each of the bis(1,2-dithiocroconato)copper(II) complex ion bind to two units of $[Cu(\mathbf{L1})(H_2O)]^+$ to form a trinuclear complex (**XV**) of formula $[Cu(\mathbf{L1})(H_2O)]_2[Cu(l,2,\text{-}dtcr)_2]$. Molecular structure of dihydrate of the trinuclear complex has been established, whose variable-temperature magnetic susceptibility measurements in the temperature range 4.2-140 K reveal that a Curie law is followed with three non-interacting copper(II) ions in the formula unit [30]. Using croconate as bridging ligand a dinuclear complex (**XVI**) of formula $[Cu_2(\mathbf{L1})_2(C_5O_5)]\cdot 3H_2O$ was isolated, which exhibit antiferromagnetic coupling interaction in the temperature range 4.2–300 K [31].

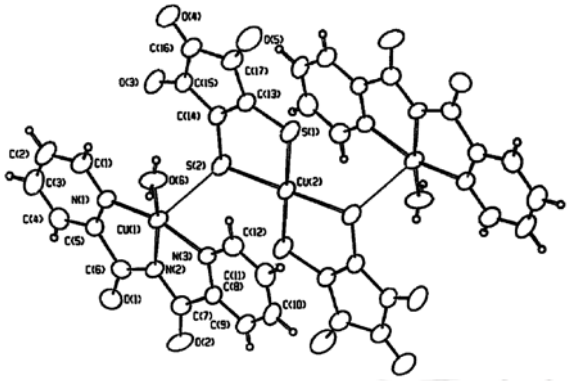

(**XV**)

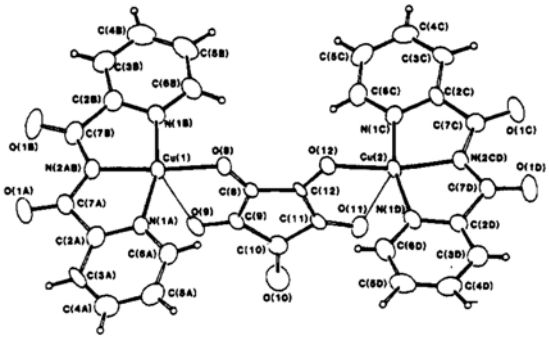

(**XVI**)

Based on broken symmetry B3LYP-DFT calculations, the magnetic behavior of [{Cu(**L1**)$_2$(H_2O)$_2$}{Cu(NO_3)$_2$}$_2$] (**XVII**) was satisfactorily interpreted using the SH of equation, $H = J(\mathbf{S1} \cdot \mathbf{S2} + \mathbf{S2} \cdot \mathbf{S3}) + J'(\mathbf{S1} \cdot \mathbf{S3})$, with $J = 14.1$ cm^{-1} and $J' = 5.5$ cm^{-1}, i.e., a ferromagnetic interaction, J, between adjacent centers and a long-range antiferromagnetic, J', interaction [32]. With these SH parameters the ground state of the complex is $S = 3/2$ with excited doublets at 1.5 and 21.1 cm^{-1}, respectively. The low-lying doublet state corresponds to antiferromagnetic arrangement of Cu(I) and Cu(III).

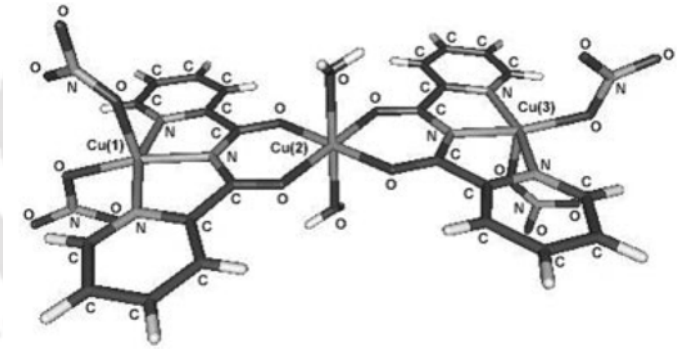

(**XVII**)

The oxalate ion bridged mixed ligand heterodinuclear compounds [Cu(**L1**)(H_2O)Cr(bpy)($ox)_2$]·2.5H_2O (**XVIII**) and [Cu(**L1**)(H_2O)Cr(phen)-($ox)_2$]·2H_2O (**XIX**) (bpy = 2,2′-bipyridine and phen = 1,10-phenanthroline) have been synthesized and characterized by single-crystal X-ray diffraction and reveal a Curie law behavior in the temperature range 1.9–290 K [33].

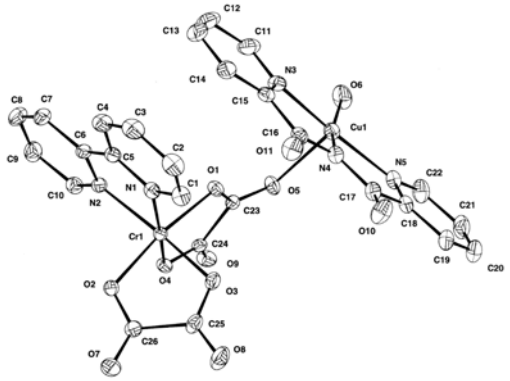

(**XVIII**)

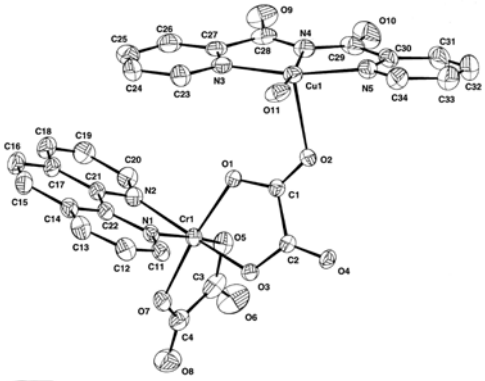

(**XIX**)

Dinuclear copper(II) complexes of formulae $[Cu_2(\mathbf{L1})_2(H_2O)_3(CrO_4)]\cdot H_2O$ (**XX**), $[Cu_2(\mathbf{L1})_2(H_2O)_3(SO_4)]\cdot H_2O$ (**XXI**), $[Cu_2(\mathbf{L1})_2(H_2O)_2(C_2O_4)]\cdot 2H_2O$ (**XXII**), and $[Cu_2(\mathbf{L1})_2(C_2O_4)]$ that contain two Cu^{II} centers bridged by chromate, sulfate and oxalate ions were synthesized and molecular structures of first three have been established by X-ray diffraction method. The chromate and sulfate bridged compounds reveal the occurrence of weak intramolecular antiferro-magnetic interactions and the oxalate bridged ones show ferro-magnetic interactions [34].

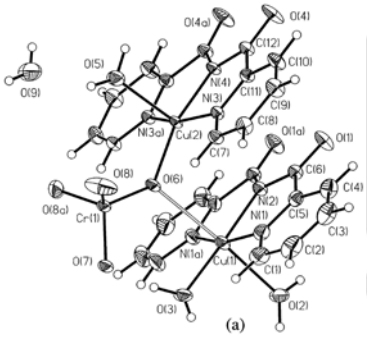

(**XX**)

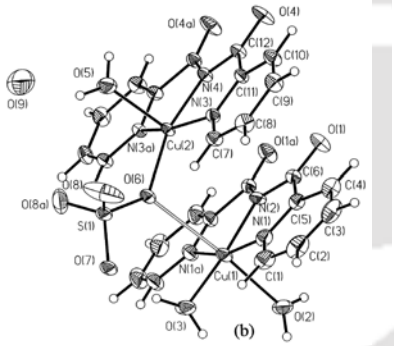

(**XXI**)

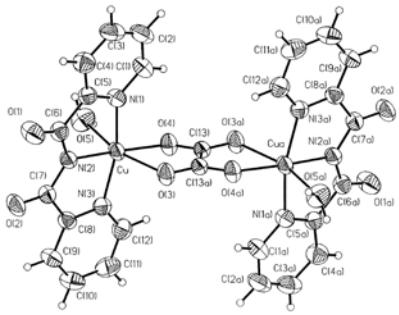

(**XXII**)

1,2-Dithiosquarate and 1,3-dithiosquarate bridged copper(II) complexes of formulae $[Cu_2(\mathbf{L1})_2(1,2\text{-dtsq})(H_2O)]\cdot 2H_2O$ (**XXIII**) and $[Cu_2(\mathbf{L1})_2(1,3\text{-dtsq})]\cdot 2H_2O$ (**XXIV**) were prepared and structurally studied. Variable temperature magnetic studies shows the exchange pathways accounting for the intermediate ferro- (J = +32.4 cm^{-1}) and antiferromagnetic (J = –33.5 cm^{-1}) couplings observed respectively in them [35].

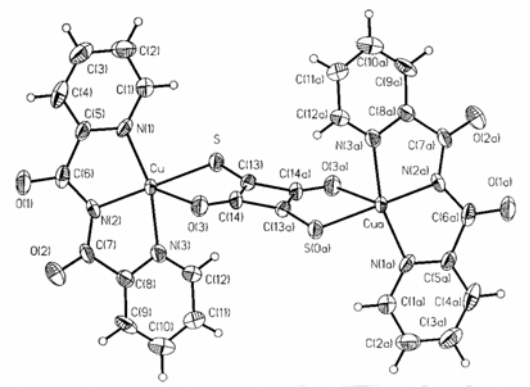

(**XXIII**)

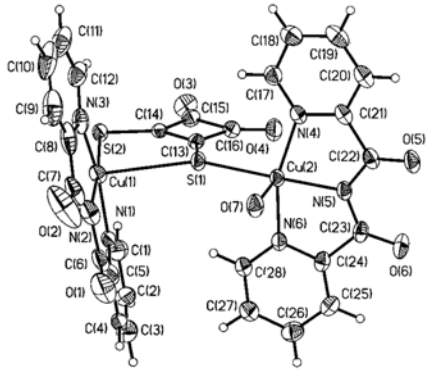

(**XXIV**)

The squarate bridged dinuclear copper(II) complex $[Cu_2(\mathbf{L1})_2(H_2O)_2(C_4O_4)]$ (**XXV**) has also been synthesized, structurally characterized, and variable-temperature magnetic susceptibility measurements (4.2–300 K**)** revealed an extremely weak exchange interaction through squarate dianion [36].

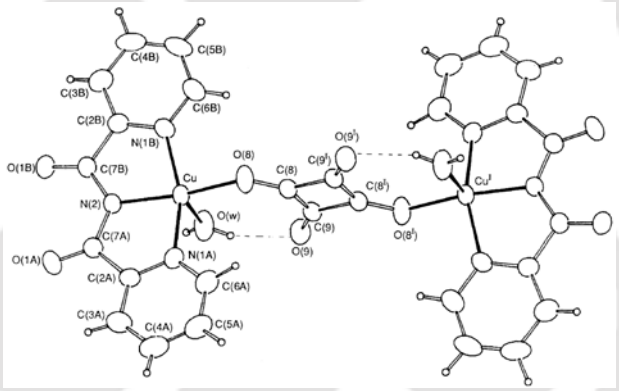

(**XXV**)

Iron(II) bischelates, $[Fe(\mathbf{L1})_2]\cdot H_2O$, and iron(III) bischelates, $[Fe(\mathbf{L1})_2](NO_3)\cdot 1.67\ H_2O$, $[Fe(\mathbf{L1})_2](C1O_4)$ as well as the monochelate $[Fe(\mathbf{L1})Cl_2(H_2O)]\cdot(CH_3)_2CO$, have been prepared, characterized by means of IR, UV-Vis and/or EPR spectroscopy, magnetic susceptibility measurements and single crystal X-ray methods. Magnetic measurements studies reveal that $[Fe(\mathbf{L1})_2]\cdot H_2O$ and $[Fe(\mathbf{L1})_2](NO_3)\cdot 1.67H_2O$ are practically in low-spin state at room temperature, $[Fe(\mathbf{L1})Cl_2(H_2O)]\cdot(CH_3)_2CO$ is in high-spin state in the temperature range 20 – 290 K, and $[Fe(\mathbf{L1})_2](C1O_4)$ shows spin-crossover behavior [37]. The iron(III) monochelates $[Fe(\mathbf{L1})Cl_2(MeOH)]$ and $[Fe(\mathbf{L1})Cl_2(EtOH)]$ have been structurally characterized and have Fe–N bond lengths lying in the range typical of high-spin Fe^{III} complexes [38].

The X-ray crystal structure of Mn^{II} bischelate having the formula $[Mn(\mathbf{L1})_2]\cdot H_2O$, has been reported and consists of discrete neutral $Mn(\mathbf{L1})_2$ entities linked through water molecules hydrogen bonded to ligand carbonyl groups. The coordination geometry around the manganese ions is very distorted compressed octahedral. The ESR spectra at X- and Q-band of $[Mn(\mathbf{L1})_2]\cdot H_2O$ as well as for manganese(II) doped into $Zn(\mathbf{L1})_2\cdot H_2O$ powder samples were examined. Zero-field splitting parameters, ***D*** and ***E,*** are calculated at 298 and 130 K. The ***D*** values are 0.073 and 0.078 cm^{-1}, respectively, whereas λ(= ***E/D)*** is far away from zero (0.23 and 0.24 cm^{-1}, respectively) in good agreement with the actual low symmetry of the MnN_6 chromophores [39].

The crystal and molecular structure of $[Cu(\mathbf{L1})_2]\cdot H_2O$ has also been determined. The structure consists of discrete neutral $[Cu(\mathbf{L1})_2]$ linked through water molecules hydrogen bonded to ligand carbonyl groups, similar to that found in $[Mn(\mathbf{L1})_2]\cdot H_2O$. The coordination geometry around copper ions is orthorhombically distorted octahedral [40]. The variable temperature EPR studies revealed that the molecular CuN_6 geometry is determined by the vibronic Jahn-Teller coupling and a compression due to rigid ligand [41]. Dimeric and polymeric copper(II) complexes of **L1** having general formulae $[Cu(\mathbf{L1})X]\cdot nH_2O$ {X = C1, Br, NCS, NCO, N_3, or CN} and $[Cu_2(\mathbf{L1})_2X]\cdot nH_2O$ {X = oxalate anion (ox), chloranilate anion (CA) or the dianion of 2, 5-dihydroxy-1, 4-benzoquinone (DHBQ)] have been synthesized by the copper(II)-assisted hydrolysis of 2,4,6-tris(2-pyridyl)-1,3,5-triazine [42]. The molecular structure of $[Cu(\mathbf{L1})(OAc)]\cdot H_2O$ has also been determined by single crystal X-ray diffraction methods [43]. Several coper(II) monochelates along with various co-ligands have been prepared and/or molecular structures been determined [44-47].

1.4 Materials

2-(Aminomethyl)pyridine, 2-quinolinecarboxaldehyde, isoquinoline, 3-cyanoisoquinoline, MCPBA, dimethylcarbamyl chloride, phenylacetylene, sodium dicyanamide, 10% Pd-C, KOCN, $CDCl_3$, KBr (Aldrich, USA), trimethylsilylcyanide (Spectrochem Pvt. Ltd. India), $Cu(OAc)_2\cdot H_2O$, $CuCl_2\cdot 2H_2O$, $FeCl_3$, $Cu(NO)_3\cdot 3H_2O$, $CoCl_2.6H_2O$, glacial acetic acid, MeOH, DMF, acetonitrile, KSCN, NaN_3, Na_2SO_4, Zn powder, KOH, K_2CO_3, Na_2EDTA, hydroxylamine hydrochloride (Merck India Ltd), EtOH

(Bengal Chemicals & Pharmaceuticals Ltd., Kolkata), and other reagent grade chemicals were used as received without further purification. Copper benzoate was prepared using the reported procedure [48].

Reagent grade dichloromethane (300 mL) was washed three times with saturated aqueous sodium bicarbonate solution (3 × 50 mL) followed by water (1 × 50 mL) and was stored overnight over fused $CaCl_2$. Thus obtained acid-free dichloromethane was refluxed for 3–4 hours over powdered P_4O_{10}, distilled afresh as and when required [49].

The same procedure described above was followed (without P_4O_{10}) treatment, for obtaining acid-free chloroform.

1.5 Instrumentation and methods

UV–Vis spectra were recorded using a Perkin–Elmer Lambda 25 UV–Vis spectrometer for solutions obtained by dissolving a calculated amount of the sample in an appropriate solvent. A Perkin–Elmer Spectrum One FT–IR spectrometer (KBr disc in the range 4000–250 cm^{-1}), has been used to record IR for air dried samples. ^1H NMR analysis were recorded in a Varian Mercury plus 400 MHz NMR Spectrometer and the chemical shifts were recorded in parts per million (ppm) on the scale using tetramethylsilane (TMS) as a reference. Perkin–Elmer Series II CHNS/O Analyzer 2400 was used obtaining for elemental analysis of samples. JEOL JES FA-200 X-band EPR spectrometer fitted with a quartz dewar for measurements at liquid nitrogen temperature was used for recording the EPR spectra, which were calibrated with Mn marker. Waters Q-TOF premier mass spectrometer is used for recording the mass spectra. Lakshore VSM Setup has been used for measurement of room temperature magnetic susceptibility data and the moment gain is calibrated using Ni standard which has magnetization of 6.92 emu / gm at 5 KOe.

1.5.1 X-ray crystallography

X-ray crystallographic data were collected using Bruker SMART APEX-CCD diffractometer with Mo Kα radiation (λ = 0.71073 Å). The intensity data were corrected for Lorentz and polarization effects and empirical absorption corrections was applied using SAINT program [50]. All the structures were solved by direct methods using SHELXS-97

[50,51]. Non-hydrogen atoms located from the difference Fourier maps were refined anisotropically by full-matrix least-squares on F^2 using SHELXL-97 [51,52]. All hydrogen atoms included at the calculated positions (except for the water/ ethanol molecules, in which some of the hydrogen atoms could neither be added at calculated positions nor be located from FMAP) were refined isotropically using a riding model.

1.5.2 Thermal Measurement

Thermogravimetry was studied by a computer controlled METTLER TOLEDO STAR^e system of module TGA/SDTA851^e under static nitrogen atmosphere using platinum pan at a heating rate of 10 °C/min in the noted temperature ranges. The instrument was calibrated using RTypSDTA sensor.

1.6 References

1. E.I. Lerner, S.J. Lippard, J. Am. Chem. Soc. 98 (1976) 5397–5398.
2. E.I. Lerner, S.J. Lippard, Inorg. Chem. 16 (1977) 1546–1551.
3. P. Paul, B. Tyagi, M.M. Bhadbhad, E. Suresh, Dalton Trans. (1997) 2273–2277.
4. P. Paul, B. Tyagi, A.K. Bilakhiya, M.M. Bhadbhade, E. Suresh, G. Ramachandraiah, Inorg. Chem. 37 (1998) 5733–5742.
5. P. Paul, B. Tyagi, A.K. Bilakhiya, M.M. Bhadbhade,; E. Suresh, J. Chem. Soc., Dalton Trans. (1999) 2009–2014.
6. P. Paul, Proc. Indian Acad. Sci. Chem. Sci., 114 (2002) 269–276.
7. H. Chowdhury, S.H. Rahaman, R. Ghosh, S.K. Sarkar, H-K. Fun, B.K. Ghosh, J. Mol. Struct. 826 (2007) 170–176.
8. S.K. Padhi, V. Manivannan, Inorg. Chem. 45 (2006) 7994–7996.
9. A. Kamiyama, T. Noguchi, T. Kajiwara, T. Ito, Inorg. Chem. 41 (2002) 507–512.
10. T. Kajiwara, T. Ito, J. Chem. Soc., Dalton Trans. (1998) 3351–3352.
11. T. Kajiwara, T. Ito, Mol. Cryst. And Liq. Cryst. 335 (1999) 73–80.
12. T. Kajiwara, R. Sensui, T. Noguch, A. Kamiyama, T. Ito, Inorg. Chim. Acta 337 (2002) 299–307.
13. A. Kamiyama, T. Noguchi, T. Kajiwara, T. Ito, Angew. Chem. Int. Ed. 39 (2000) 3130–3132.

14. A. Kamiyama, T. Noguchi, T. Kajiwara, T. Ito, CrystEngComm. 5 (2003) 231–237.
15. A.M. Madalan, K. Bernot, F. Pointillart, M. Andruh, A. Caneschi, Eur. J. Inorg. Chem. (2007) 5533–5540.
16. F. Pointillart, K. Bernot, R. Sessoli, D. Gatteschi, Chem. Eur. J. 13 (2007) 1602–1609.
17. T. Kajiwara, M. Nakano, Y. Kaneko, S. Takaishi, T. Ito, M. Yamashita, A.I. Kamiyama, H. Nojiri, Y. Ono, N. Kojima, J. Am. Chem. Soc. 127 (2005) 10150–10151.
18. Y. Kaneko, T. Kajiwara, H. Yamane, M. Yamashita, Polyhedron, 26 (2007) 2074–2078.
19. T. Kajiwara, I. Watanabe, Y. Kaneko, S. Takaishi, M. Enomoto, N. Kojima, M. Yamashita, J. Am. Chem. Soc. 129 (2007) 12360–12361.
20. M. Ferbinteanu, T. Kajiwara, K-Y. Choi, H. Nojiri, A. Nakamoto, N. Kojima, F. Cimpoesu, Y. Fujimura, S. Takaishi, M. Yamashita,. J. Am. Chem. Soc. 128 (2006) 9008–9009.
21. M. Ferbinteanu, T. Kajiwara, F. Cimpoesu, K. Katagiri, M. Yamashita, Polyhedron 26 (2007) 2069–2073.
22. M. Ferbinteanu, F. Cimpoesu, T. Kajiwara, M. Yamashita, Solid State Sciences 11 (2009) 760–765.
23. R. Lescouëzec, J. Vaissermann, L.M. Toma, R. Carrasco, F. Lloret, M. Julve, Inorg. Chem. 43 (2004) 2234–2236.
24. H-R. Wen, C-F. Wang, J-L. Zuo, Y. Song, X-R. Zeng, X-Z. You, Inorg. Chem. 45 (2006) 582–590.
25. H. Casellas, F. Costantino, A. Mandonnet, A. Caneschi, D. Gatteschi, Inorg.Chim. Acta 358 (2005) 177–185.
26. H-R. Wen, C.F. Wang, Z.Y. Du, J.L. Zuo, Inorg. Chim. Acta 361 (2008) 2901–2908.
27. T. Kajiwara, T.Ito, Angew. Chem. Int. Ed. 39 (2000) 230–233.
28. L.M. Toma, R. Lescouëzec, D. Cangussu, R. Llusar, J. Mata, S. Spey, J.A. Thomas, F. Lloret, M. Julve, Inorg. Chem. Commun. 8 (2005) 382–385.
29. W. Liu, C-F. Wang, Y-Z. Li, J-L. Zuo, X-Z. You, Inorg. Chem. 45 (2006) 10058–10065.

30. J. Sletten, M. Julve, F. Lloret, I. Castro, G. Seitz, K. Mann, Inorg. Chim. Acta 250 (1996) 219–225.
31. I. Castro, J. Sletten, J. Faus, M. Julve, Y. Journaux, F. Lloret, S. Alvarez, Inorg. Chem. 31 (1992) 1889–1894.
32. A. Bencini, F. Totti, Int. J. Quantum Chem. 101 (2005) 819–825.
33. R. Lescouëzec, G. Marinescu, J. Vaissermann, F. Lloret, J. Faus, M. Andruh, M. Julve, Inorg. Chim. Acta 350 (2003) 131–142.
34. M.L. Calatayud, I. Castro, J. Sletten, F. Lloret, M. Julve, Inorg. Chim. Acta 300–302 (2000) 846–854.
35. I. Castro, M.L. Calatayud, J. Sletten, F. Lloret, J. Cano, M. Julve, G. Seitz, K. Mann, Inorg. Chem. 38 (1999) 4680–4687.
36. I. Castro, J. Faus, M. Julve, Y. Journaux, J. Sletten, J. Chem. Soc., Dalton Trans. (1991) 2533–2538.
37. S. Wocadlo, W. Massa, J-V. Folgado, Inorg. Chim. Acta 207 (1993) 199–206.
38. T. Kajiwara, T. Ito, Acta Cryst. C56 (2000) 22–23.
39. D. Marcos, J.V. Folgado, D. Beltrán-Porter, M.T. Do Prado-Gambardella, S.H. Pulcinelli, R.H. De Almeida-Santos, Polyhedron, 9 (1990) 2699–2704.
40. D. Marcos, R. Martinez-Mañe, J.-V. Folgado, A. Beltrán-Porter, D. Beltrán-Porter, A. Fuertes, Inorg. Chim. Acta, 159 (1989) 11–18.
41. J-V. Folgado, W. Henke, R. Allmann, H. Stratemeier, D. Beltrin-Porter, T. Rojo, D. Reinen, Inorg. Chem. 29 (1990) 2035–2042.
42. J.V. Folgado, E. Escriva, A. Beltrán-Porter, D. Beltrán-Porter, Transition Met. Chem. 12 (1987) 306–310.
43. J.V. Folgado, E. Martínez-Tamayo, A. Beltran-Porter, D. Beltrán-Porter, A. Fuertes, C. Miravitlles, Polyhedron, 8 (1989) 1077–1083.
44. B. Vangdal, J. Carranza, F. Lloret, M. Julve, J. Sletten, J. Chem. Soc., Dalton Trans. (2002) 566–574.
45. X–P. Zhou, D. Li, S-L. Zheng, X. Zhang, T. Wu, Inorg. Chem. 45 (2006) 7119–7125.
46. D.C. de Castro Gomes, L.M. Toma, H.O. Stumpf, H. Adams, J.A. Thomas, F. Lloret, M. Julve, Polyhedron, 27 (2008) 559–573.
47. P. Halder, E. Zangrando, T.K. Paine, Polyhedron, 29 (2010) 434–440.

48. R.E. Del Sesto, A.M. Arif, J. S. Miller, Inorg. Chem. 39 (2000) 4894-4902.
49. K.M. Kadish, J.E. Anderson, Pure & App. Chem. 59 (1987) 703–714.
50. G.M. Sheldrick, SADABS, University of Göttingen, Göttingen, Germany, 1996.
51. SMART and SAINT, Siemens Analytical X-ray Instruments Inc., Madison, WI, 1996.
52. G.M. Sheldrick, SHELXS-97 and SHELXL-97, University of Göttingen, Göttingen, Germany, 1997.

Chapter 2

Conversion of 2-(Aminomethyl) Substituted Pyridine and Quinoline to Their Bis(carbonyl)amides Using Copper(II) Acetate*

Abstract

In air, hydrated ethanolic (95%) solution of 2-(aminomethyl) substituted pyridine and quinoline, on stirring with half equivalent of $Cu(OAc)_2 \cdot H_2O$, respectively afforded $[Cu(\mathbf{L1})(OAc)(H_2O)] \cdot H_2O$ (**1**) and $[Cu(\mathbf{L2})(OAc)(H_2O)]$ (**2**) {**L1** = bis(2-pyridylcarbonyl)amide ion and **L2** = bis(2-quinolylcarbonyl)amide ion} in good yields. These two reactions involve oxidation of the methylene group and formation of the bond between nitrogen and carbon in N–C(=O) through coupling. The complex $[Cu(\mathbf{L3})(OAc)(H_2O)]_3[Cu_2(OAc)_4(EtOH)_2]_{1.5}$ (**3**) {**L3** = (2-pyridylcarbonyl)(2-quinolylcarbonyl)amide ion} was synthesized by stirring ethanolic solution of the Schiff base [(2-pyridyl)-N-((2-quinolyl)methylene)methanamine] (**L**) and with one equivalent of $Cu(OAc)_2 \cdot H_2O$. A plausible mechanism for the conversion has been proposed. The free ligands were isolated as crystalline solids from the compounds **1–3**, by extrusion of Cu^{2+} ion using $EDTA^{2-}$. The molecular structures of **1**–**3** and **L2H** were established by X-ray crystallography and compounds having quinolyl group exhibit π–stacking interactions.

*This work has been published in:

R. Sahu, S.K. Padhi, H.S. Jena, V. Manivannan, *Inorg. Chim. Acta* **2010**, *363*, 1448–1454.

2.1 Introduction

Oxidation of alkyl and aromatic substrates by copper containing enzymes and by the model complexes using dioxygen is an active area of research [1]. However, oxidation of the $–CH_2–$ group flanked by a 2-pyridyl and an amide/imine function in presence of a suitable metal ion is rare [2, 3]. In such cases the final ligand that was found using the amide/imine function as 2-pyridylcarbonylamide/2-pyridylaldimine is bis(2-pyridylcarbonyl)amide ion (**L1**) and as 2-pyridylmethylketimine is 4′-(2-pyridyl)-2,2′:6′,2′′-terpyridine. The chemical reactivity of the methylene group flanked by a 2-pyridyl and an amine function is: (a) deprotonation of the coordinated bis(picolyl)amine (**bpa**) using a strong base, firstly at the secondary nitrogen atom, [{Rh(nbd)}$_2$(μ-**bpa**-H)]Cl and then at the methylene group to PyCH=N–CH_2Py as in [{Rh(nbd)}$_2$(μ-**bpa**-2H)] followed by its oxidation to [PyC(O)–N–CH_2Py]$^-$ (bpam-H) as in [Rh(nbd)(bpam-H)] using O_2 [4] and (b) double deprotonation of the coordinated bis(picolyl)amine using KO^{t}Bu as in K[Ir(**bpa**-2H)(cod)] followed by chemical oxidation to a ligand radical complex [Ir(**bpa**-2H)(cod)] using Ag^+ or O_2 [5], as shown in Scheme 1.

The **L1H** ligand was obtained through the Cu(II) ion mediated hydrolysis of 2,4,6-tris(2-pyridyl)-1,3,5-triazine [6, 7] and has been used for the synthesis of complexes of several transition metal ions. In metal chelates the three nitrogen atoms are coordinated to the metal center leaving the two oxygen atoms available for further coordination. Thus the metal chelates of **L1** can act as a bidentate ligand and such coordination by the oxygen atoms has been exploited to build supramolecular assemblies having extended structures [8–18].

Our laboratory has the interest in using picolylamines as synthon for synthesis of nitrogenous ligands [19]. This Chapter describes the method in which 2-(aminomethyl) attached to a pyridine or quinoline ring can be readily converted to respective bis(carbonyl)amides, using copper(II) acetate. The compounds obtained, by using 2-(aminomethyl)pyridine (**2-amp**) is [Cu(**L1**)(OAc)(H_2O)]·H_2O and by using 2-(aminomethyl)quinoline (**2-amq**) is [Cu(**L2**)(OAc)(H_2O)] {**L2** = bis(2-quinolyl-carbonyl)amide ion}. In addition, synthesis of [Cu(**L3**)(OAc)(H_2O)]$_3$ [Cu_2(OAc)$_4$(EtOH)$_2$]$_{1.5}$ {**L3** = (2-pyridylcarbonyl)(2-quinolylcarbonyl)amide ion} from a Schiff base [(2-pyridyl)-N-((2-quinolyl)methylene)methanamine] and copper(II) acetate is

also described. The structural evaluation of these compounds and that of **L2H** are discussed.

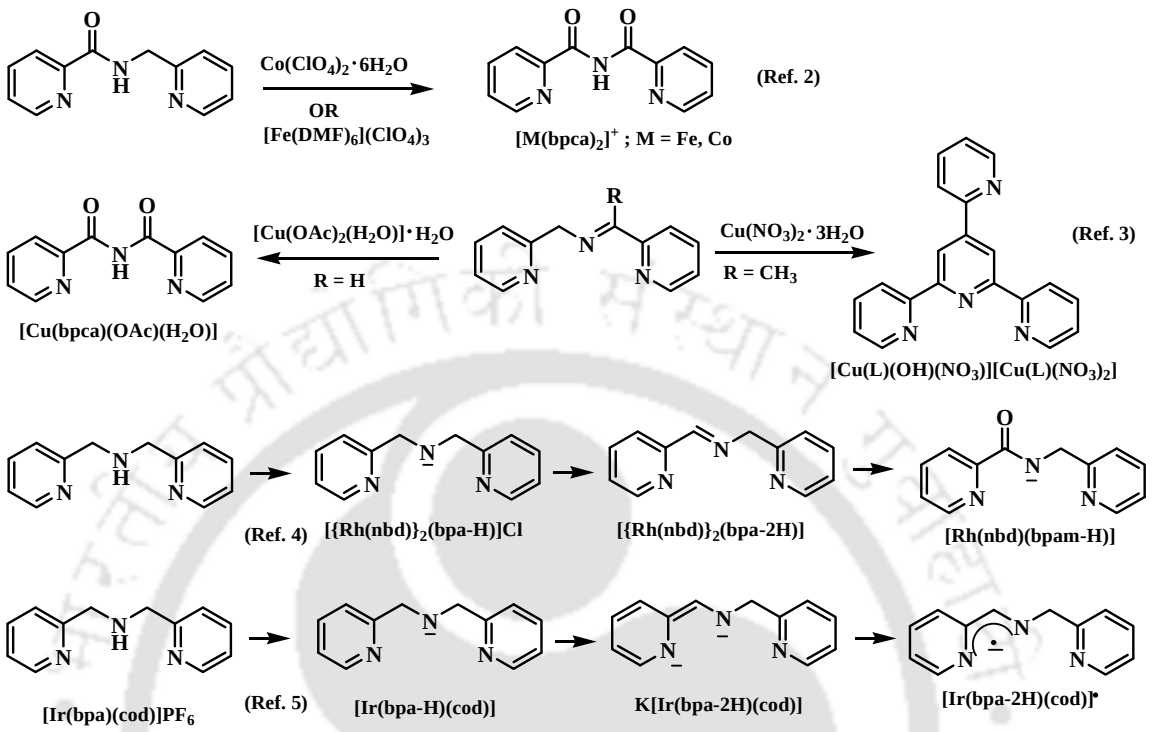

Scheme 1

2.2 Experimental Section

Bis(picolyl)amine was prepared by following the reported procedures [20].

2.2.1 Syntheses

2-Quinolinecarbaldoxime: To a solution of 2-quinolinecarboxaldehyde (1 g, 6.3 mmol) and hydroxylamine hydrochloride (1g, 14.4 mmol) in ethanol (10 mL), pyridine (1 mL) was added and refluxed for 6 h. After removing the solvent, ice-cold water (10 mL) was added, and a yellow precipitate of the 2-quinolinecarboxaldoxime was isolated by filtration, washed with ice-cold water and dried in desiccators [21]. The crude product was used directly in the next step without further purification. Yield: 0.9 g, 83%. IR (KBr, cm^{-1}): 3415 (m), 1635(s), 1603(m), 1563(m), 1504(m), 1489(w), 1455(m), 1427(m), 1354(m), 1321(w), 1302(w), 1238(w), 1206(w), 1141(w), 1118(w), 1022(s), 1007(s), 944(m), 922(m), 903(m), 839(m), 828(s), 792(m), 776(w), 741(s), 680(m), 633(m), 588(m),

476(m). 400 MHz ^{1}H NMR (δ (*J,* Hz), $CDCl_3$), **Fig 1**.: 7.57(1H, t, 7.4), 7.74 (1H, t, 7.6), 7.73 (1H, d, 8.0), 7.94 (1H, d, 8.4), 8.11 (1H, d, 8.8), 8.16 (1H, d, 8.4), 8.41 (1H, s), 8.63 (OH, b).

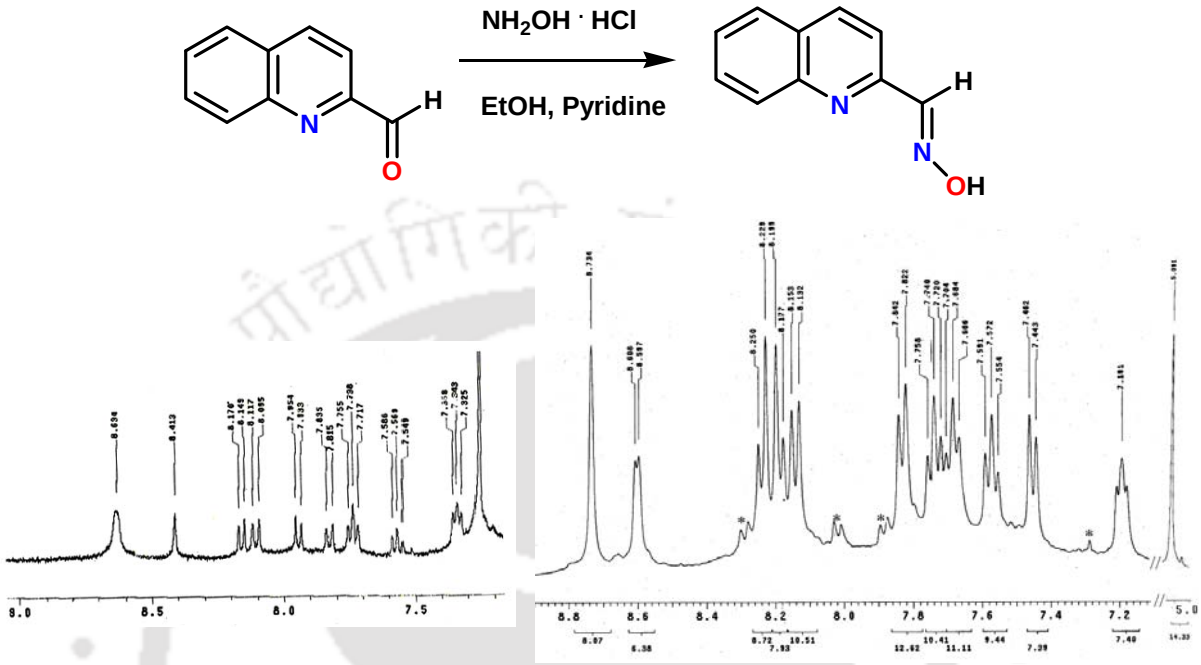

Fig. 1. ^{1}H NMR spectrum of 2-quinolinecarbaldoxime (left) and **L** (right)
Peaks marked * are due to impurity.

2-(Aminomethyl)quinoline: In a 200 mL round-bottomed flask equipped with overhead mechanical stirring, the 2-quinolinecarboxaldoxime (3.5 g, 20 mmol) and acetic acid (32 mL) were dissolved in ethanol (50 mL). Zinc dust (32 g) was added in small increments over 1 h and the mixture was stirred at room-temperature for another 12 h. The mixture was filtered, washed with ethanol and the combined filtrate and the washings were concentrated in *vacuo*. The concentrate was made strongly basic (pH > 12) using saturated aqueous KOH solution and extracted with ether. The ether solution was dried over anhydrous Na_2SO_4 and **2-amq** was recovered as oil after removal of ether [22]. Yield: 2.4 g, 73%. IR (KBr, cm^{-1}): 3400(m), 2962(s), 2926(s), 1606(s), 1583(m), 1484(s), 1418(m), 1376(m), 1309(m), 1290(m), 1261(m), 1176(w), 1155(w), 1109(m), 1086(w), 1034(w), 905(w), 746(s), 481(w). 400 MHz ^{1}H NMR (δ (*J,* Hz), $CDCl_3$) **Fig. 2**.: 1.98 (NH_2, s), 4.14 (CH_2, s), 7.37 (1H, d, 8.4), 7.49 (1H, t, 7.2), 7.68 (1H, t, 6.8), 7.78 (1H, d, 8.0), 8.04 (1H, d, 8.4), 8.09 (1H, d, 8.8).

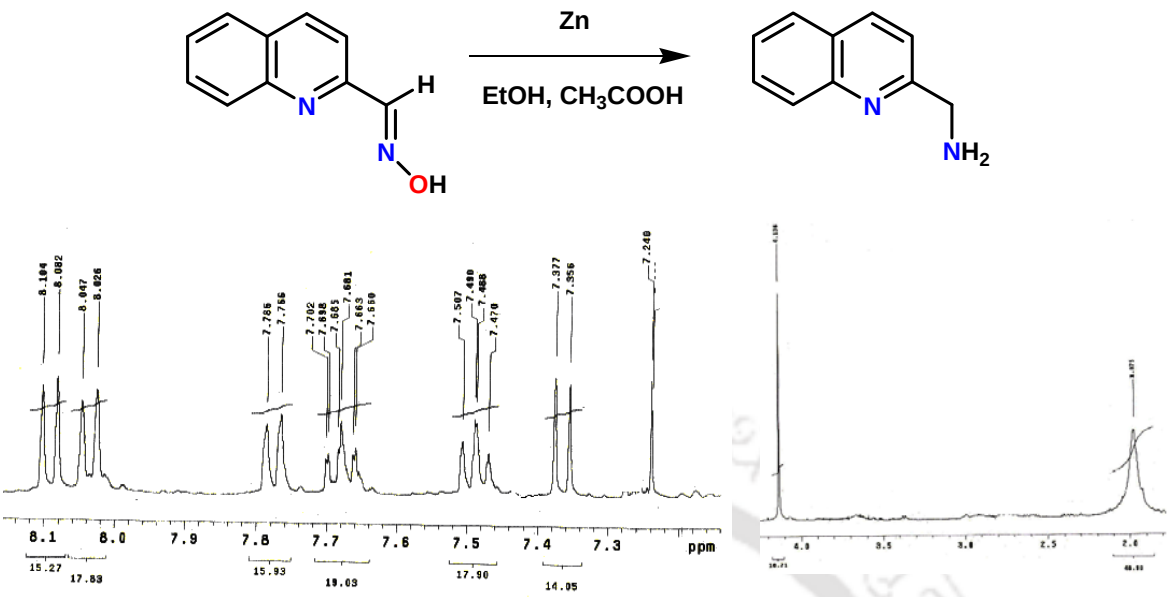

Fig. 2. ^{1}H NMR spectrum of 2-(aminomethyl)quinoline

[Cu(L1)(OAc)(H$_2$O)]·H$_2$O (1): To Cu(OAc)$_2$·H$_2$O (1.1 g, 5.5 mmol) dissolved in ethanol (60 mL) was added **2-amp** (1.2 g, 11 mmol) and stirred for 24 h. The solution was left undisturbed, blue crystals of **1** deposited after a week were collected and washed with ice-cold ethanol. Yield: 1.3 g, 61%. Selected IR frequencies (KBr, cm^{-1}) **Fig. 3**.: 1717(s), 1635(s), 1566(m), 1413(m), 1383(s), 1361(s), 1291(m). Anal Calcd. for $C_{14}H_{15}N_3O_6Cu$ (384.8): C 43.69, H 3.93, N 10.92. Found: C 43.61, H 3.91, N 10.75.

[Cu(L2)(OAc)(H$_2$O)] (2): Was prepared by following the same procedure described for **1**, and using 3 mmol of **2-amq** (0.506 g) and 1.5 mmol of Cu(OAc)$_2$·H$_2$O (0.300 g). Yield: 0.400 g, 58%. IR (KBr, cm^{-1}) **Fig. 3**.: 1707(s), 1633(s), 1512(w), 1462(m), 1379(s), 1345(w), 1270(w), 1218(w), 1151(w), 1118(w), 1026(w), 854(m), 779(s), 615(w). UV–Vis [λ_{max}, nm(ε, M^{-1}cm^{-1}), CH$_3$OH solution]: 730 (65); 510 (70); 240 (38595). EPR (DMF solution, 77 K): $g_{\|}$ = 2.263, $A_{\|}$ = 82 G; $g_{\perp}$ = 2.082. μ_{eff} (polycrystalline, 25 ºC) = 2.20 B. M. Anal Calcd. for $C_{22}H_{16}N_3O_5Cu$ (466): C 56.71, H 3.46, N 9.02. Found: C 56.62, H 3.43, N 9.11.

[Cu(L3)(OAc)(H$_2$O)]$_3$[Cu$_2$(OAc)$_4$(EtOH)$_2$]$_{1.5}$ (3): A mixture of **2-amp** (0.11 g, 1 mmol) and 2-quinolinecaboxaldehyde (0.16 g, 1 mmol) in methanol (30 mL) were heated at reflux for 5 h and then evaporated to dryness, which afforded [(2-pyridyl)-N-((2-quinolyl)methylene)methanamine] (**L**) as a reddish brown oil. IR (KBr, cm^{-1}):1633(s),

1595 (m), 1503 (m), 1471 (w), 1458 (w), 1434 (m), 1384 (m), 1307 (w), 1148 (w), 1116(w), 1093 (w), 1054 (w), 999 (w), 913 (w), 830 (m), 750 (s), 624 (m), 477 (w). 400 MHz ^{1}H NMR (δ (*J,* Hz), $CDCl_3$) **Fig 1**.(*vide supra*) : 5.09 (CH_2, s), 7.19 (1H, t, 5.8), 7.45 (1H, d, 7.6), 7.57 (1H, t, 7.4), 7.68 (1H, t, 7.6), 7.74 (1H, t, 7.6), 7.83 (1H, d, 8.0), 8.14 (1H, d, 8.4), 8.19 (1H, d, 8.0), 8.24 (1H, d, 8.4), 8.60 (1H, d, 4.4), 8.73 (1H, s). The crude **L** was dissolved in ethanol (30 mL) and a ethanolic solution (30 mL) of $Cu(OAc)_2{\cdot}H_2O$ (0.2 g, 1 mmol) was added and was stirred for 48 h. The solution was left undisturbed and green crystals deposited after 2 weeks were collected after washing with ice-cold ethanol. Yield: 0.167g, 52% (per copper atom). IR (KBr, cm^{-1}) **Fig. 3**.: 1706(s), 1632(s), 1461(m), 1376(s), 1342(m), 1217(w), 1117(w), 851(w), 803(m), 778(s), 725(m), 512(w). UV–Vis [λ_{max}, nm (ε, $M^{-1}cm^{-1}$), CH_3OH solution]: 680 (190); 450 (160) 321 (6885), 283 (11040), 243 (27820). EPR (CH_3OH solution, 77 K): $g_{\|}$ = 2.237, $A_{\|}$ = 75 G; $g_{\perp}$ = 2.041. μ_{eff} (polycrystalline, 25 ºC) = 1.97 B. M. (per Cu atom). Anal Calc. for $C_{72}H_{81}N_9O_{30}Cu_6$ (1933.7): C 44.72, H 4.22, N 6.52. Found: C 44.60, H 4.18, N 6.45.

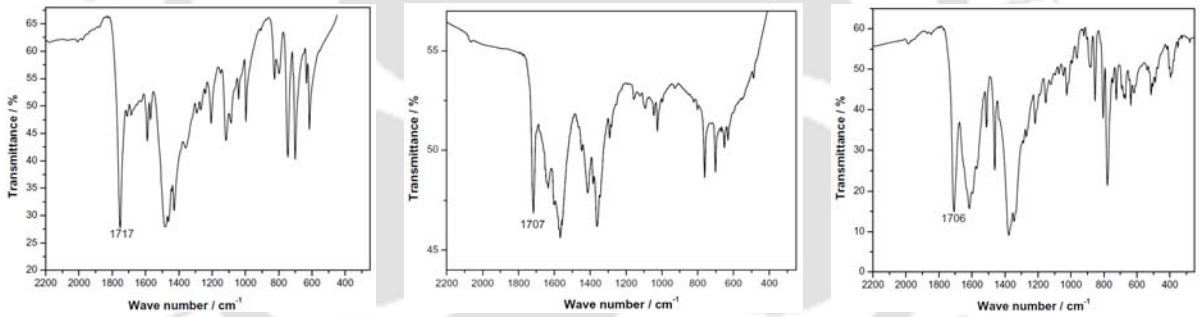

Fig. 3. IR spectra of **1** (left), **2** (middle) and **3** (right)

$[Cu(bpa)(OAc)_2]{\cdot}3H_2O$: To 0.2 g (1 mmol) of the **bpa** dissolved in 10 mL of 95% ethanol and a ethanolic (20 mL) solution of 0.2 g (1mmol) of $Cu(OAc)_2.H_2O$ was added. The solution was stirred for 6 h, which afforded a green gummy substance after few days of standing, which was dissolved in acetonitrile and left undisturbed. The blue crystals deposited were collected, which lost its crystallinity quickly, were finely ground and kept in vacuum desiccators over P_4O_{10}. Yield: 0.20 g, 46%. IR (KBr, cm^{-1}): 2962(m), 2923(m), 2853(m), 1586(s), 1567(s), 1409(s), 1261(s), 1093(s), 1025(s), 803(s). UV–Vis [λ_{max}, nm(ε, $M^{-1}cm^{-1}$), CH_3OH solution]: 637 (60); 450 (25), 256 (12470). Anal Calc. for $C_{16}H_{25}N_3O_7Cu$ (434.9): C 44.18, H 5.79, N 9.66. Found: C 44.12, H 5.70, N 9.55.

Free Ligands: Free **L1**H, **L2**H and **L3**H {**L3**H = (2-pyridylcarbonyl)(2-quinolylcarbonyl)amide} were obtained respectively from **1**, **2** and **3** by extrusion of Cu^{2+} ion using Na_2EDTA.

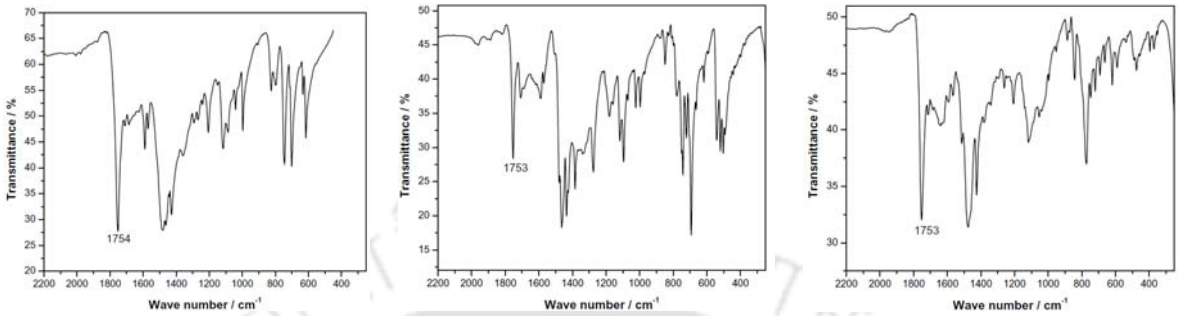

Fig. 4. IR spectra of **L1H** (left), **L2H** (middle) and **L3H** (right)

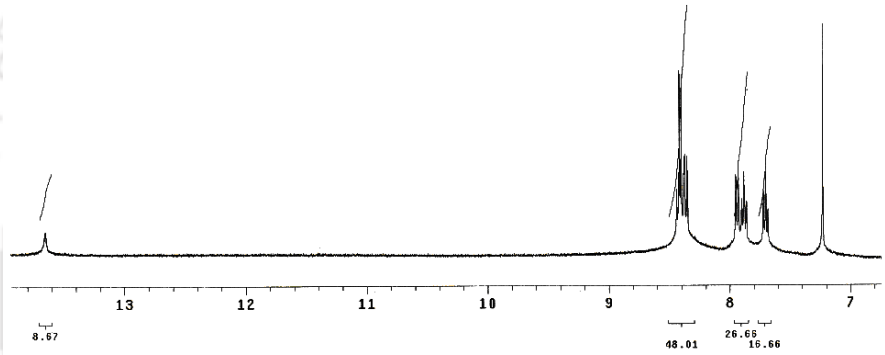

Fig. 5. ^1H NMR spectrum of **L2H**

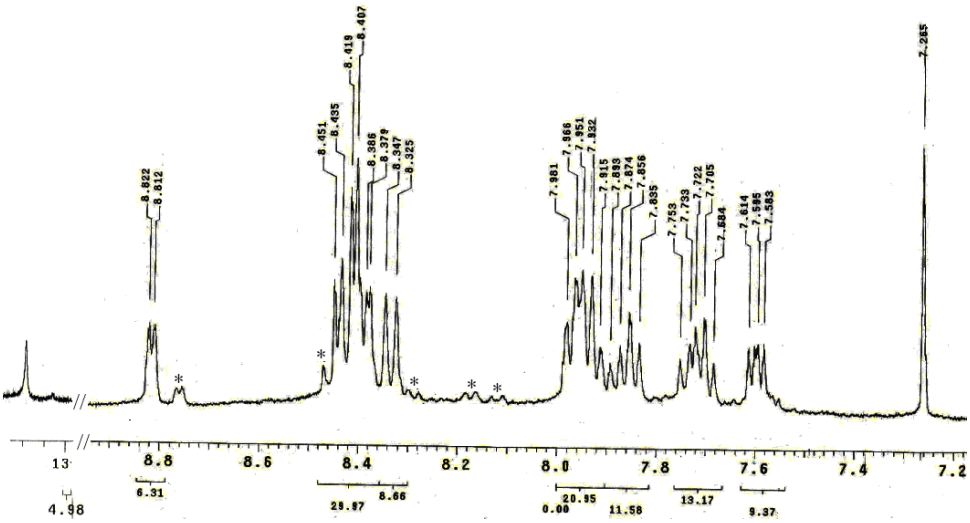

Fig. 6. ^1H NMR spectrum of **L3H**. Peaks marked * are due to impurity.

In a typical procedure, the complex (0.1 mmol) and Na_2EDTA (100 mg, 0.27 mmol) were dissolved in H_2O (50 mL) and stirred vigorously with 50 mL of $CHCl_3$, for 2 h. The

$CHCl_3$ layer was separated, dried with anhydrous Na_2SO_4, and the free ligands were obtained in quantitative yields after removing $CHCl_3$. **L2H**: m.p. 242 ºC. ESI-MS: *m/z* calcd. for $C_{20}H_{13}N_3O_2$ 327.10 found (M^-–H) 325.94. IR, (KBr, cm^{-1}) **Fig. 4**.: 1753 (s), 1708(m), 1588(w), 1478(w), 1463(s), 1434(s), 1384(m), 1275(m), 1180(w), 1117(m), 1095(m), 848(w), 778(w), 742(m), 722(m), 693(s), 663(w), 618(w), 541(m), 492(w). 400 MHz ^{1}H NMR (δ (*J,* Hz), $CDCl_3$) **Fig. 5**.: 7.70 (2H, t, 7.2), 7.88 (2H, t, 7.6), 7.94 (2H, d, 8.4), 8.40 (6H, m), 13.65 (NH, s). **L3H**: m.p. 182 ºC. ESI-MS: *m/z* calcd. for $C_{16}H_{11}N_3O_2$ 277.09 found (M^-–H) 275.95. IR, (KBr, cm^{-1}) **Fig. 4**.: 1753(s), 1588(w),1469(s), 1424(s), 1261(s), 1205(m), 1100(s), 1024(w), 996(w), 871(w), 846(m), 798(w), 772(m), 746(m), 691(m), 663(m), 618(m), 591(w), 477(w). 400 MHz ^{1}H NMR (δ (*J,* Hz), $CDCl_3$) **Fig. 6**.: 7.57(1H, t, 6.2), 7.71(1H, t, 6.0), 7.88(3H, m), 8.31(1H, d, 8.0), 8.4(3H, m), 8.79(1H, d, 4.8), 13.27 (NH, s).

2.3 Results and Discussions

2.3.1 Syntheses

In air, hydrated ethanolic (95%) solution of **2-amp** on stirring with half equivalent of $Cu(OAc)_2{\cdot}H_2O$ generated a green solution which on standing deposited blue crystals of composition [Cu(**L1**)(OAc)(H_2O)]·H_2O (**1**) in good yields (Scheme 2).

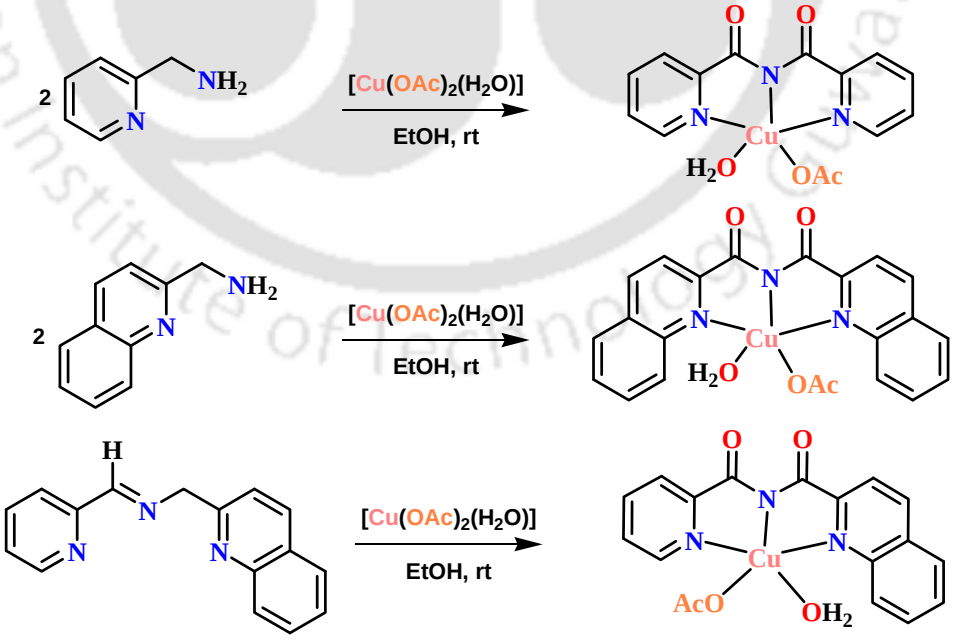

Scheme 2. Synthesis of **1–3**.

Under the same conditions by using **2-amq**, green crystals of [Cu(**L2**)(OAc)(H_2O)] (**2**) were obtained. These reactions clearly involve two categories of reactivities under mild conditions: (1) the oxidation of the methylene function and (2) formation of the bond between nitrogen and carbon in N–C(=O) through coupling.

A plausible mechanism for the conversion is shown in Scheme 3. Coordination of one molecule of **2-amp** at each of the copper atoms in dicopper(II) center form **I**. Oxidation of the methylene group might occur at this stage leading to an amide intermediate **II**. Coordination of another molecule of **2-amp** through the pyridine nitrogen atom with a pendent 2-aminomethyl group will lead to **III**. Since the carbonyl carbon of the amide function is now electrophilic in character due to loss of conjugation with the lone-pair on –NH_2 group (which is coordinated to copper), will be attacked by pendent 2-aminomethyl group, forming the intermediate **IV** containing tetrahedral carbon centers. Elimination of ammonia from tetrahedral carbon and collapse of the dicopper core to intermediate **V** that contain *N*-(2-picolyl)picolinamide moiety coupled with its oxidation to bis(2-pyridylcarbonyl)amide lead to the final product **1**.

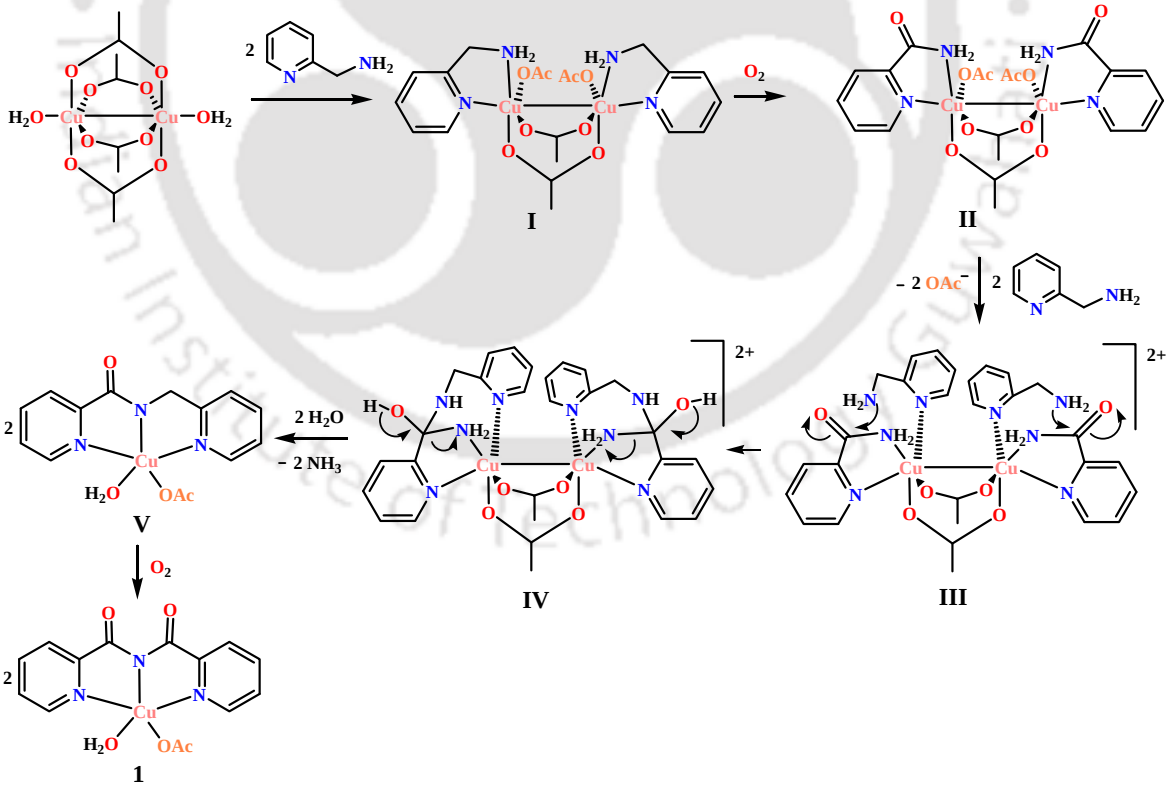

Scheme 3. Plausible mechanism for the conversion of **2-amp** to **1**.

Under the same experimental conditions, **bpa** and $Cu(OAc)_2 \cdot H_2O$ yielded the compound of composition $[Cu(\mathbf{bpa})(OAc)_2] \cdot 3H_2O$, in which coordination of the tridentate ligand to the copper(II) center occurs and above noted reactivity was not observed (Scheme 4). It is pertinent to note that the oxidation of the methylene group adjacent to a pyridine-2-carboxamido moiety in N-(2-picolyl)picolinamide by Fe(III), Co(III) ions and adjacent to a

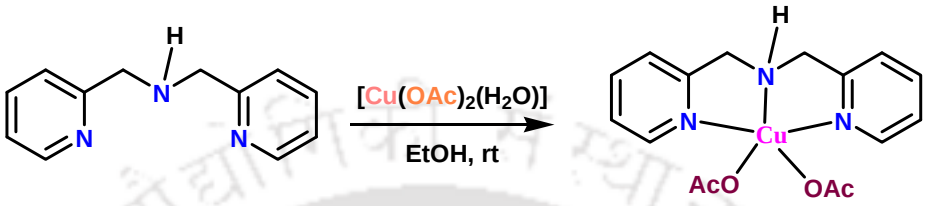

Scheme 4. Reaction of **bpa** with $Cu(OAc)_2 \cdot H_2O$.

pyridine-2-methylketimine function in N-(2-pyridylmethyl)pyridine-2-methylketimine by $Cu(NO_3)_2 \cdot 3H_2O$ were reported earlier [2,3]. The complex $[Cu(\mathbf{L3})(OAc)(H_2O)]_3[Cu_2(OAc)_4(EtOH)_2]_{1.5}$ (**3**) was synthesized by using the Schiff base [(2-pyridyl)-N-((2-quinolyl)methylene)methanamine] (**L1**) and one equivalent of $Cu(OAc)_2 \cdot H_2O$. In this reaction the imine moiety is oxidized to the 2-quinoline-2-carboxamido moiety, which probably aids the oxidation of the adjacent methylene group. It is relevant to note that reaction of **2-amp** with $Cu(OAc)_2 \cdot H_2O$ in acetonitrile produced a simple bischelate [22]. The free ligands were isolated as crystalline solids from the compounds **1–3**, by the extrusion of the Cu^{2+} ion using $EDTA^{2-}$.

2.3.2 Molecular Structures

The molecular structures of **1**–**3** and of **L2H** were established by single crystal X-ray diffraction methods and the crystal data are listed in Table 1. The crystallographic and the bond parameters of **1** prepared by this method, are identical to that reported for the **1** prepared from the other two routes *viz.,* by reacting $Cu(OAc)_2 \cdot H_2O$ with 2,4,6-tris(2-pyridyl)-1,3,5-triazine [23] and with N-(2-pyridylmethyl)pyridine-2-carbaldimine [3], hence its structural details are not elaborated further, a schematic view is shown in Fig 7.. The selected bond distances and angles for **2, 3** and **L2H** are listed in Table 2.

Compound **2** crystallized in the space group $Cmc2_1$ and the asymmetric unit contain 2 half molecules. Compound **3** is a co-crystal that crystallized in the space group P-1 and the

Table 1. Crystallographic and refinement parameters.

	1	**2**	**3**	**4**
Formula	$C_{14}H_{15}CuN_3O_6$	$C_{22}H_{16}N_3O_5Cu$	$C_{72}H_{81}N_9O_{30}Cu_6$	$C_{20}H_{13}N_3O_2$
CCDC Number	284749	754807	754808	754809
Formula weight	384.84	465.93	1933.73	327.33
Cryst. color, habit	Blue, Blocks	Green, Blocks	Green, Blocks	Brown, Blocks
T, K	298(2)	298(2)	298(2)	298(2)
cryst. syst.	Triclinic	Orthorhombic	Triclinic	Monoclinic
space group	*P*-1	$Cmc2_1$	*P*-1	$P2_1/n$
a, Å	7.3954(2)	16.2378(13)	14.764(2)	9.1492(4)
b, Å	8.6190(3)	15.5732(13)	16.575(3)	13.1027(6)
c, Å	13.0051(4)	15.9288(14)	17.431(3)	13.4468(6)
α, deg	74.610(2)	90.00	72.615(12)	90.00
β, deg	84.771(2)	90.00	76.271(12)	96.080(3)
γ, deg	81.008(2)	90.00	80.499(11)	90.00
V, Å^3	788.34(4)	4028.0(6)	3934.0(12)	1602.92(12)
Z	2	8	2	4
D_{calcd}, gcm^{-3}	1.621	1.537	1.633	1.356
μ, mm^{-1}	1.422	1.125	1.683	0.090
F(000)	1031	1856	1980	680
GOF[a] on F^2	1.79	1.050	1.039	1.040
R[$I > 2\sigma(I)$]	[b]R_1 = 0.0179, [c]wR_2 = 0.0179	[b]R_1 = 0.1075, [c]wR_2 = 0.2147	[b]R_1 = 0.0789, [c]wR_2 = 0.1688	[b]R_1= 0.0420, [c]wR_2= 0.0978
Rindices(all data)	[b]R_1 = 0.0514, [c]wR_2 = 0.0514	[b]R_1 = 0.1077, [c]wR_2 = 0.2147	[b]R_1 = 0.1297, [c]wR_2 = 0.1927	[b]R_1= 0.0797, [c]wR_2= 0.1128

[a] GOF = $[\sum[w(F_0^2 - F_c^2)^2] / M - N]^{1/2}$ (M =number of reflections, N = number of parameters refined).
[b] $R_1 = \sum \| F_0 | - | Fc \| / \sum | F_0 |$.
[c] $wR_2 = [\sum[w(F_0^2 - F_c^2)^2] / \sum[w(F_0^2)^2]]^{1/2}$.

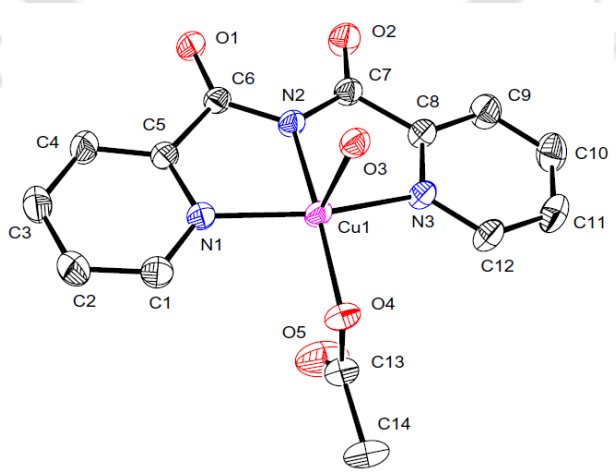

Fig. 7. ORTEP diagram (30%) of **1**. Hydrogen atoms are omitted for clarity.

Table 2. Selected bond distance (Å) and Angles (deg).

		2	
Cu1–N1	2.109(8)	Cu2–O6	2.293(10)
Cu1–N2	1.931(12)	Cu2–O7	1.974(9)
Cu1–O2	2.320(10)	C10–N2	1.346(12)
Cu1–O3	1.966(10)	C10–O1	1.204(12)
Cu2–N3	2.109(7)	C22–N4	1.334(11)
Cu2–N4	1.891(11)	C22–O5	1.245(13)
N1–Cu1–N1	161.1(4)	N3–Cu2–N3	159.9(4)
N1–Cu1–N2	81.0(2)	N3–Cu2–N4	80.7(2)
N1–Cu1–O2	89.3(3)	N3–Cu2–O6	90.1(2)
N1–Cu1–O3	99.4(2)	N3–Cu2–O7	100.0(2)
N2–Cu1–O2	103.4(4)	N4–Cu2–O6	112.4(4)
N2–Cu1–O3	157.9(5)	N4–Cu2–O7	155.3(5)
O2–Cu1–O3	98.7(4)	O6–Cu2–O7	92.3(4)
O1–C10–N2	128.9(11)	O5–C22–N4	129.7(11)
C10–N2–C10	121.1(13)	C22–N4–C22	120.2(13)
C10–N2–Cu1	119.4(6)	C22–N4–Cu2	119.6(6)
		3	
Cu1–N1	2.088(5)	Cu3–O15	2.301(4)
Cu1–N2	1.966(5)	O1–C6	1.183(7)
Cu1–N3	2.035(5)	O2–C7	1.219(7)
Cu1–O3	1.969(4)	N2–C6	1.378(8)
Cu1–O5	2.300(4)	N2–C7	1.337(8)
Cu2–N4	2.062(5)	O6–C24	1.220(8)
Cu2–N5	1.966(5)	O7–C25	1.278(7)
Cu2–N6	2.089(5)	N5–C24	1.340(8)
Cu2–O8	1.967(4)	N5–C25	1.318(8)
Cu2–O10	2.278(4)	O11–C42	1.184(8)
Cu3–N7	1.969(5)	O12–C43	1.256(7)
Cu3–N8	1.951(5)	N8–C42	1.355(8)
Cu3–N9	2.142(5)	N8–C43	1.333(8)
Cu3–O13	1.965(4)		
N1–Cu1–N2	81.6(2)	N5–Cu2–O8	163.2(2)
N1–Cu1–N3	163.0(2)	N5–Cu2–O10	106.3(2)
N2–Cu1–N3	81.5(2)	N6–Cu2–O8	105.9(2)
N1–Cu1–O3	91.1(2)	N6–Cu2–O10	93.8(2)
N1–Cu1–O5	90.9(2)	O8–Cu2–O10	89.3(2)
N2–Cu1–O3	163.4(2)	N7–Cu3–N8	81.1(2)
N2–Cu1–O5	106.2(2)	N7–Cu3–N9	162.9(2)
N3–Cu1–O3	105.5(2)	N8–Cu3–N9	82.0(2)
N3–Cu1–O5	93.0(2)	N7–Cu3–O13	95.5(2)

O3–Cu1–O5	88.7(2)	N7–Cu3–O15	92.0(2)
N4–Cu2–N5	81.7(2)	N8–Cu3–O13	165.7(2)
N4–Cu2–N6	161.7(2)	N8–Cu3–O15	104.1(2)
N5–Cu2–N6	80.0(2)	N9–Cu3–O13	100.4(2)
N4–Cu2–O8	92.1(2)	N9–Cu3–O15	94.4(2)
N4–Cu2–O10	89.9(2)	O13–Cu3–O15	89.9(2)
		L2H	
O1–C10	1.2138(14)	N2–C10	1.3783(18)
O2–C11	1.2127(15)	N2–C11	1.3721(19)
O1–C10–N2	125.13(14)	C10–N2–C11	129.56(11)
O2–C11–N2	125.13(14)		

unit cell contain 3 units of the [Cu(**L3**)(OAc)(H_2O)] (**3a**) and 1.5 units [$Cu_2(OAc)_4(EtOH)_2$] (**3b**). A perspective view of one molecule each of **2** and **3a** are depicted in Fig. 8. The copper(II) centers in **2** and **3a** are penta-coordinated and is bound by the three nitrogen atoms of the anionic ligand in a meridional fashion, a monodentate acetate ion and a water molecule. Overall N_3O_2 coordination environment around the copper atom has a distorted square pyramidal geometry as is evident from the τ values that are lying in the range 0.01–0.05 in **2** and **3a** [24]. In general the Cu–N_D (N_D = amide–N) is shorter than that of the Cu–$N_{P/Q}$ (N_P = pyridine–N and N_Q = quinoline–N). The Cu–N_P lengths are comparable between those observed in **1** and **3a**, and within **3a** the Cu–N_Q lengths are shorter than that of Cu–N_P. In **2**, each of the individual quinolinimide rings are planar and in a given ligand the dihedral angle between the two quinolinimide rings lies in the range 3.5–4.2º.

In **2**, packing reveals the presence of π···π interactions between the quinoline rings, with the non-bonded distances of C5···C13 3.32(2) Å and C9···C15 3.31(2) Å. The significant intermolecular H-bonding interactions present are O1···O6 2.913(12) Å, O2···O5 2.840(13) Å, O2···O7 2.906(9) Å. The packing diagram of **3** on viewing down the *c*-axis is shown in Fig. 9. It consists of separate layers made up of **3a** and **3b** units. The layers of **3a** and **3b** are segregated and commingled alternatively. The two layers are interlinked by hydrogen-bonding interactions viz., O3···O30 2.658(5) Å, O5···O26 2.895(7) Å, O8···O24 2.650(6) Å, O10···O20 2.899(7) Å, O13···O25 2.620(6) Å, O15···O23 2.944(7) Å. Within the **3a**-layers, the hydrogen-bonding that occur are O2···O15 2.937(6) Å, O5···O11 2.884(7) Å, O6···O10 2.872(7) Å, O7···O10 2.880(6) Å, O1···O15 2.877(7) Å. In addition π···π

interactions exist between the quinoline rings with the non-bonded distances of C8···C30 3.361(9) Å and C12···C26 3.356(8) Å. Within the layers of **3b**, the molecules are isolated and no significant hydrogen-bonding interactions are found to occur.

The ORTEP plot of **L2H** is shown in Fig. 9. Two quinoline rings are planar and the packing diagram reveal the presence of π···π interactions. A cg···cg distance of 3.638(1) Å is present between the centers (cg) of two six-membered rings containing the nitrogen atom. Other significant non-bonded interactions present are C4···C4 3.291(2) Å, O2···C10, 3.142(2) Å, O1···C11 3.222(2) Å. The non-bonded distance between the two amide oxygen atoms in **2** are O1···O1 2.741(9) Å, O5···O5 2.744(9) Å while that in **3a** are O1···O2 2.838(7) Å, O6···O7 2.765(9) Å, O11···O12 2.920(9) Å and that in **L2H** is O1···O2 2.911 (2) Å. On comparison the values observed in **2** are comparable to those in **1** but shorter than that in **3a** and **L2H**.

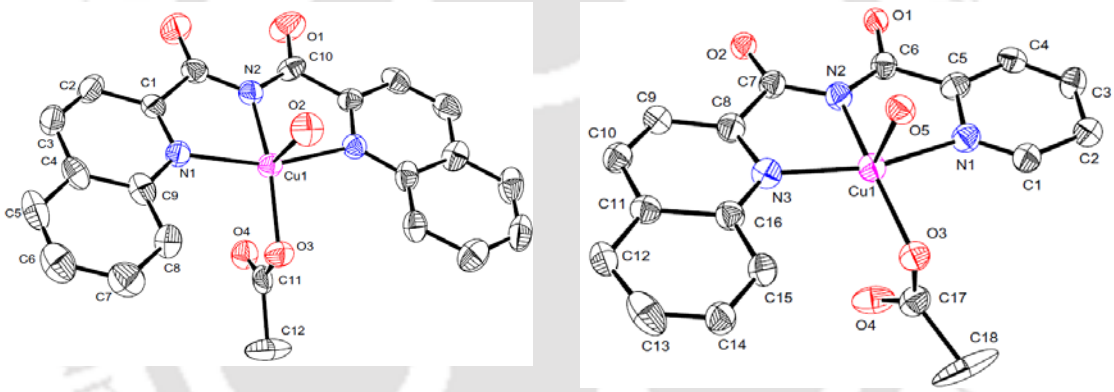

Fig. 8. ORTEP diagram (30% probability level) of **2** (left) and **3a** (right). Hydrogen atoms are omitted for clarity.

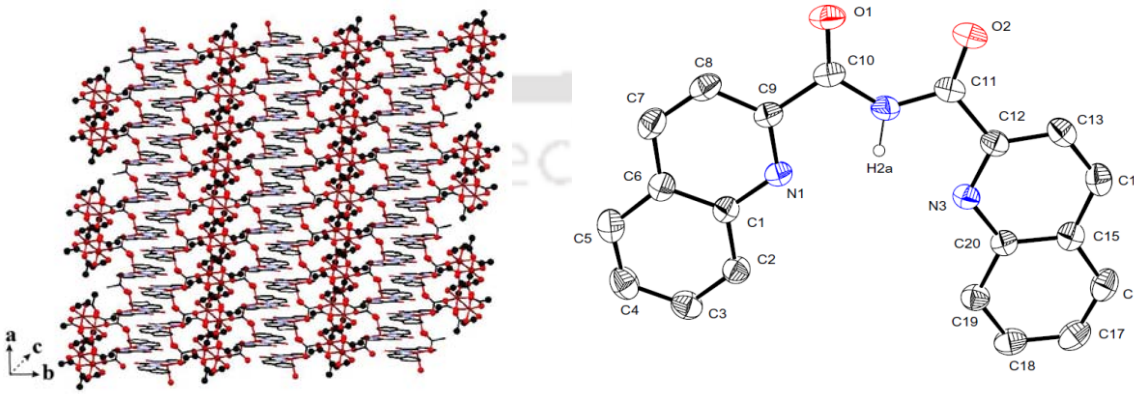

Fig. 9. Packing diagram of **3** (left) on viewing down the *c*-axis and ORTEP diagram (30%) of **L2H** (right) in which hydrogen atoms except H2a are omitted for clarity.

2.3.3 Optical Spectra and Magnetism

Complexes **1**–**3** exhibit a characteristic strong intensity band for the $\nu_{(CO)}$ in the range 1705–1720 cm^{-1} and the free ligands exhibit the same at around 1750 cm^{-1}. The characteristic feature of the electronic spectra of **2** and **3** is the presence of a broad band in the visible region along with a shoulder on to its higher-energy side. These are of *d*–*d* transition in origin, the broad absorption and the shoulder may be arising from the transition $d_{x^2-y^2}$ to d_{z^2} and $d_{x^2-y^2}$ to d_{xy}, respectively. The intra-ligand transitions occur in the 325–240 nm region. The room temperature μ_{eff} values are consistent with the presence of one unpaired electron in **2** and **3a**. The overall value of 1.97 B. M. for the co-crystal **3** may be due the lesser magnetic moments shown by the dimeric copper(II) carboxylates [25]. The EPR spectra of **2** and **3** show the pattern of an axial spectrum (Fig. 10.) with $g_{\|} > g_{\perp} > 2$ signifying that the signals arise from **2** and **3a** and the odd electron being in the $d_{x^2-y^2}$ orbital. This observation also shows the **3b** is EPR silent under these conditions [26].

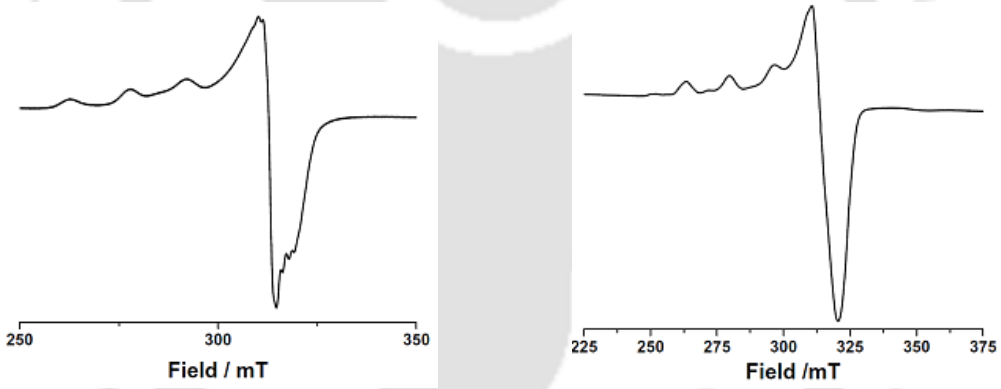

Fig. 10. EPR spectrum of **2** (left) and **3** (right) in MeOH at 77K.

2.4 Conclusion

In summary, in hydrated ethanolic medium 2-(aminomethyl) substituted pyridine and quinoline were converted respectively to bis(2-pyridylcarbonyl)amide and bis(2-quinolylcarbonyl)amide species under mild conditions by stirring with copper(II) acetate. This reaction involve the oxidation of the methylene function as well as the formation of the bond between nitrogen and carbon in N–C(=O) through coupling and also show that the $–CH_2–$ group flanked by pyridyl/quinolyl group can be oxidized under mild conditions. The co-crystals of $[Cu(\mathbf{L3})(OAc)(H_2O)]_3[Cu_2(OAc)_4(EtOH)_2]_{1.5}$ were synthesized by stirring the ethanolic solution of the Schiff base [(2-pyridyl)-N-((2-

quinolyl)methylene)methanamine] (**L1**) and with one equivalent of $Cu(OAc)_2 \cdot H_2O$, which involve the oxidation of both the imine and $–CH_2–$ groups. The free ligands were isolated as crystalline solids from the compounds **1–3** by the extrusion of the Cu^{2+} ion using $EDTA^{2–}$. In both **2** and **3a**, the copper(II) center has a distorted square pyramidal geometry and N_3O_2 coordination environment. The packing diagram of **3** consists of separate layers made up of **3a** and **3b** units that are segregated and commingled alternatively. Compounds having quinolyl group show the presence of π–stacking interactions.

2.5 References

1. E.A. Lewis, W.B. Tolman, Chem. Rev. 104 (2004) 1047–1076.
2. J.M. Rowland, M.M. Olmstead, P.K. Mascharak, Inorg. Chem. 41 (2002) 2754 – 2760.
3. S.K. Padhi, V. Manivannan, Inorg. Chem. 45 (2006) 7994–7996.
4. C. Tejel, M.A. Ciriano, M.P. del Río, F.J. van den Bruele, D.G.H. Hetterscheid, N.T. Spithas. B. de Bruin, J. Am. Chem. Soc. 130 (2008) 5844–5845.
5. C. Tejel, M.A. Ciriano, M.P. del Rio, D.G.H. Hetterscheid, N. . Spithas, J.M.M. Smits, D. de Bruin, Chem. Eur. J. 14 (2008) 10932–10936.
6. E.I. Lerner, S.J. Lippard, J. Am. Chem. Soc. 98 (1976) 5397–5398.
7. E.I. Lerner, S.J. Lippard, Inorg. Chem. 16 (1977) 1546–1551.
8. T. Kajiwara, T. Ito, J. Chem. Soc., Dalton Trans. (1998), 3351–3352.
9. T. Kajiwara T. Ito, Angew. Chem. Int. Ed. 39 (2000) 230–233.
10. A. Kamiyama, T. Noguchi, T. Kajiwara, T. Ito, Angew. Chem., Int. Ed. 39 (2000) 3130–3132.
11. A. Kamiyama, T. Noguchi, T. Kajiwara, T. Ito, Inorg. Chem. 41 (2002)507–512.
12. A. Kamiyama, T. Noguchi, T. Kajiwara, T. Ito, CrystEng Comm. 5 (2003) 231–237.
13. R. Lescouëzec, J. Vaissermann, L.M. Toma, R. Carrasco, F. Lloret, M. Julve, Inorg. Chem. 43 (2004) 2234–2236.
14. T. Kajiwara, M. Nakano, Y. Kaneko, S. Takaishi, T. Ito, M. Yamashita, A. Igashira-Kamiyama, H. Nojiri, Y. Ono, N. Kojima, J. Am. Chem. Soc. 127 (2005) 10150–10151.

15. H.-R. Wen, C.-F. Wang, J.-L. Zuo, Y. Song, X.-R. Zeng, X.-Z. You, Inorg. Chem. 45 (2006) 582–590.
16. A. M. Madalan, K. Bernot, F. Pointillart , M. Andruh, A. Caneschi, Eur. J. Inorg. Chem. (2007) 5533–5540.
17. F. Pointillart, K. Bernot, R. Sessoli, D. Gatteschi, Chem. Eur. J. 13 (2007) 1602-1609.
18. T. Kajiwara, I. Watanabe, Y. Kaneko, S. Takaishi, M. Enomoto, N. Kojima, M. Yamashita, J. Am. Chem. Soc. 129 (2007) 12360–12361.
19. V.K. Fulwa, R. Sahu, H.S. Jena, V. Manivannan, Tetrahedron Lett. 50 (2009) 6264–6267.
20. W.A. Chomitz, S.G. Minasian, A.D. Sutton, A. Arnold, Inorg. Chem. 46 (2007) 7199–7209.
21. J.W. Canary, Y. Wang, R. Roy, L. Que, H. Miyake, Inorg. Synth. 32 (1998) 70–75.
22. M. Barquín, M.J.G. Garmendia, L. Larrínaga, E. Pinilla, M.R. Torres, Inorg. Chim. Acta 362 (2009) 2334–2340.
23. J.V. Folgado, E. Martínez-Tamayo, A. Beltran-Porter, D. Beltrán-Porter, Polyhedron 8 (1989) 1077–1083.
24. A.W. Addison, T.N. Rao, J. Reedijk, J. van Rijn, G.C. Verschor, J. Chem. Soc. Dalton Trans. (1984) 1349–1356.
25. M. Kato, H.B. Jonassen, J.C. Fanning, Chem. Rev. 64 (1964), 99–128.
26. D.P. Dalal, S.S. Eaton, G.R. Eaton, J. Magn. Reson. 42 (1981) 277–286.

Chapter 3

Copper(II) Acetate Mediated Conversion of *Ortho* Aminomethyl Substituted Isoquinolines to Bis(isoquinolylcarbonyl)amides

Abstract

Ethanolic (95%) solutions of *ortho* aminomethyl substituted isoquinolines, on stirring in air with half equivalent of $[Cu(OAc)_2(H_2O)]$, respectively afforded [Cu(**1-L4**)(OAc)] (**1**) and [Cu(**3-L4**)(OAc)] (**2**) {**1-L4** = bis(1-isoquinolylcarbonyl)amide ion and **3-L4** = bis(3-isoquinolylcarbonyl)amide ion}. This novel reaction involves oxidation of methylene group and formation of the bond between nitrogen and carbon in N–C(=O) through coupling. A plausible mechanism for this conversion has been proposed. The free ligands can be isolated as crystalline solids from the compounds **1–2**, by extrusion of the Cu^{2+} ion using $EDTA^{2-}$. The molecular structure of $[Cu(\mathbf{1\text{-}L4})(OAc)]\cdot 2.5H_2O$ has been established using single crystal X-ray diffraction studies. The copper(II) center has pseudo square-planar N_3O environment and has a distorted geometry. Packing diagram shows the existence of a centrosymmetric dimer in which two copper centers are intermolecularly linked by the O2 atom of the amide function leading to a diamond shaped Cu_2O_2 core. The aromatic groups form the hydrophobic layers and water molecules are amalgamated between these hydrophobic layers but are further confined into the channel with methyl group of acetate ion serving as the separator. The water molecules exist as two tetrameric and a nanomeric clusters.

3.1 Introduction

Oxidation of alkyl and aromatic substrates is an important quest for synthetic chemists. In this aspect, role of copper containing enzymes and their model complexes has been reviewed [1]. There are few reports on oxidation of the $–CH_2–$ group flanked by a 2-pyridyl and an amide or imine function in presence of a suitable metal ion [2,3]. In another case, a methylene group flanked by 2-pyridyl and an amine undergoes deprotonation on coordination to Rh(-I, I) dimer and Ir(I) centers [4,5]. In Chapter-2, it has been demonstrated that an unprecedented formation of bis(carbonyl)amides from 2-aminomethyl substituted pyridine and quinoline, using copper(II) acetate is achievable [6]. This has prompted to explore the applicability of this novel method to other substrates and in this Chapter, a ready conversion of *ortho* aminomethyl substituted isoquinolines to their bis(isoquinolylcarbonyl)amides has been described.

3.2 Experimental Section

3.2.1 Syntheses

Isoquinoline-N-oxide: To an ice-cold (0–5 °C) solution of isoquinoline (5.0 g, 38.7 mmol) in $CHCl_3$ (200 mL) was added solid MCPBA (11.3 g, 65.8 mmol) and stirred for 4 days at room temperature. The reaction mixture was washed with a 5% solution of K_2CO_3 (6 × 60 mL), organic layer was dried over sodium sulfate and concentrated under reduced pressure. The desired product was isolated as a crystalline solid. Yield: 5.0 g, 89%. IR (KBr, cm^{-1}): 1645(s), 1603(s), 1573(s), 1499(s), 1456(s), 1424(m), 1383(m), 1332(s), 1302(s), 1275(s), 1255(s), 1206(s), 1171(vs), 1127(s), 981(w), 912(m), 868(m), 820(s), 748(s), 736(s), 629(m), 534(m), 494(m), 471(m). 400 MHz ^{1}H NMR (δ (*J*, Hz), $CDCl_3$), **Fig. 1**: 7.614–7.633 (2H, m), 7.696 (1H, d, 6.8), 7.755 (1H, d, 7.2), 7.812 (1H, d, 8.8), 8.167 (1H, d, 8.4), 8.812 (1H, s).

Isoquinoline–1–carbonitrile: To isoquinoline–N–oxide (2.0 g, 13.8 mmol) in dry CH_2Cl_2 (30 mL), were added trimethylsilylcyanide (1.5 g, 15.1 mmol) and dimethylcarbamyl chloride (1.5 g, 13.9 mmol). After stirring the reaction mixture for 3 days at room temperature, a 10% aqueous K_2CO_3 (20 mL) was added and stirred for further 15 min. The organic phase was separated and the aqueous layer was extracted

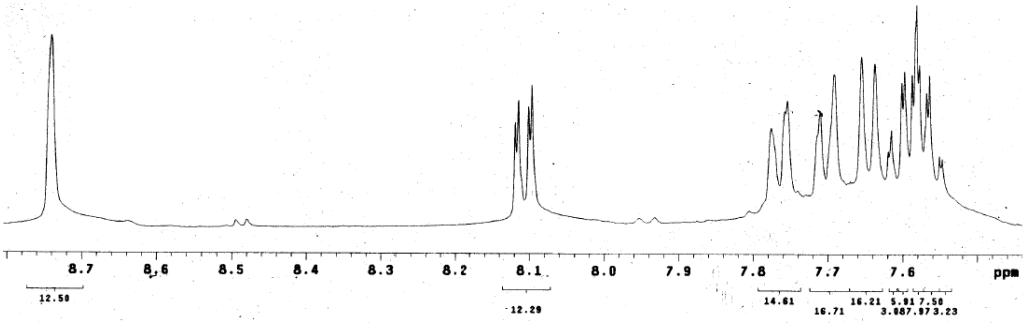

Fig. 1. ^{1}H NMR spectrum of isoquinoline-N-oxide.

twice with CH_2Cl_2 (2 × 30 mL). The combined organic phase was dried over anhydrous Na_2SO_4 and the solvent was evaporated. Yield: 2.0 g, 94%. IR (KBr, cm^{-1}): 2228(s), 1637(s), 1622(s), 1580(m), 1552(m), 1492(m), 1455(m), 1389(s), 1344(m), 1322 (w), 1297(w), 1226(w), 1198(w), 1032(m), 877(s), 838(s), 788(m), 746(s), 695(w), 660(m), 539(m), 464(m). 400 MHz ^{1}H NMR (δ (*J*, Hz), $CDCl_3$), **Fig. 2**: 7.718 (2H, t, 7.6), 7.855 (1H, d, 5.2), 7.911 (1H, d, 8.0), 8.168 (1H, d, 8.4), 8.333 (1H, d, 8.4).

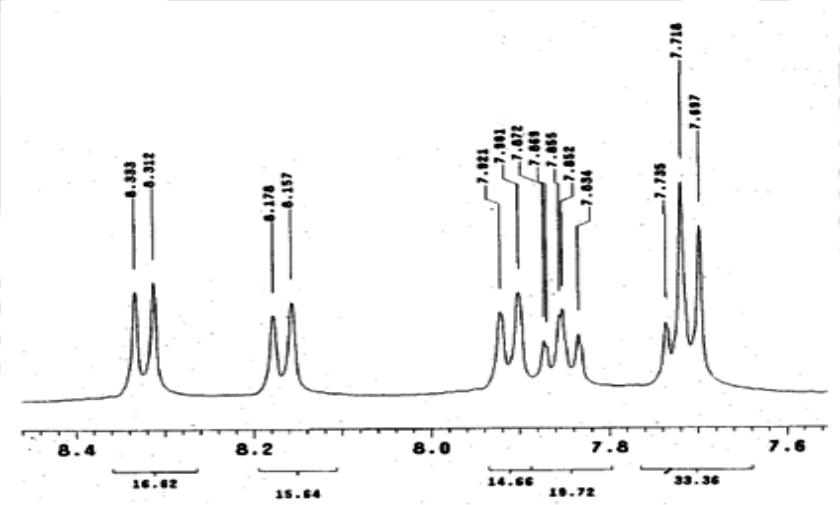

Fig. 2. ^{1}H NMR spectrum of isoquinoline–1–carbonitrile.

1–Aminomethylisoquinoline (1-ami): A solution of isoquinoline-1-carbonitrile (2.0 g, 13.0 mmol) in acetic acid (120 mL) was kept at 2 atm. of dihydrogen at room temperature in the presence of 10% palladium on carbon (0.40 g) in a hydrogenation apparatus for about 4 h. The reaction mixture was then filtered and the solution was evaporated under reduced pressure. The oily residue was dissolved in dichloromethane, washed to alkaline pH with a 10% aqueous NaOH. The organic phase was dried over Na_2SO_4, the solvent was

evaporated and **1–ami** was isolated as a reddish solid. Yield: 1.9 g, 92%. IR (KBr, cm^{-1}): 3425(b), 1681(s), 1622(s), 1584(s), 1558(s), 1502(s), 1446(s), 1378(s), 1314(s), 1258(m), 1188(m), 1142(s), 1107(s), 1008(m), 956(m), 870(m), 827(s), 800(m), 746(s), 665(w), 634(w), 617(w), 593(w), 528(w), 503(w), 464(m), 439(w). 400 MHz ^{1}H NMR (δ (*J*, Hz), $CDCl_3$), **Fig. 3**: 2.351 (NH_2, s), 4.543 (CH_2, s), 7.577(1H, d, 5.2), 7.626 (1H, t, 7.8), 7.705 (1H, t, 7.4), 7.852 (1H, d, 8.4), 8.108 (1H, d, 8.8), 8.468 (1H, d, 5.6).

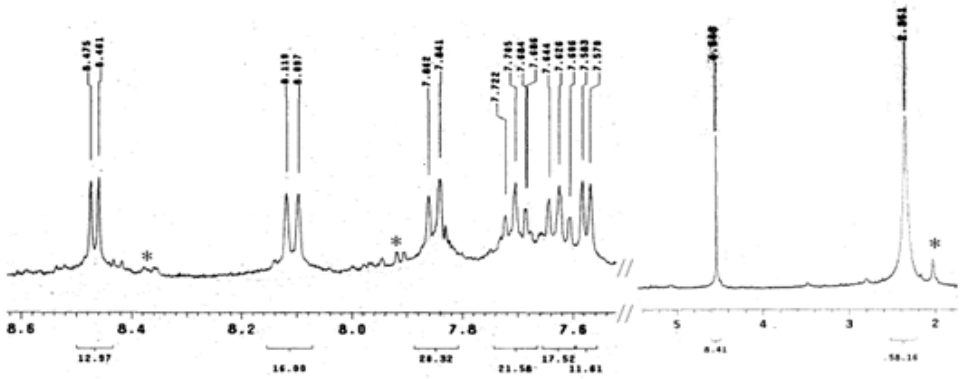

Fig. 3. ^{1}H NMR spectrum of 1–aminomethylisoquinoline. Peaks marked * are due to impurity.

3–Aminomethylisoquinoline (**3-ami**)**:** A solution of isoquinoline-3-carbonitrile (1.0 g, 6.5 mmol) in acetic acid (60 mL) was kept at 2 atm of dihydrogen at room temperature in the presence of 10% palladium on carbon (0.20 g) in a hydrogenation apparatus for about 4 h. The reaction mixture was then filtered and the solution was evaporated under reduced pressure. The oily residue was dissolved in dichloromethane, washed to alkaline pH with a 10% aqueous NaOH. The organic phase was dried over Na_2SO_4, the solvent was evaporated and **3–ami** was isolated as a reddish solid. Yield: 0.925 g, 90%. IR (KBr, cm^{-1}): 3282(b), 1630(s), 1593(s), 1584(s), 1558(s), 1502(s), 1493(s), 1439(s), 1387(s), 1345(s), 1327(s), 1262(s), 1196(w), 1124(m), 1091(s),1064(s), 1028(s), 957(s), 870(m), 881(s), 801(s), 751(s), 628(w), 488(w), 470(m). 400 MHz ^{1}H NMR (δ (*J*, Hz), $CDCl_3$), **Fig. 4**: 2.772 (NH_2, s), 4.013 (CH_2, s), 7.440-7.601 (3H, m), 7.673 (1H, d, 8.0), 7.830 (1H, d, 8.4), 9.092 (1H, d, 11.2).

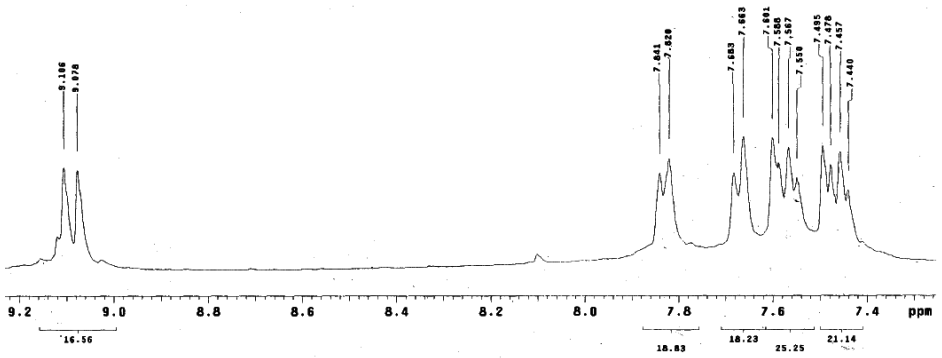

Fig. 4. ^{1}H NMR spectrum of 3–aminomethylisoquinoline.

[Cu(1-L4)(OAc)] (1): To $Cu(OAc)_2 \cdot H_2O$ (0.250 g, 1.25 mmol) dissolved in ethanol (80 mL) was added **1–ami** (0.396 g, 2.50 mmol) and stirred for 24 h with occasional purging of air. The solution was left undisturbed, green precipitate deposited after two weeks of standing, were collected and washed with ice-cold ethanol. Yield 0.380 g, 67%. IR (KBr, cm^{-1}): 1708(s), 1618(s), 1586(s), 1555(s), 1500(m), 1450(m), 1408(s), 1359(m), 1312(s), 1228(w), 1163(m), 1101(w), 1048(w), 1020(m), 929(w), 881(m), 834(m), 817(m), 763(m), 746(m), 710(w), 672(w), 636(m), 591(w), 518(w), 473(m), 288(w). [λ_{max}, nm(ε, $M^{-1}cm^{-1}$), DMF solution]: 710 (147), 373 (16975), 326 (29020). EPR (CH_3OH solution, 77 K): $g_{\|}$ = 2.169, $A_{\|}$ = 85 G; $g_{\perp}$ = 2.029. μ_{eff} (polycrystalline, 25 ºC) = 2.30 B. M. ESI-MS (**Fig. 5.**): *m*/*z* calcd. for $[^{63}Cu(\mathbf{1\text{-}L4})]^{+}$ 389.0226, Found 389.0224. Violet crystals of composition $\mathbf{1} \cdot 2.5H_2O$ were obtained by slow evaporation of methanol solution of **1**.

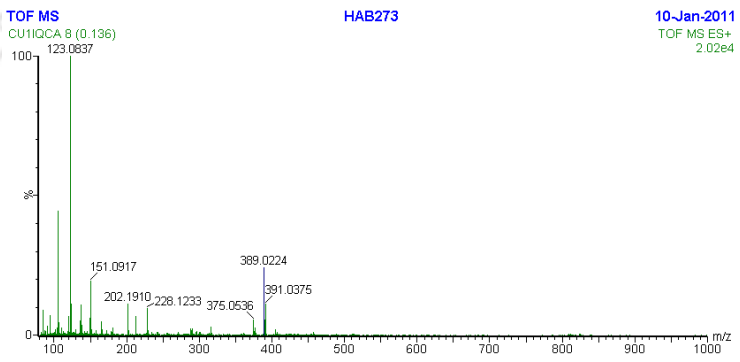

Fig. 5. ESI-MS of **1**.

[Cu(3-L4)(OAc)] (2): To $Cu(OAc)_2 \cdot H_2O$ (0.250 g, 1.25 mmol) dissolved in ethanol (50 mL) was added **3–ami** (0.396 g, 2.50 mmol) and stirred for 24 h with occasional purging

of air. The solution was left undisturbed, green precipitate of **2** deposited after a week were collected, washed with ice-cold ethanol and dried in *vacuo* over P_2O_5. Yield: 0.360 g, 65%. IR (KBr, cm^{-1}): 1701(s), 1613(s), 1578(s), 1494(w), 1460(s), 1390(m), 1332(s), 1313(s), 1254(m), 1149(w), 1111(w), 1052(w), 1018(w), 980(m), 912(m), 802(m), 786(w), 775(w), 747(m), 688(m), 651(w), 621(w), 588(w), 541(m), 498(w), 469(m), 371(w). [λ_{max}, nm(ε, $M^{-1}cm^{-1}$), MeOH solution]: 700 (126), 400(7455), 365(16280), 336 (22400). EPR (DMF solution, 77 K): $g_{\|}$ = 2.164, $A_{\|}$ = 80 G; $g_{\perp}$ = 2.016. μ_{eff} (polycrystalline, 25 ºC) = 2.31 B. M. ESI-MS (**Fig. 6**): *m/z* calcd. for $[^{63}Cu(\mathbf{3\text{-}L4})]^+$ 389.0226, Found 389.0223.

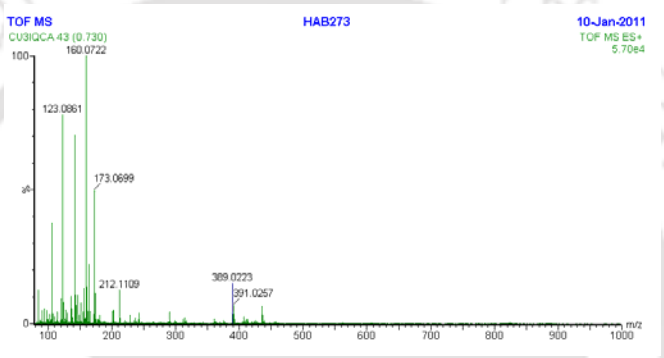

Fig. 6. ESI-MS of **1**.

Bis(1-Isoquinolylcarbonyl)amide (1-L4H): The complex **1** (1.0 g, 2.02 mmol) and Na_2EDTA (1.50 g, 4.04 mmol) were dissolved in H_2O (50 mL) and stirred vigorously with 50 mL of $CHCl_3$, for 2 h. The $CHCl_3$ layer was separated, the aqueous layer was washed with $CHCl_3$ (2 × 30 mL) and the combined $CHCl_3$ solution was dried with anhydrous Na_2SO_4. After removal of the solvent, **1-L4H** was obtained as yellow solid. Yield: 0.60 g, 91%. IR (KBr, cm^{-1}): 1745(s), 1636(s), 1583(m), 1556(m), 1446(s), 1419(m), 1379(m), 1340(w), 1307(m), 1260(w), 1230(w), 1145(w), 1106(w), 1082(w), 1040(w), 1021(w), 913(w), 877(m), 831(m), 799(m), 746(m), 710(w), 640(w), 621(m), 511(w), 466(w). ESI-MS (**Fig. 7.**): *m/z* calcd. for $C_{20}H_{13}N_3O_2$ 327.1041, found (M^+–H) 328.1042 400 MHz ^1H NMR (δ (*J*, Hz), $CDCl_3$), **Fig. 7.**: 7.754-7.779 (2H, m), 7.887-7.937 (2H, m), 8.671 (1H, d, 5.6), 9.638-9.663 (1H, m), 13.537 (NH, s). Anal Calcd. for $C_{20}H_{13}N_3O_2$ (327.34): C 73.38, H 4.00, N 12.84. Found: C 73.31, H 3.98, N 12.80.

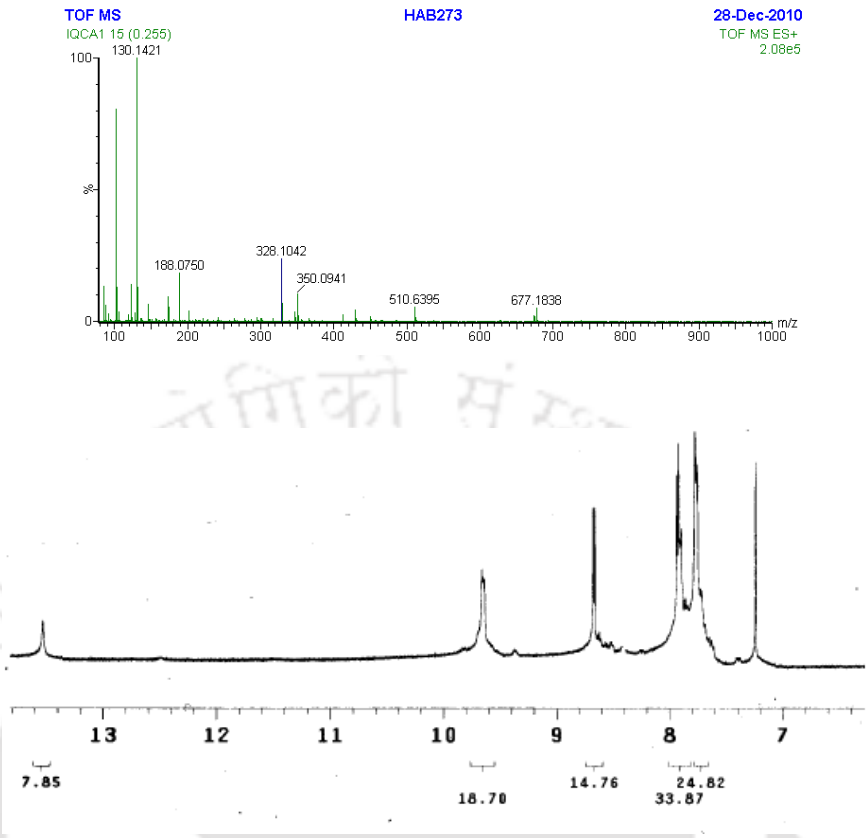

Fig. 7. ESI-MS (above) and ^{1}H NMR Spectra of **1**.

3.3 Results and Discussion

3.3.1 Syntheses

It has been demonstrated in Chapter 2 that 2-aminomethyl substituted pyridine and quinoline were readily converted to the respective bis(carbonyl)amides. In order to test the applicability of this reaction with other *ortho*-aminomethyl containing simple nitrogen heterocycles, 1–aminomethylisoquinoline (**1-ami**) and 3–aminomethylisoquinoline (**3-ami**) were chosen for the scrutiny. Following synthetic methodology [7] was adopted for the synthesis of **1-ami**. In the first step, isoquinoline was converted to isoquinoline-*N*-oxide using *meta*-chloroperbenzoic acid in chloroform. Cyano group was introduced at the 1-position of the isoquinoline nucleus, using trimethylsilylcyanide in the presence of dimethylcarbamylchloride. This method offered 1-cyanoisoquinoline from isoquinoline-*N*-oxide in good yields. 1-Cyanoisoquinoline was then converted to **1-ami** by reduction with molecular hydrogen in the presence Pd/C catalyst in acetic acid. Commercially available 3-

cyanoisoquinoline was converted to **3-ami** in the similar manner by reduction with molecular hydrogen in the presence Pd/C catalyst in acetic acid.

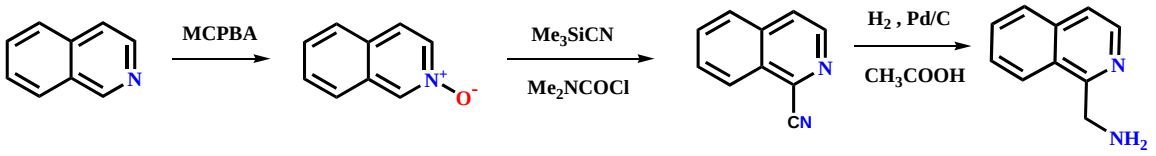

Ethanolic solution of **1-ami** on stirring with half equivalent of $[Cu(OAc)_2(H_2O)]$ in air generated a green solution which on standing deposited green precipitate of composition [Cu(**1-L4**)(OAc)] (**1**) in good yields as shown in Scheme 1.

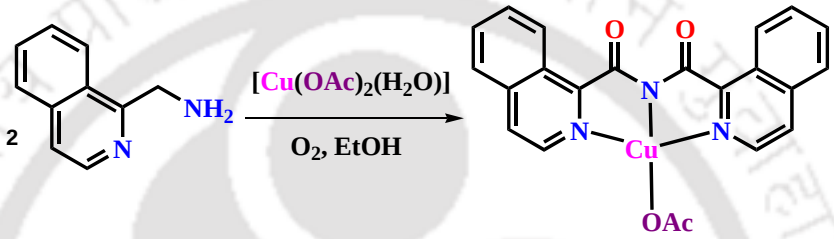

Scheme 1. Synthesis of **1** from **1-ami**.

The free ligand **1-L4H** was isolated as yellow crystalline solid from the compound **1**, by the extrusion of the Cu^{2+} ion using Na_2EDTA, as shown in Scheme 2.

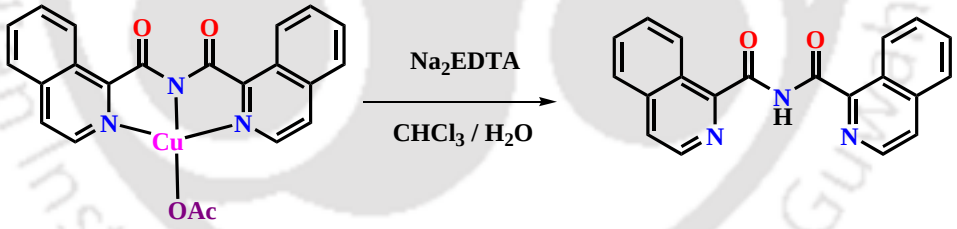

Scheme 2. Extrusion of **1-L4H** from **1**.

Similarly, **3-ami** also reacted with copper(II) acetate affording the [Cu(**3-L4**)(OAc)] (**2**) {**3-L4** = bis(3-isoquinolylcarbonyl)amide ion} in similar yields.

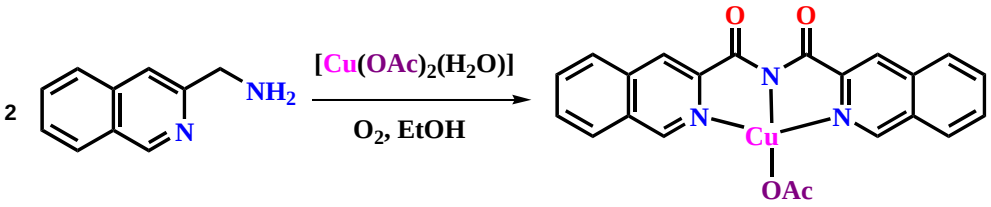

Scheme 3. Synthesis of **2** from **3-ami**.

The mechanism similar to that described in Chapter 2 for the formation of bis(2-pyridylcarbonyl)amide from picolylamine, could be operating for the 1-aminomethylisoquinoline. Hence, a plausible mechanism for the conversion is shown in Scheme 4. One molecule of **1-ami** coordinate at each copper atom with retention of the dicopper(II) center to form the complex **I**. Upon coordination of **1-ami**, oxidation of the methylene group could occur leading to an amide intermediate **II**. Coordination of another molecule of **1-ami** at both the copper atoms in the intermediate **II**, by replacing the acetate ion, through the pyridine nitrogen atom with a pendent *ortho*-aminomethyl group will lead to complex **III**. Due to binding of the amide function through the nitrogen atom to the copper atom, the carbonyl carbon is now electrophilic in character due to loss of its conjugation with the lone-pair on $–NH_2$ group. Hence carbon atom can be attacked by pendent *ortho*-aminomethyl group, forming the intermediate **IV** that contains tetrahedral carbon centers. Elimination of ammonia from tetrahedral carbon and subsequent collapse of the dicopper core to intermediate **V** having the *N*-(1-isoquinolyl)isoquinolinamide moiety. Oxidation of the intermediate **V** leads to the final product **1** containing the copper(II) complex of bis(1-isoquinolylcarbonyl)amide ion, which was also observed in a related case [3]. This proposed mechanism retains the dicopper core, because mononuclear copper(II) salts do not show the observed conversion [8-10]. Also since a related 2-(aminomethyl)pyridine in acetonitrile yield simple coordination product [10], probably ethanol plays a crucial role in retaining the dicopper core till formation of intermediate **IV**. It has also been previously observed that bis(2-picolyl)amine yields simple coordinated complex and did not show oxidation of methylene group under same [6] and other conditions [11], hence rules out the involvement of bis(1-isoquinolyl)amine as a possible intermediate.

3.3.2 Molecular Structure

The molecular structure of **1**·2.5H_2O has been established using single crystal X-ray diffraction method. The complex crystallized in *P*–1 space group (Table 1) and the asymmetric unit contains [Cu(**1-L4**)(OAc)] and water molecules of crystallization. The copper(II) center has pseudo square-planar N_3O environment and has a distorted geometry. The two chelate bite angles have a value of 81. 5(1) and 81.9(1)°, while the two non-

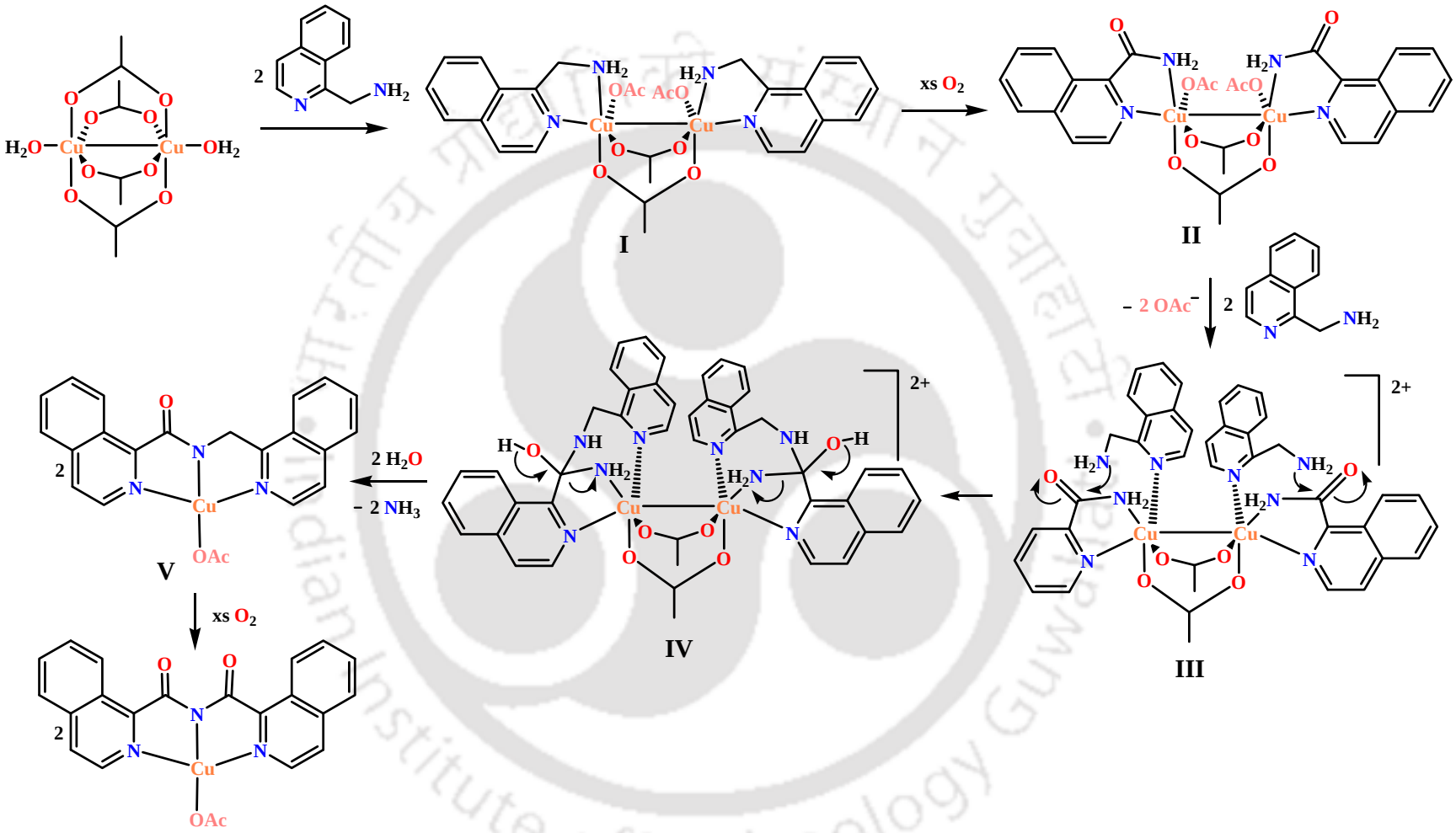

Scheme 4. A plausible mechanism.

Table 1. Crystallographic Data for **1**·2.5H_2O.

	1·2.5H_2O
Formula	$C_{22}H_{20}N_3O_{6.5}Cu$
Formula weight	493.96
T, K	293(2)
Cryst syst	Triclinic
Space group	*P*-1
a, Å	10.5812(7)
b, Å	11.0568(7)
c, Å	11.3189(8)
α, deg	80.081(4)
β, deg	66.806(4)
γ, deg	78.244(4)
V, Å^3	1185.44(14)
Z	2
D_{calcd}, gcm^{-3}	1.482
μ, mm^{-1}	0.977
GOF[a] on F^2	1.054
R[I > 2σ(I)]	[b]R_1 = 0.0532; [c]wR_2 = 0.1560
Rindices (all data)	[b]R_1 = 0.0690; [c]wR_2 = 0.1689

[a] GOF = $[\sum[w(F_0^2 - F_c^2)^2] / M - N]^{1/2}$ (M =number of reflections, N = number of parameters refined).
[b] $R_1 = \sum \| F_0 | - | Fc \| / \sum | F_0 |$.
[c] $wR_2 = [\sum[w(F_0^2 - F_c^2)^2] / \sum[w(F_0^2)^2]]^{1/2}$.

chelated *cis* angles are 97.9(1) and 98.7(1)°. The two *trans* angles are N1–Cu1–N3, 163.4(1) and N2–Cu1–O3, 179.2(1)°. The Cu–N_Q (N_Q = isoquinolyl-N and N_A = amide-N) distances are longer by 0.085(3) and 0.066(3) Å than Cu–N_A and Cu–O distances, respectively. The ORTEP diagram of the complex is shown in Fig. 8.

In the packing diagram the complex exists as a centrosymmetric dimer in which two copper centers being intermolecularly linked by the O2 atom of the amide function. As a result a diamond shaped Cu_2O_2 core is present with the Cu1–O2 contact having a length of

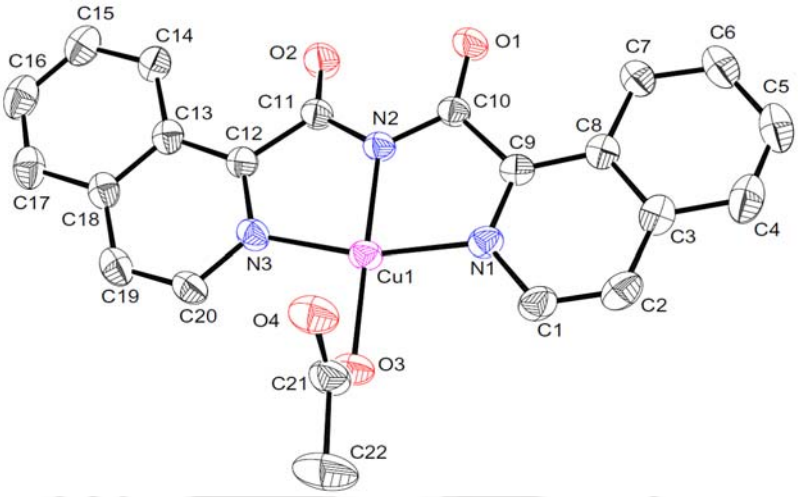

Fig. 8. ORTEP (30% probability ellipsoids) digram of **1**.

2.753(3) Å. In this core, the non-bonded Cu···Cu, O2···O2 and O2···Cu distances respectively are 5.1218(5), 4.528(3) and 3.973(2) Å. The angles subtended at Cu1 and O2 respectively are 82.5(1)° and 97.5(1)°. As a result of O2 linking, the C11 and O2 atoms of the amide function deviate respectively by 0.18 and 0.64 Å, from the plane containing the atoms O1C10N2C12. A perspective view of the dimer is shown in Fig. 9.

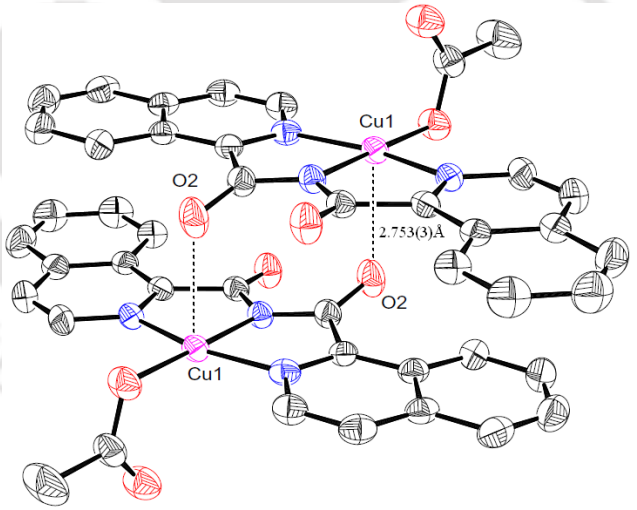

Fig. 9. ORTEP (30%) diagram depicting dimer containing diamond shaped Cu_2O_2 core.

Also π···π interaction between quinolyl rings is present with a distance of 3.57 Å between the centroids formed by N1C1C2C3C8C9 and C13C14C15C16C1718 atoms. Aromatic rings of the complex form the hydrophobic layers and water molecules are amalgamated between these layers. The water molecules are further confined into a channel in which

methyl group of acetate ion serving as a separator of the layers containing water molecules. The water molecules are present as two separate tetramers O7···(O5, O6, O9) and O9···(O7, O10, O10) and a nonamer O6···O5···O7···O6(···O5)···O10(O9, O9, O10). These water clusters are linked to the complex molecule through hydrogen bonds with carbonyl oxygen atom O1 through O6···O1, 2.88(1) Å as well as to acetate oxygen atom O4, through O4···O5, 2.83(1) Å and O4···O9, 2.77(1) Å non-bonded interactions. A perspective view of the packing diagram is shown in Fig. 10.

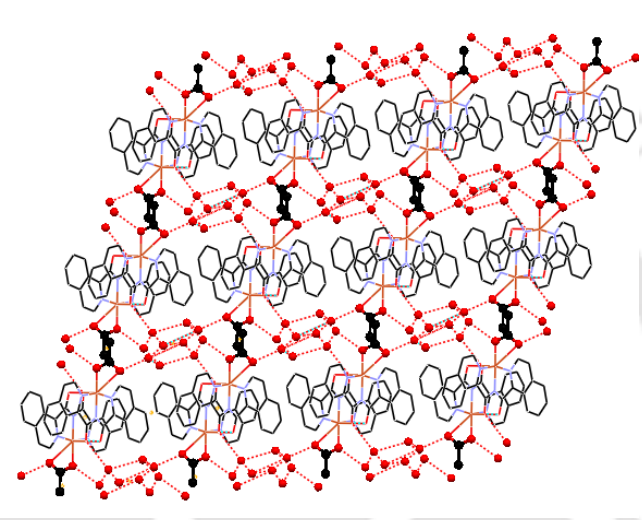

Fig. 10. Packing diagram of **1** on viewing down the *b*-axis.

3.3.3 Optical Spectra and Magnetism

The IR spectrum of **1** (Fig. 11), show a characteristic 1708 cm^{-1} peak for ν_{CO}, which shifts to 1745 cm^{-1} in free **1-L4H**, and **2** shows the same at 1701 cm^{-1}. The ESI-MS mass spectra of **1** exhibit m/z = 389.0224 (calcd. 389.0226) that can be assigned to $[^{63}Cu(\mathbf{1\text{-}L4})]^+$ fragment. In case of **2** peaks at m/z = 389.0223 corresponding to $[^{63}Cu(\mathbf{3\text{-}L4})]^+$ fragment was observed. Free **1-L4H** show m/z = 328.1042 peak ESI-MS for $\mathbf{L4}H_2^+$ fragment. TGA profiles of **1**, **1**·2.5H_2O and **2** are consistent with the anhydrous or observed hydration levels. Room temperature magnetic moment of **1** and **2** are ~2.30 B. M. for being assigned as a one electron paramagnet. EPR spectra of both complexes in frozen solution (77 K) exhibit a typical axial spectrum with $g_{\|} > g_{\perp}$ consistent with b_1^1 ground electronic configuration for Cu^{2+} ion (Fig. 12).

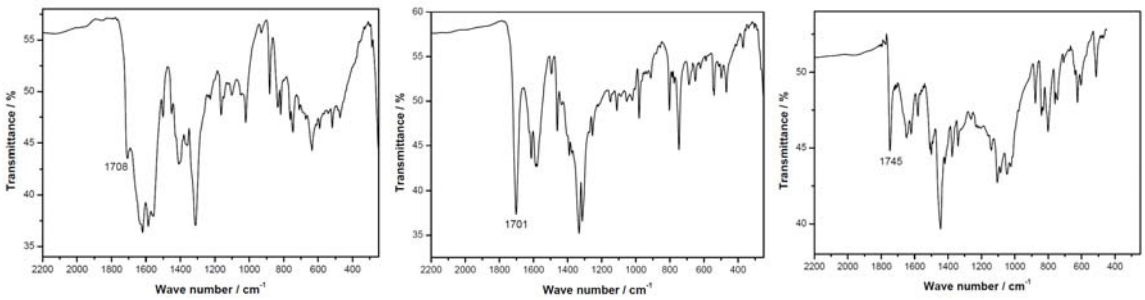

Fig. 11. IR Spectra of **1** (left), **2** (middle) and **1-L4H** (right).

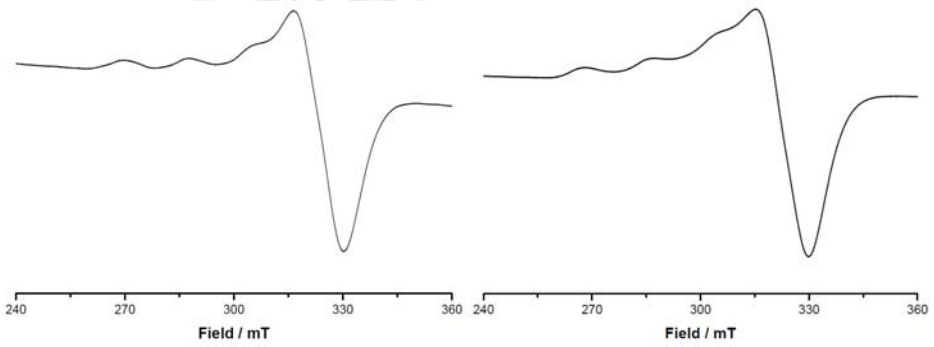

Fig. 12. EPR Spectra of **1** (left) and **2** (right) in frozen DMF solution (77 K).

3.4 Conclusion

In conclusion, o*rtho* aminomethyl substituted isoquinolines readily form respective bis(isoquinolylcarbonyl)amide complexes on treating with $[Cu(OAc)_2(H_2O)]$ in air and in hydrated ethanol. This reaction involves oxidation of the methylene group and formation of the bond between nitrogen and carbon in N–C(=O) through coupling. Determination of molecular structure of **1**·2.5H_2O confirmed the presence of bis(1-isoquinolylcarbonyl)amide complex of copper(II) ion. Other spectroscopic evidence corroborates the observed conversion. The copper(II) center has pseudo square-planar N_3O environment and has a distorted geometry. Packing diagram shows the existence of a centrosymmetric dimer in which two copper centers are intermolecularly linked by the O2 atom of the amide function leading to result a diamond shaped Cu_2O_2 core. The water molecules exist as two tetrameric and a nanomeric clusters. With this result we believe that a *ortho* aminomethyl substituted pyridine nucleus having alkyl/aryl substituents or having fused aromatic/carbocyclic ring can be converted to respective bis(carbonyl)amides using copper(II) acetate in ethanol and in presence of molecular oxygen.

3.5 References

1. E.A. Lewis, W.B. Tolman, Chem. Rev. 104 (2004) 1047–1076.
2. J.M. Rowland, M.M. Olmstead, P.K. Mascharak, Inorg. Chem. 41 (2002) 2754–2760.
3. S.K. Padhi, V. Manivannan, Inorg. Chem. 45 (2006) 7994–7996.
4. C. Tejel, M.A. Ciriano, M.P. del Río, F.J. van den Bruele, D.G.H. Hetterscheid, N.T. Spithas. B. de Bruin, J. Am. Chem. Soc. 130 (2008) 5844–5845.
5. C. Tejel, M.A. Ciriano, M.P. del Rio, D.G.H. Hetterscheid, N.T. Spithas, J.M.M. Smits, D. de Bruin, Chem. Eur. J. 14 (2008) 10932–10936.
6. R. Sahu, S.K. Padhi, H.S. Jena, V. Manivannan, Inorg. Chim. Acta 363 (2010) 1448–1454.
7. W. Baratta, M. Ballico, S. Baldino, G. Chelucci, E. Herdtweck, K. Siega, S. Magnolia, P. Rigo, Chem. Eur. J. 14 (2008) 9148–9160.
8. H. M. Helis, W. H. Goodman, R. B. Wilson, J. A. Morgan, D. J. Hodgson, Inorg. Chem. 16(1977) 2412–2416.
9. C. J. O'Connor, E. E. Eduok, F. R. Fronczek, O. Kahn, Inorg. Chim. Acta 105 (1985) 107–113.
10. M. Barquín, M. J. G. Garmendia, L. Larrínaga, E. Pinilla, M. R. Torres, Inorg. Chim. Acta 362 (2009) 2334–2340.
11. M. Palaniandavar, S. Mahadevan, M. Kockerling, G. Henkel, Dalton (2000) 1151–1154.

Chapter 4

Syntheses and Molecular Structures of Co^{3+}–Na^{+} And Co^{3+}–K^{+} Coordination Polymers Constructed Using Mono- and Bis-Chelated Cobalt(III) Complexes of Bis(2-Pyridylcarbonyl)Amide Ion*

Abstract

Four new hetero-bimetallic Co^{3+}–Na^{+} and Co^{3+}–K^{+} coordination polymers having the molecular formulae $[Na(H_2O)Co(\mathbf{L1})(N_3)_3]_n$ (**1**), $[Na_2Co(\mathbf{L1})(N_3)_3(H_2O)_5][Co(\mathbf{L1})(N_3)_3]$ (**2**), $K[Co(\mathbf{L1})(NCS)_3]\cdot H_2O$ (**3**) and $K[Co(\mathbf{L1})_2][Co(NCS)_4]\cdot 0.5H_2O$ (**4**), {**L1** = bis(2-pyridylcarbonyl)amide ion} were synthesized. Compounds **1–4** were characterized by single crystal X-ray diffraction, IR, UV-Vis, and thermogravimetric methods. These bimetallic systems have EE, EO azide bridge (in **1**, **2**) as well as bent (in **1**, **2**, **3**) and linear (in **1**, **4**) aquo bridges. Important features observed among them were: a Z–shaped and diamond–shaped Co_2Na_2 clusters in **1**, a centrosymmetric double–ladder like polymer based on Na_4 cluster in **2**, and a linear KOK core having paddle–wheel structure in **4**.

---

*This work has been published in

R. Sahu, V. Manivannan, *Inorg. Chim. Acta* **2010**, *363*, 4008–4016.

4.1 Introduction

Synthesis and structural elucidation of coordination polymers [1–3] continue to attract attention due to their potential applications in diverse areas that include catalysis [4, 5], chirality [6, 7], luminescence [8], magnetism [9–13] and porous materials [14–17]. Synthesis and applications of such polymers depends on nature of the metal ion and bridging ligand. One such bridging ligand is bis(2-pyridylcarbonyl)amide ion (**L1**) and its mono-chelated metal complexes have been used as motifs for the synthesis and magnetic evaluations of mixed valent $Fe^{II}Fe_2^{III}$ (S = 3/2), $Fe_3^{II}Fe_4^{III}$ (S = 12/2) clusters [18], Cu(II) 1D-chains [19] as well as DFT calculations [20]. The structural and magnetic characteristics of mixed-metal trinuclear complexes [21–23], linear-chains [24–27], honeycombs [28, 29], 3d-4f species [30–32] synthesized using transition metal bis-chelates have been reported.

The deprotonated tridentate ligand **L1** usually coordinate through the three nitrogen atoms to the metal ion in meridional fashion. This leaves the two carbonyl oxygen atoms for further coordination to other metal ions leading to formation of weakly linked polynuclear entities. Such coordination can be in the following modes: (a) bidentate chelate having a six-membered ring (b) each oxygen atom being linked to one metal atom $\mu_{1,1}$ (c) one oxygen atom being linked to one metal atom and the other oxygen to two metal atoms and (d) both oxygen atoms being linked to two metal atoms. These coordination modes shown in Scheme 1 can be utilized for the construction of coordination polymers in conjunction with co-ligands and in this Chapter the structural characterization of Co^{3+}–Na^+ and Co^{3+}–K^+ polymers were described. These polymers exhibit the presence of Z and diamond shaped Co_2Na_2 clusters, a centrosymmetric double ladder like polymer based on Na_4 cluster, and a linear KOK core having paddle-wheel structure.

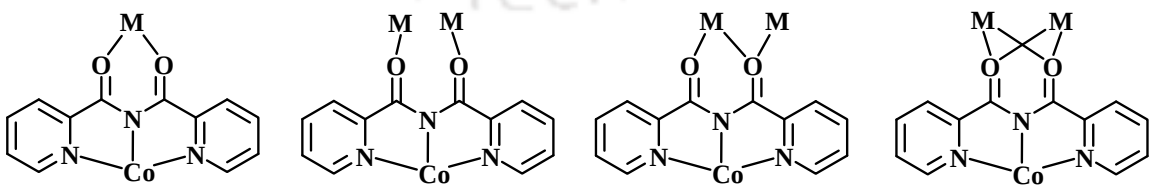

Scheme 1. Coordination modes of chelated **L1**.

4.2 Experimental Section

The ligand **L1H** was prepared using the procedure reported in chapter 2 [33].

4.2.1 Syntheses

$Na[Co(L1)(N_3)_3]\cdot H_2O$ (1): Methanolic solution (40 mL) of $CoCl_2\cdot 6H_2O$ (50 mg, 0.2 mmol), NaN_3 (40 mg, 0.60 mmol) was stirred for 10 minutes and then solid **L1H** (45 mg, 0.2 mmol) was added and stirred for another 6 h. The reaction mixture was allowed to evaporate to dryness at ambient temperature, the contents were dissolved in acetonitrile, filtered to remove the brown residue and the green solution was left undisturbed from which green hexagonal prismatic crystals deposited after a week. Yield: 27 mg (28%). Anal Calcd. for **1**: C 31.87, H 2.23, N 37.17 %. Found: C 31.76, H 2.26, N 37.10 %. IR (KBr, cm^{-1}) **Fig. 1**.: 3480(s), 2073(s), 2032(s),1710(s), 1625(m), 1603(m), 1470(w), 1447(w), 1376(w), 1343(s), 1294(w), 1279(w), 1157(w), 1095(w), 1052(w), 808(w), 763(m), 704(m), 631(m), 589(w), 503(w), 455(m), 457(w), 410(m).

$[Na_2Co(L1)(N_3)_3(H_2O)_5][Co(L1)(N_3)_3]$ (2): To the solution of **L1H** (42 mg, 0.18 mmol) and phenylacetylene (62 mg, 0.6 mmol) in methanol (50 mL), $CoCl_2\cdot 6H_2O$ (43 mg, 0.18 mmol) and NaN_3 (40 mg, 0.61mmol) were added and the mixture was stirred for 6 h. The reaction mixture was allowed to evaporate to dryness at ambient temperature, the content was dissolved in acetonitrile and was filtered to remove the brown gummy residue. The green solution was left undisturbed from which green parallelepiped crystals deposited after a week. Yield: 20 mg (22%). Anal Calcd. for **2**: C 30.07, H 2.73, N 35.07%. Found: C 30.01, H 2.66, N 34.92 %. IR (KBr, cm^{-1}) **Fig. 1**.: 3445(s), 2060(s), 2021(s), 1710(s), 1600(s), 1467(w), 1441(w),1383(s), 1350(s), 1293 (m), 1095(w), 1053 (w), 1030(w), 769 (m), 704 (m), 630 (m).

$K[Co(L1)(NCS)_3]\cdot H_2O$ (3): Blue blocks of **3** was prepared by following the procedure described for **2** by using KSCN (76mg 0.7 mmol) instead of NaN_3. Yield: 20 mg (20%). Anal Calcd. for **3**: C 34.88, H 1.95, N 16.27%. Found: C 34.76, H 1.91, N 16.21 %. IR (KBr, cm^{-1}) **Fig. 1**.: 3418(s), 2113(s), 2071(s), 1719(s), 1634(s), 1603(s), 1472(w), 1445(m), 1371(m), 1336(s), 1296(s), 1258(m), 1153(w), 1095(m), 1053(m), 1027(w), 829(w), 803(w), 768(s), 752(m), 698(s), 629(s), 479(m), 432(m).

K[Co(L1)$_2$][Co(NCS)$_4$]·0.5H$_2$O (4): Green plate of **4** was obtained by following the procedure described for **1** by using KSCN (76mg 0.7 mmol) instead of NaN_3. Yield: 18 mg (21%). Anal Calcd. for **4**: C 39.53, H 2.01, N 16.46%. Found: C 39.48, H 1.98, N 16.40 %. IR (KBr, cm^{-1}) **Fig. 1**.: 3418(s), 2115(s), 2068(s), 1720(s), 1634(s), 1605(s), 1471(m), 1445(m), 1371(m), 1334(s), 1296(s), 1257(s), 1153(m), 1096(m), 1053(m), 1032(m), 826(w), 802(w), 769(s), 752(s), 698(s), 629(s), 501(m), 478(m), 431(m).

4.3 Results and Discussion

4.3.1 Syntheses and Characterization

The complexes **1–4** were synthesized (Scheme 2) using the free ligand **L1H** and $CoCl_2·6H_2O$ in 1:1 ratio in the presence of three equivalents of NaN_3 (**1** and **2**) or KSCN (**3** and **4**). Compounds **2** and **3** were obtained by using three equivalents of phenylacetylene in addition to other reagents and the role of phenylacetylene is not clear. Apart from the crystals of **1–4**, a brown acetonitrile-insoluble residue was present which could not be

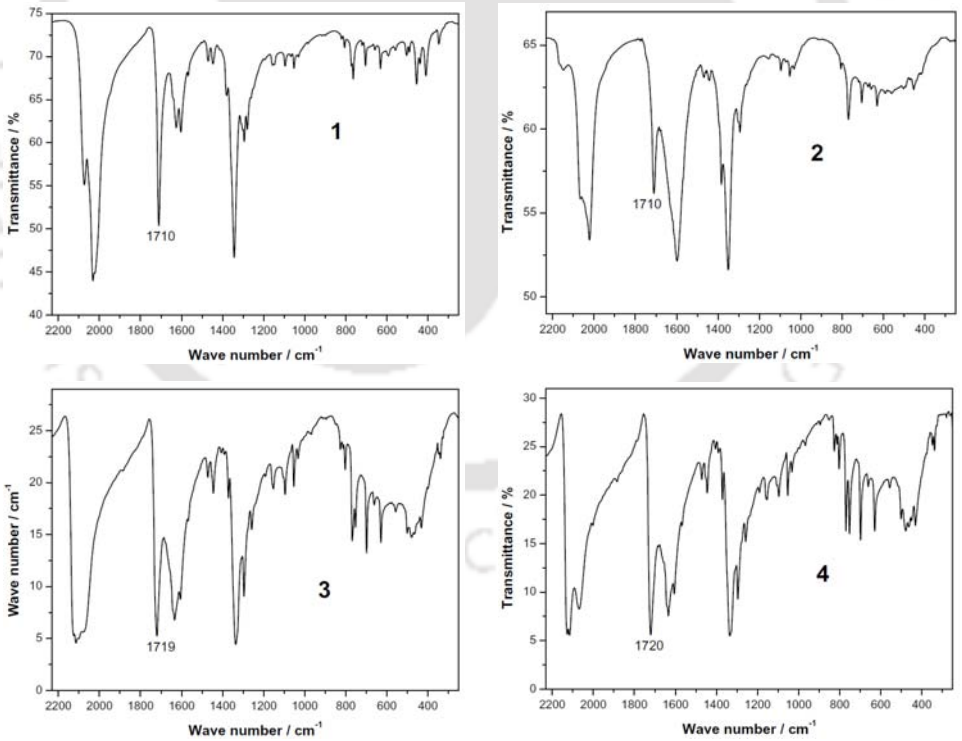

Fig. 1. IR spectra of **1–4**.

characterized due to its insolubility in common solvents. In **1–4** as a result of coordination of **L1** to cobalt(III), *ν*(CO) has been shifted from 1754 cm^{-1} to 1710 cm^{-1}. In case of **1** and

2, the bands at 2073–2060 and 2032–2021 cm^{-1} can be assigned to $\nu(N_3)$ the EE and EO coordination modes respectively. The ν(NC) of thiocyanate in **3**–**4** occurs at ~2115 and ~2070 cm^{-1} that the former can be assigned to the terminal coordination through the N-atom and the later to bridging mode [34]. Complexes **1** and **2** absorb around 580 nm while **3** and **4** absorb around 610 and 580 nm (Table 1), which are of d–d in origin. Complexes **1–3** are diamagnetic while **4** shows a room temperature magnetic moment of 4.427 B. M. which is consistent with the presence of 3 unpaired electrons and is very much comparable with those values reported [35] for tetrahedral thiocyanate complexes of Co^{2+} ion having $e_2^4t_2^3$ electronic configuration.

Table 1. UV-Vis data[^]

Complex	λ_{max}, nm (ε, M^{-1} cm^{-1})
1	583(765), 360(2515), 330(2375), 260(2950).
2	580(560), 360(3250), 264(3500).
3	618(435), 585(403), 362(690), 304(995), 270(1440).
4	614(192), 570(228), 370(3255), 310(4255), 273(5915).

[^] Acetonitrile solution

TGA measurements of **1–4** were taken after the adsorbed water molecules were removed by storing the freshly prepared samples in desiccators overnight and the profiles were analyzed only for the loss of water molecules (Fig. 1). In **1**, loss of one water molecule occur in the temperature range 40–120°C (found 4.24, *ca*. 4.29%) with a mid-point temperature of 86°C. Removal of five water molecules in **2** occur gradually in two steps having the mid-point temperatures 70 and 102°C in the combined temperature range of 40–120°C (found 10.23, *ca*. 10.06%). The loss of one molecule of water in **3** occurs in the range 43–145°C (found 4.21, *ca*. 3.50%), and that of half molecule in **4** in the range 44–125°C (found 3.63, *ca*. 1.10%). The large discrepancy in the values observed in **4** may be due to artifacts.

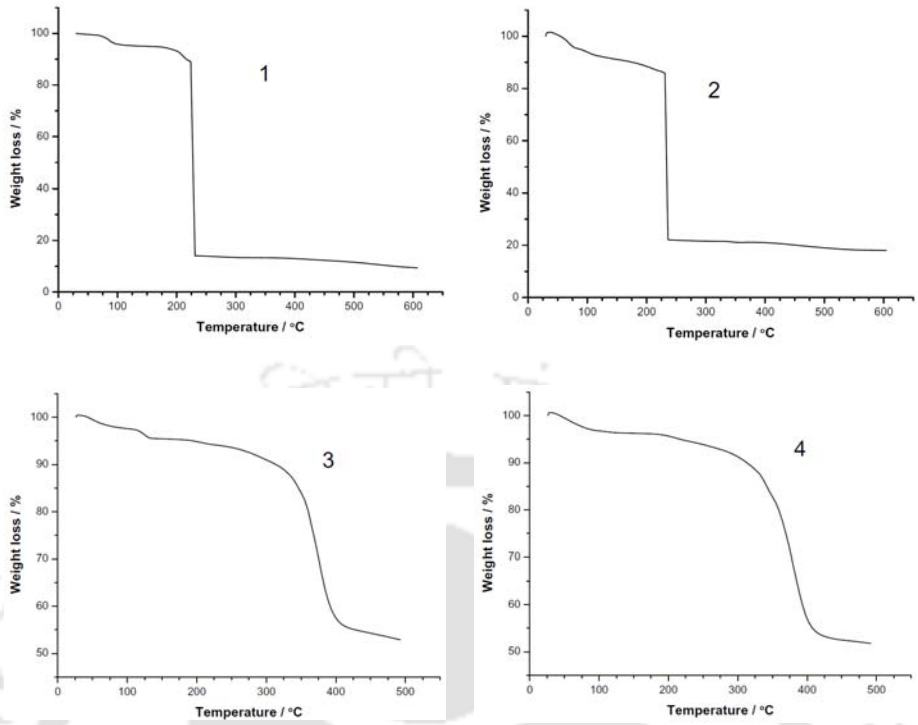

Fig. 1. TG profiles of **1**–**4.**

4.3.2 Molecular Structures

The molecular structures of **1–4** were determined and the crystallographic data are listed in Table 2.

Compound **1** crystallized in the space group $P2_1/c$ contain a 3D-coordination network structure built up on a repeating unit having the formula $Na_2[Co(\mathbf{L1})(N_3)_3]_2{\cdot}2H_2O$. This 3D-coordination network has two distinct types of tetrametallic Co_2Na_2 clusters *viz*., Z-shaped Co···Na···Na···Co and planar diamond-shaped Co_2Na_2 units. There are two different hexa-coordinated low-spin cobalt(III) centers namely Co1 and Co2, each of which is bound by **L1** and three azide ions. Among the three azide ions that are bound to Co1, (i) one is bound in the end-on-bent fashion through N7; (ii) second is involved in bridging Co1 and Na1 centers in $\mu_{1,1}$ fashion using N4 and (iii) third bridges through the N10 atom to Co1, Na1 as well as through N12 to Na2, in $\mu_{1,1,3}$ fashion. Thus N4, N10 binding to Na1 brings Co1 and Na1 to a closer proximity within the non-bonded Co1···Na1 distance of 3.5304(7) Å. Two oxygen atoms of **L1** from the {Co(1)**L1**} fragment is chelated (mode **I**) to Na1 center. A center of symmetry is present between two Na1 atoms which are bridged by two

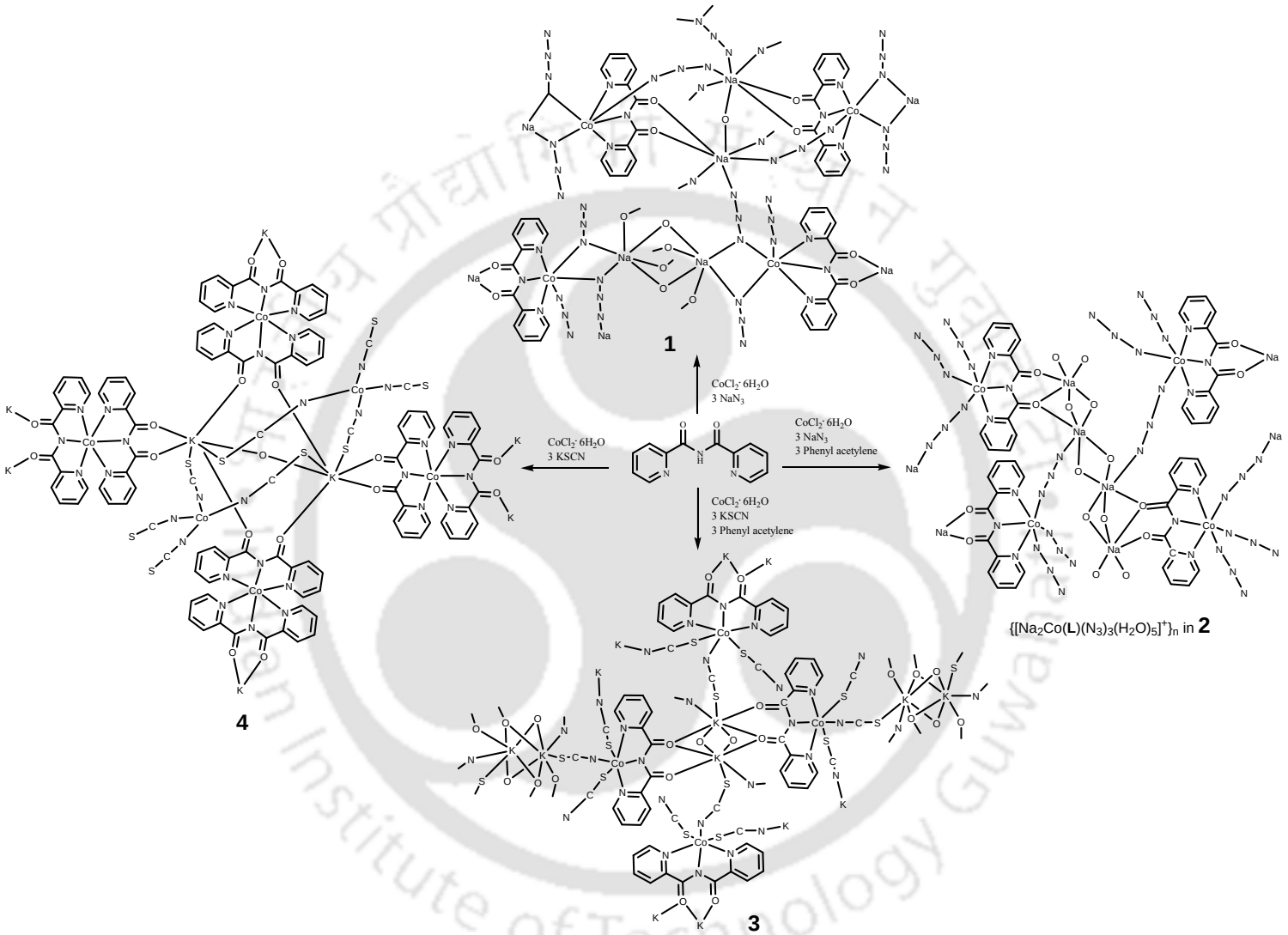

Scheme 2. Synthesis of **1–4**.

Table 2. Crystallographic Data for **1–4**.

	1	**2**	**3**	**4**
Formula	$C_{48}H_{32}Co_4N_{48}Na_4O_{11}$	$C_{24}H_{16}Co_2N_{24}Na_2O_9$	$C_{15}H_8CoKN_6O_3S_3$	$C_{56}H_{32}Co_4K_2N_{20}O_9S_8$
Mol wt	1784.90	958.45	514.51	1699.50
Cry color, habit	Green, hexagonal prismatic	Green, parallelepiped	Blue, block	Green, plates
T, K	298(2)	298(2)	298(2)	298(2)
Cryst syst	Monoclinic	Triclinic	Monoclinic	Monoclinic
Space group	$P2_1/c$	P-1	$P2_1/c$	$P2_1/n$
a, Å	15.8679(2)	11.7419(3)	7.3163(2)	12.8579(2)
b, Å	15.0535(2)	11.7459(3)	15.6024(3))	16.6994(3)
c, Å	14.7390(2)	15.8925(4)	17.9687(4)	16.3316(3)
α, deg	90.00	96.774(1)	90.00	90.00
β, deg	96.401(1)	109.248(1)	99.310(1)	98.726(1)
γ ,deg	90.00	108.782(1)	90.00	90.00
V, Å^3	3498.72(8)	1896.59(9)	2024.14(8)	3466.12(10)
Z	2	2	4	2
D_{calcd}, g cm^{-3}	1.694	1.661	1.688	1.628
μ, mm^{-1}	1.050	0.981	1.393	1.370
GOF[a] on F^2	1.057	1.000	1.026	1.031
R_1,[b] %	3.34	2.11	4.64	5.97
wR_2,[c] %	10.49	10.64	13.04	18.28

[a] GOF = $[\sum[w(F_0^2 - F_c^2)^2] / M - N]^{1/2}$ (M =number of reflections, N = number of parameters refined).

[b] $R_1 = \sum \| F_0 | - | Fc \| / \sum | F_0 |$. [c] $wR_2 = [\sum[w(F_0^2 - F_c^2)^2] / \sum[w(F_0^2)^2]]$.

Table 3. Selected Bond Distances (Å)

1			
Co1–N1	1.9343(12)	Na1···Na1	3.754(2)
Co1–N2	1.8883(11)	Na1–O1	2.328(1)
Co1–N3	1.9295(12)	Na1–O2	2.323(1)
Co1–N4	1.9921(14)	Na1–O5	2.389(2)
Co1–N7	1.9733(14)	Na1–O5[a]	2.536(2)
Co1–N10	1.9561(12)	Na1–N4	2.414(1)
Co2–N13	1.9211(14)	Na1–N10	2.582(2)
Co2–N14	1.8836(14)	Na2–O3	2.652(3)
Co2–N15	1.9307(14)	Na2–O4	2.380(2)
Co2–N16	1.9789(15)	Na2–O6	2.395(1)
Co2–N19	1.9660(16)	Na2–N12	2.879(3)
Co2–N22	1.9542(14)	Na2–N16	2.540(2)
Co1···Na1	3.5304(7)	Na2–N21	2.717(3)
Co2···Na2	3.5527(11)	Na2–N22	2.492(2)
2			
Co1–N1	1.9292(13)	Na1···Na2	3.419(1)
Co1–N2	1.8944(14)	Na1–O1	2.547(2)
Co1–N3	1.9175(13)	Na1–O5	2.442(2)
Co1–N4	1.9566(14)	Na1–O5[b]	2.375(2)
Co1–N7	1.9424(14)	Na1–O6	2.409(2)
Co1–N10	1.9765(14)	Na1–O7	2.433(2)
Co2–N13	1.9133(13)	Na1–N12	2.509(2)
Co2–N14	1.8940(13)	Na2–O1	2.609(2)
Co2–N15	1.9348(14)	Na2–O2	2.311(2)
Co2–N16	1.9609(14)	Na2–O6	2.504(2)
Co2–N19	1.9525(15)	Na2–O7	2.545(2)
Co2–N22	1.9702(15)	Na2–O8	2.384(3)
Na1···Na1	3.6057(15)	Na2–O9	2.385(2)
3			
Co1–N1	1.918(2)	K1···K1	3.633(2)
Co1–N2	1.882(2)	K1–O1	2.710(3)
Co1–N3	1.928(2)	K1–O2	2.886(2)
Co1–N4	1.901(2)	K1–O3	2.726(3)
Co1–S2	2.336(1)	K1–N5	2.937(4)
Co1–S3	2.310(1)	K1–S1	3.330(1)
4			
Co1–N1	1.944(4)	Co2–N10	1.960(6)
Co1–N2	1.908(4)	K1–O1	2.860(5)
Co1–N3	1.936(4)	K1–O2	2.796(4)
Co1–N4	1.950(4)	K1–O3	2.709(5)
Co1–N5	1.941(4)	K1–O4	3.049(6)
Co1–N6	1.900(4)	K1–O5	2.745(2)
Co2–N7	1.956(7)	K1–S1[c]	3.735(3)
Co2–N8	1.943(6)	K1–S3	3.258(3)
Co2–N9	1.971(6)	K1–S4	3.265(3)

[a] -x+2, -y+1, -z+1; [b] -x, -y+1, -z+1; [c] -x+3/2, y-1/2, -z+3/2.

Table 4: Selected Bond Angles (°) for **1**.

O1[b]–Na1–O5	85.33(6)	O4–Na2–N21[e]	128.14(9)
O1[b]–Na1–N4	156.67(6)	O4–Na2–N22[d]	108.39(8)
O1[b]–Na1–N10	91.59(5)	O6–Na2–N12	116.75(7)
O2[b]–Na1–N4	106.29(5)	O6–Na2–N16[d]	106.23(6)
O2[b]–Na1–N10	92.18(5)	O6–Na2–N21[e]	78.03(6)
O2[b]–Na1–O1[b]	77.39(5)	O6–Na2–N22[d]	165.97(8)
O2[b]–Na1–O5	154.46(6)	O6–Na2–O3	78.03(6)
O5–Na1–N4	97.05(6)	N16[d]–Na2–N12	118.29(7)
O5–Na1–N10	107.11(5)	N16[d]–Na2–N21[e]	76.60(7)
N4–Na1–N10	65.46(5)	N16[d]–Na2–O3	84.43(7)
O3–Na2–N12	144.10(8)	N21[e]–Na2–N12	71.82(7)
O3–Na2–N21[e]	143.71(9)	N22[d]–Na2–O3	90.13(7)
O4–Na2–O3	69.80(7)	N22[d]–Na2–N12	77.27(7)
O4–Na2–O6	74.76(6)	N22[d]–Na2–N16[d]	64.65(5)
O4–Na2–N12	82.38(7)	N22[d]–Na2–N21[e]	108.57(7)
O4–Na2–N16[d]	153.59(9)	N19–Co2–Na2[a]	131.69(6)
N1–Co1–Na1	89.39(4)	N21[e]–Na2–Co2[d]	90.60(6)
N2–Co1–Na1	130.99(4)	N22-Co2-Na2[a]	42.54(5)
N3–Co1–Na1	99.80(4)	N22[d]–Na2–Co2[d]	32.02(4)
N4–Co1–Na1	41.06(4)	O1[b]–Na1–Co1	124.50(5)
N4–Na1–Co1	32.83(3)	O1[b]–Na1–Na1[c]	89.43(5)
N4–Na1–Na1[c]	107.84(4)	O2[b]–Na1–Co1	97.75(4)
N7–Co1–Na1	135.71(4)	O2[b]–Na1–Na1[c]	118.51(5)
N10–Co1–Na1	45.83(5)	O3–Na2–Co2[d]	89.80(6)
N10–Na1–Co1	32.92(3)	O5–Na1–Co1	107.56(4)
N10–Na1–Na1[c]	148.68(5)	O5[c]–Na1–Na1[c]	38.90(3)
N12–Na2–Co2[d]	96.09(6)	O5[c]–Na1–Co1	141.13(4)
N13–Co2–Na2[a]	90.33(5)	O5–Na1–Na1[c]	41.80(4)
N14–Co2–Na2[a]	135.19(5)	Co1–Na1–Na1[c]	135.87(3)
N15–Co2–Na2[a]	98.30(5)	O4–Na2–Co2[d]	137.26(7)
N16[d]–Na2–Co2[d]	32.88(4)	O6–Na2–Co2[d]	138.86(5)
N16–Co2–Na2[a]	44.16(5)		

[a] -x+1,y-1/2,-z+1/2;[b] -x+2,y+1/2,-z+1/2; [c] -x+2,-y+1,-z+1; [d] -x+1,y+1/2,-z+1/2; [e] -x+1,-y+1,-z

Table 5: Selected Bond Angles (°) for **2**.

O5[a]–Na1–N12[b]	96.36(7)	O2–Na2–O1	71.56(5)
O5[a]–Na1–O7	84.63(6)	O2-Na2-O6	133.45(8)
O5–Na1–O1	173.50(6)	O2–Na2–O7	134.74(8)
O5[a]–Na1–O1	92.31(5)	O2–Na2–O8	87.02(10)
O5[a]–Na1–O6	158.59(6)	O2–Na2–O9	92.65(8)
O5–Na1–N12[b]	83.40(6)	O6–Na2–O1	77.63(5)
O5[a]–Na1–O5	83.08(6)	O6–Na2–O7	71.17(6)
O6–Na1–O1	80.56(5)	O7–Na2–O1	81.74(6)
O6–Na1–O5	102.13(6)	O8–Na2–O1	127.25(10)
O6–Na1–O7	74.72(6)	O8–Na2–O7	80.83(9)
O6–Na1–N12[b]	104.82(7)	O8–Na2–O6	139.49(10)
O7–Na1–O1	85.23(6)	O8–Na2–O9	86.74(11)
O7–Na1–O5	89.76(6)	O9–Na2–O1	139.93(8)
O7–Na1–N12[b]	172.90(8)	O9–Na2–O6	89.06(8)
N12[b]–Na1–O1	101.73(6)	O9–Na2–O7	129.54(8)
O1–Na1–Na1[a]	134.39(5)	O6–Na2–Na1	44.77(4)
O1–Na1–Na2	49.26(4)	O7–Na1–Na1[a]	86.30(5)
O1–Na2–Na1	47.70(3)	O7–Na1–Na2	48.01(5)
O2–Na2–Na1	119.19(5)	O7–Na2–Na1	45.27(4)
O5[a]–Na1–Na2	113.81(5)	O8–Na2–Na1	124.55(9)
O5–Na1–Na2	128.80(5)	O9–Na2–Na1	133.77(7)
O5–Na1–Na1[a]	40.83(4)	N12[b]–Na1–Na2	136.55(6)
O5[a]–Na1–Na1[a]	42.25(4)	N12[b]–Na1–Na1[a]	89.72(6)
O6–Na1–Na1[a]	139.06(6)	Na2–Na1–Na1[a]	133.65(4)
O6–Na1–Na2	47.06(4)		

[a] -x,-y+1,-z+1;[b] -x,-y,-z+1

Table 6: Selected Bond Angles (°) for **3**.

O1[a]–K1–O2[d]	166.35(7)	O3–K1–O2[d]	67.04(8)
O1[a]–K1–O2[a]	62.49(7)	O3[b]–K1–O2[a]	67.83(7)
O1[a]–K1–O3[b]	110.33(8)	O3–K1–O2[a]	66.46(7)
O1[a]–K1–O3	103.21(9)	O3–K1–O3[b]	98.07(8)
O1[a]–K1–S1	101.35(6)	O3–K1–S1	155.05(6)
O1[a]–K1–N5[c]	101.26(9)	O3[b]–K1–S1	77.34(6)
O2[a]–K1–O2[d]	104.09(5)	O3[b]–K1–N5[c]	143.76(10)
O2[a]–K1–S1	130.76(6)	O3–K1–N5[c]	91.38(11)
O2[d]–K1–S1	89.43(5)	N5[c]–K1–O2[d]	88.84(9)
O2[a]–K1–N5[c]	146.17(10)	N5[c]–K1–S1	79.49(9)
O3[b]–K1–O2[d]	63.58(7)	O3[b]–K1–K1[b]	47.97(6)
O1[a]–K1–K1[b]	116.14(6)	S1–K1–K1[b]	120.68(4)
O2[a]–K1–K1[b]	53.70(5)	N5[c]–K1–K1[b]	130.02(9)
O2[d]–K1–K1[b]	50.39(5)	O3–K1–K1[b]	50.11(6)

[a] -x+1,y+1/2,-z+1/2;[b] -x+2,-y+2,-z+1;[c] x+1,y,z;[d] x+1,-y+3/2,z+1/2

Table 7: Selected Bond Angles (°) for **4**.

O1–K1–S3[c]	96.86(11)	O3[a]–K1–O4[b]	111.96(19
O1–K1–S4	74.81(10)	O3[a]–K1–O5	63.20(15)
O1–K1–O4[b]	138.32(16)	O4[b]–K1–S3[c]	75.65(13)
O2–K1–O1	59.80(13)	O4[b]–K1–S4	86.32(14)
O2–K1–O4[b]	80.56(15)	O5–K1–O1	162.33(12)
O2–K1–S3[c]	65.20(13)	O5–K1–O2	126.66(12)
O2–K1–S4	79.20(10)	O5–K1–O4[b]	55.62(13)
O3[a]–K1–S3[c]	114.85(18)	O5–K1–S3[c]	74.83(7)
O3[a]–K1–S4	102.79(15)	O5–K1–S4	121.31(7)
O3[a]–K1–O1	108.36(18)	S3[c]–K1–S4	142.05(11)
O3[a]–K1–O2	167.34(18)	O5–K1–S1[d]	96.31(6)
O3[a]–K1–S1[d]	68.66(13)	O2–K1–S1[d]	100.73(10)
O1–K1–S1[d]	66.04(11)	O4[b]–K1–S1[d]	140.07(14)
S3[c]–K1–S1[d]	69.22(9)	S4–K1–S1[d]	133.43(8)

[a] x-1/2,-y+1/2,z+1/2; [b] -x+3/2,y+1/2,-z+1/2; [c] -x+1,-y+1,-z+1; [d] -x+3/2,y-1/2,-z+3/2

O5 atoms of water molecules in a bent fashion. Overall, Na1 is bound by two carbonyl oxygen atoms, two nitrogen atoms of the bridged azide ions and two bridged water molecules. This results in the formation of a centrosymmetric Z-shaped Co1···Na1···Na1···Co1 cluster, in which the non-bonded Na1···Na1 distance is 3.7544(15) Å and the angle at Na1 atom is 135.87(2)°. Both Na1 centers are hexa-coordinated and have an identical N_2O_4 environment. Sharing an edge of individual octahedra of metal ions constitute the Z-shaped Co···Na···Na···Co cluster. A shaded-ball and stick diagram depicting the features discussed above is shown in Fig. 2. The selected bond distances are listed in Table 3 and selected angles in Table 4–7. Two oxygen atoms from the {Co(2)**L1**} fragment is chelated (mode **I**) to Na2. Three azide ions coordinated to Co2 are further bound to Na2, two in EO ($\mu_{1,1}$) and one in EE ($\mu_{1,3}$) fashions. Also two Na2 atoms are bridged by an O6 atom of water molecule in a linear fashion having a Na2–O6 distance of 2.3947(12) Å, with O6 sitting at the center of symmetry. Overall the Na2 and Co2 cores together form a planar diamond shaped Co_2Na_2 cluster having a non-bonded Na2···Na2 distance of 4.789(2) Å and Co2···Na2 distances of 5.765(1) and 6.190(1)Å.The Na–O and Na···Na distances observed here is comparable with that observed in the reported compounds [36–39]. The Na2 atom is hepta-coordinated by N_4O_3 environment and has distorted pentagonal bipyramidal geometry. The N12 bound diamond-shaped Co_2Na_2 core is further linked by this azide group to the linear Co_2Na_2 cluster. A shaded-ball and stick diagram depicting the features discussed above is shown in Fig. 3.

Complex **2** crystallized in the P-1 space group contain a 2D-polymeric $\{[Na_2Co(\mathbf{L1})(N_3)_3(H_2O)_5]^+\}_n$ and discrete $[Co(\mathbf{L1})(N_3)_3]^-$ anion. The Co2 center in $[Co(\mathbf{L1})(N_3)_3]^-$ ion is hexa-coordinated in which the low-spin Co(III) is bound by **L1** and three azide ions in EO bent mode. A perspective view is shown in Fig. 4. The two amide oxygen atoms of $[Co(\mathbf{L1})(N_3)_3]^-$ ion has contacts of O4···Na2, 3.208(2) Å and O3···Na1, 3.672(3) Å with sodium ions in the polymeric $[Na_2Co(\mathbf{L1})(N_3)_3(H_2O)_5]^+$ species. The Co1 center in $[Na_2Co(\mathbf{L1})(N_3)_3(H_2O)_5]^+$ ion has similar environment as Co2 center, but two azide ions are bound in EO bent mode and one azide ion in EE bridging fashion, which are simultaneously linked to the Na1 center. The oxygen atoms of the **L1** bound to the Co1 is linked to Na1 and Na2 in the mode **III**. In this mode the oxygen atom O1 binds both Na1

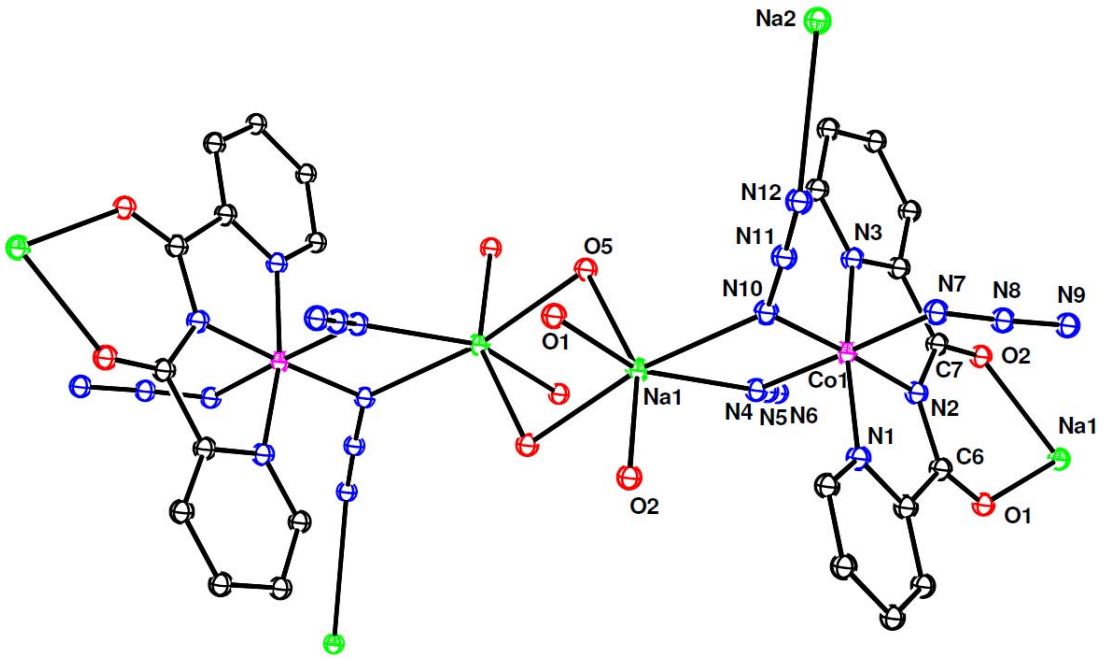

Fig. 2. A shaded-ball and stick diagram of Z-shaped Co···Na···Na···Co cluster in **1**.

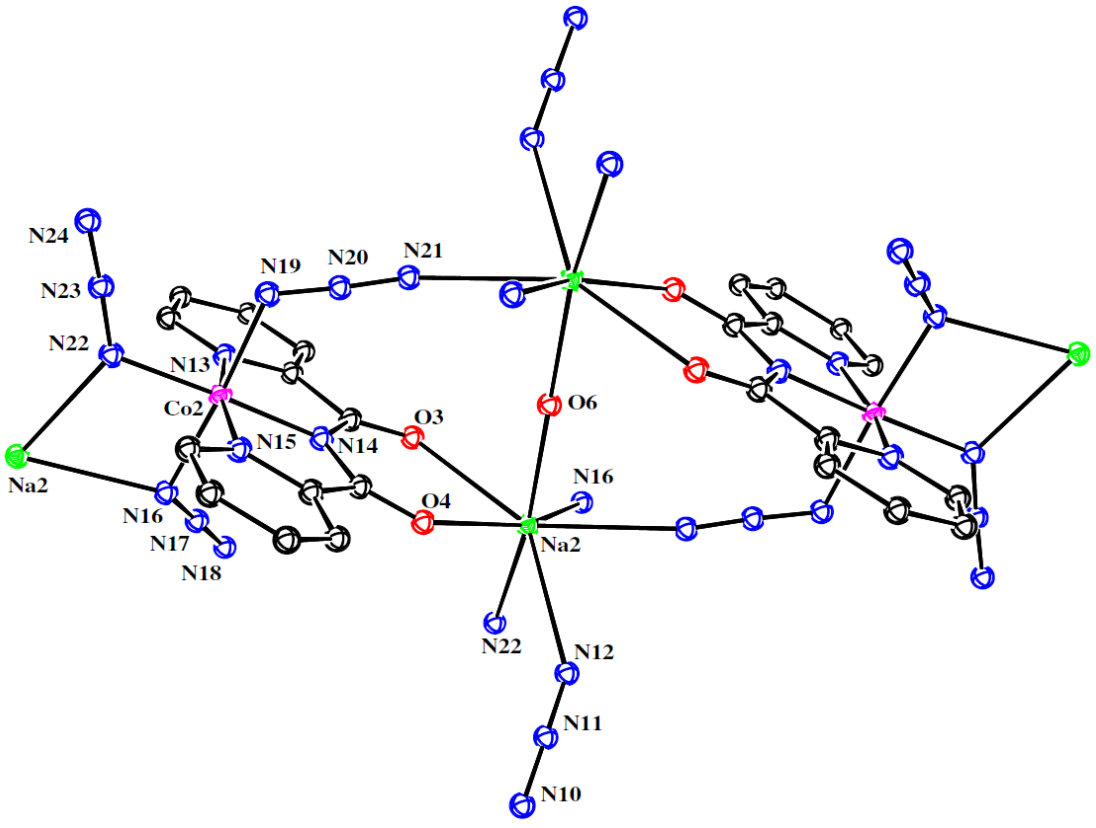

Fig. 3. A shaded-ball and stick diagram of diamond-shaped Co_2Na_2 cluster in **1**.

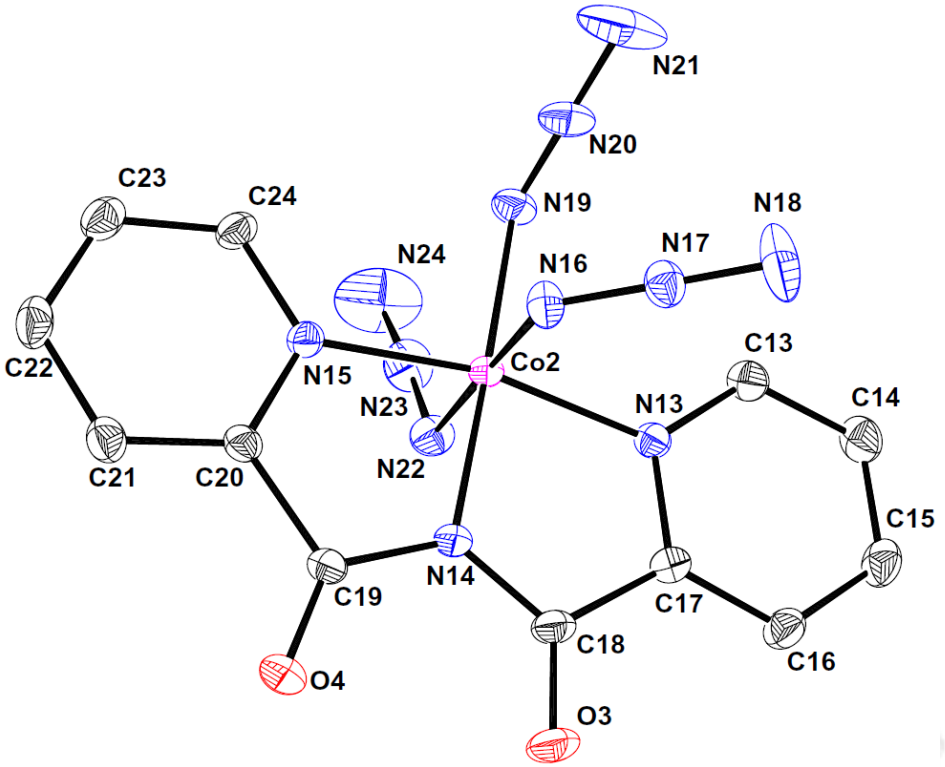

Fig. 4. ORTEP diagram (20% probability level) of $[Co(\mathbf{L1})(N_3)_3]^-$ in **2**. Hydrogen atoms are omitted for clarity.

and Na2, while O2 is bound only to Na2. The O6, O7 atoms of water molecules bridge Na1, Na2 atoms and O5 bridge two Na1 centers all in bent fashions. The other two oxygen atoms O8 and O9 are terminal, coordinated to Na2. Therefore, the carbonyl oxygen and water bridging generates a Z-shaped Na_4 cluster, viz., Na2···Na1···Na1···Na2 with an angle at Na1 of 133.65(4)º. This cluster has an inversion center at the middle of Na1···Na1 bond. The non-bonded distances are Na1···Na2, 3.4185(13) Å and Na1···Na1, 3.6057(15) Å. The Na1 has a pseudo octahedral geometry having a NO_5 coordination environment and Na2 is hexa-coordinated by six oxygen atoms in distorted trigonal prism geometry. Therefore, Na_4 cluster is constituted by sharing a face from trigonal prism of Na2 with octahedron of Na1 and sharing an edge between the two octahedra of Na1. Overall, 2D centrosymmetric double ladder like polymer is generated by the repeating $[Na_2Co(\mathbf{L1})(N_3)_3(H_2O)_5]^+$ cation. A shaded-ball and stick diagram depicting the features is shown in Fig. 5 and that of the polyhedral sharing in Na_4 cluster is shown in Fig. 6.

Complex **3** crystallized in the space group $P2_1/c$ contain a 3D-coordination polymer based on the formula K[Co(**L1**)(*N*CS)(*S*CN)$_2$]·H_2O. The low-spin cobalt(III) domain is a monochelate of **L1**, further coordinated by nitrogen end of thiocyanate ion at the equatorial

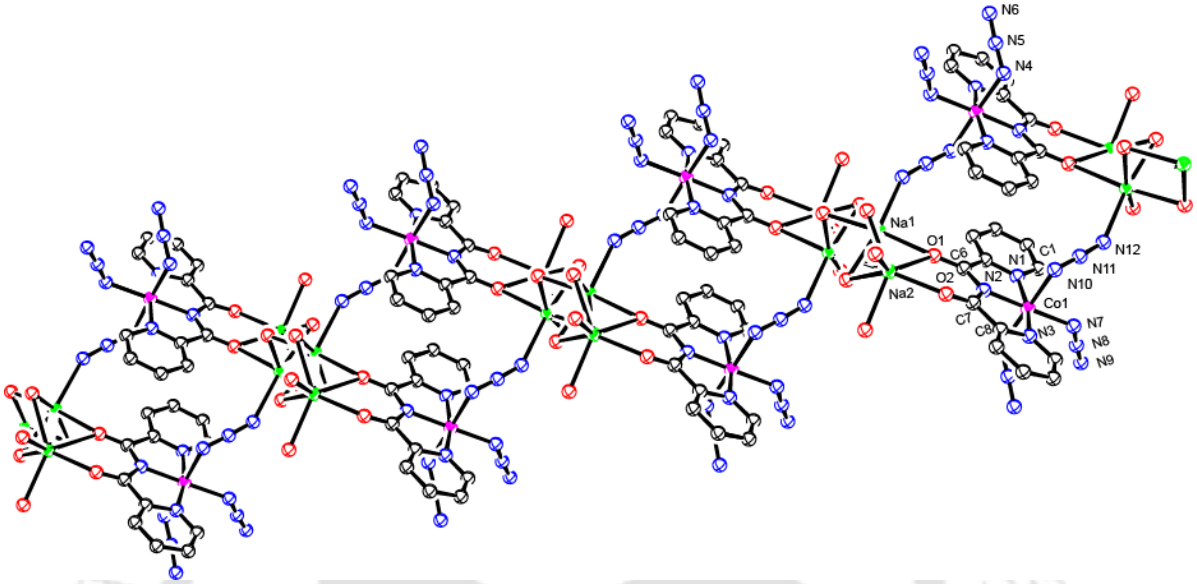

Fig. 5. A shaded-ball and stick diagram of 2D-polymeric ladder-like $\{[Na_2Co(\mathbf{L1})(N_3)_3(H_2O)_5]^+\}_n$ ion in **2**.

plane and sulfur end of two thiocyanate ions at axial sites. The potassium domain contain a centrosymmetric K_2 core bound by the oxygen atoms of the {Co(1)**L1**} fragment in the coordination mode **III**. In this mode the O2 atom is bound to two K1 centers while O1 is bound to one K1. In addition, each potassium ion is bound by (i) sulfur end of the

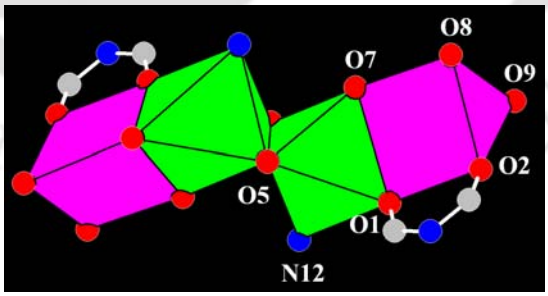

Fig. 6. Polyhedral presentation of Z-shaped Na_4 cluster present in 2D-polymeric ladder-like $\{[Na_2Co(\mathbf{L1})(N_3)_3(H_2O)_5]^+\}_n$ ion of **2**.

equatorial thiocyanate ligand (ii) N5 of axial thiocyanate ion and (iii) O3 of water molecule. Therefore K_2 unit contain the two bridged water molecules bound in a bent

fashion with the non-bonded K···K distance and the K–O–K angles are respectively 3.633(2) Å and 81.93(8)º. A disposition of alternating O2 and O3 atoms that bridge the two potassium atoms has the bond parameters at the rhombic bridge are O2···O3, 3.181(4) Å, O3···O2, 3.078(3) Å, the angle at O2 and O3 respectively are 83.9(1)º and 96.1(1)º. The bond parameters observed in **3** are comparable with those observed in reported complexes [40–42]. Each of the K^+ ions is hepta-coordinated and has O_5NS coordination environment. In addition to the carbonyl oxygen linking present in the K_2O_4 core, coordination by thiocyanate nitrogen and sulfur atoms from two adjacent cobalt domains link them to a three dimensional coordination polymeric network structure. The K–O distances lie in the range 2.710(3) – 3.019(2) Å. A shaded-ball and stick diagram depicting the features discussed above is shown in Fig. 7.

Complex **4** is an admixture containing two kinds of cobalt centers viz., $[Co(\mathbf{L1})_2]^+$, $[Co(NCS)_4]^{2-}$ and K^+ ions. In $[Co(NCS)_4]^{2-}$ ion, the high-spin cobalt(II) is coordinated by nitrogen atoms of the thiocyanate ion and has a distorted tetrahedral geometry. In the bis-chelated $[Co(\mathbf{L1})_2]^+$ ion, the low-spin cobalt(III) has a distorted octahedral geometry having coordination environment of N_6. The Co(III)–N and Co(II)–N bond lengths lie in the range 1.900(4) – 1.950(4) Å and 1.943(6) – 1.971(6) Å, respectively. Two of the thiocyanates in $[Co(NCS)_4]^{2-}$ ion, are further involved in the coordination to two potassium

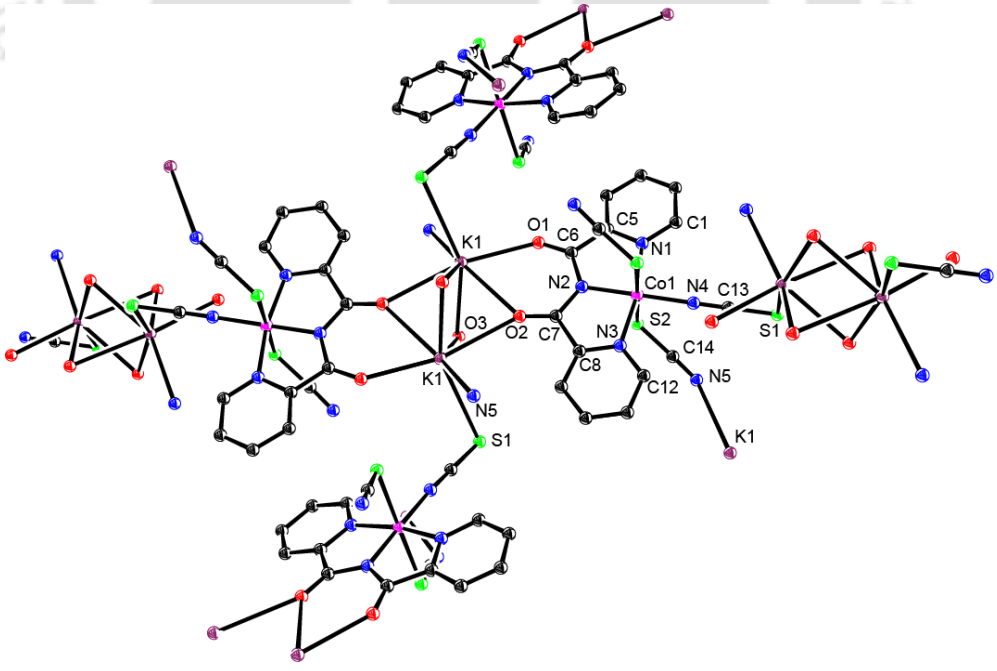

Fig. 7. A shaded-ball and stick diagram of **3**.

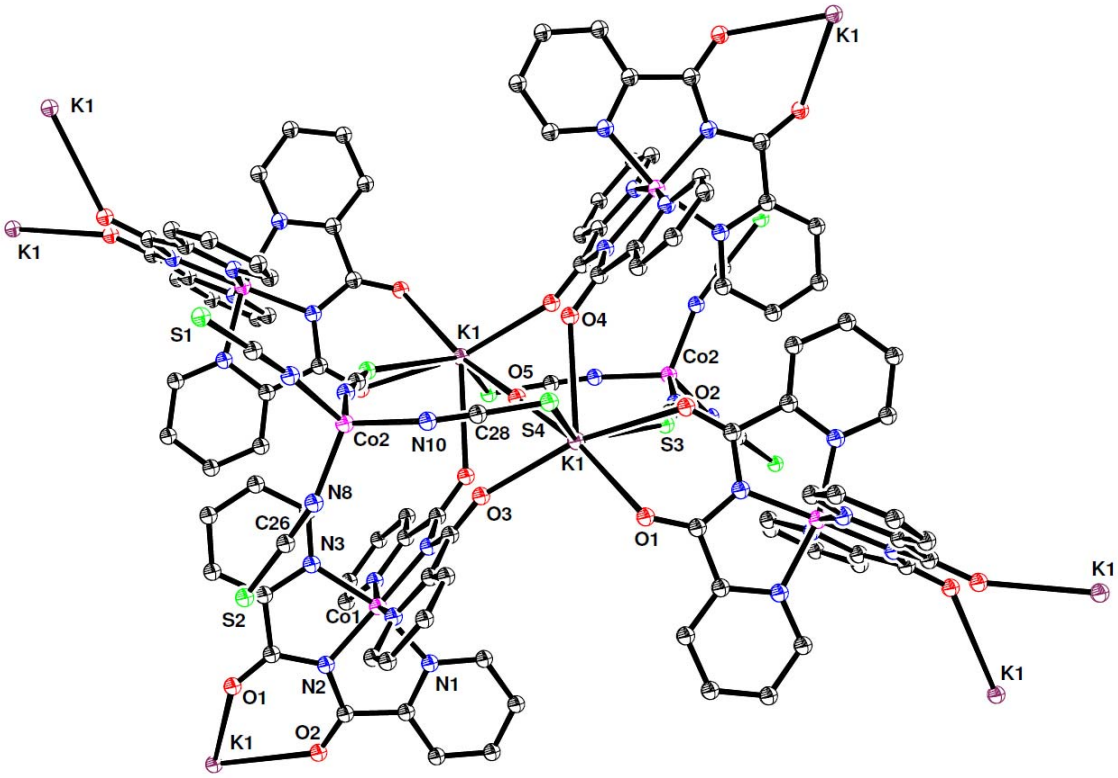

Fig. 8. A shaded-ball and stick diagram of **4**.

ions through the sulfur atoms. Among the two sets of carbonyl oxygen atoms in $[Co(\mathbf{L1})_2]^+$, one set is chelated to a potassium ion (mode **I**), the other set is bound to two potassium ions in the coordination mode **II** and this leads to a 3D-coordination polymer. The two potassium ions are also bridged by O5 of water molecule which sits at the center of symmetry and hence the KOK angle and the K···K non-bonded distance respectively are 180.0º and 5.489(3) Å. A weak K1–S1 contact of 3.735(3) Å is also present, however potassium ion can be considered as hepta-coordinated. A shaded-ball and stick diagram depicting the features is shown in Fig. 8. The linearly water bridged centrosymmetric K_2 core in which both the potassium centers are chelated by the carbonyl groups from one $[Co(\mathbf{L1})_2]^+$ ion, is bridged through oxygen atoms from two adjacent $[Co(\mathbf{L1})_2]^+$ ions and by two $[Co(NCS)_4]^{2-}$ ions through two sulfur atoms results in the existence of a paddle-wheel structure around the KOK core, as shown in Fig. 9.

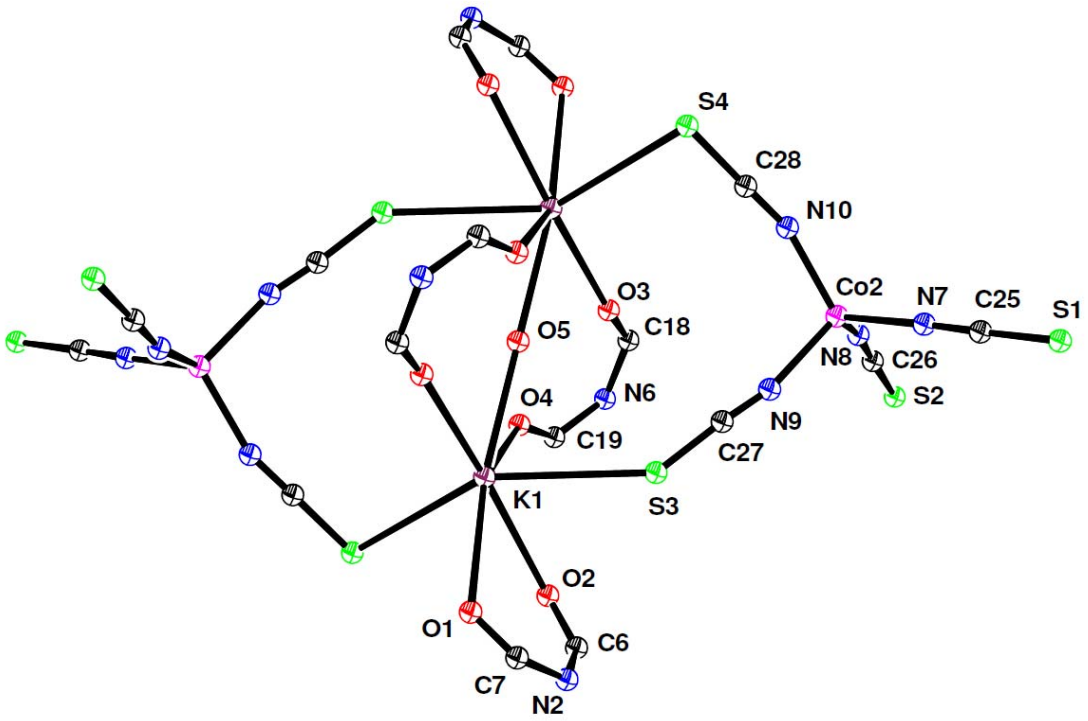

Fig. 9. A shaded-ball and stick diagram showing the paddle-wheel like structure around the centrosymmetric K_2O core in **4**.

In **1**, the six-membered chelate ring formed by the carbonyl oxygen atoms coordinated to Na1 has an envelope conformation in which Na1 is displaced out of the plane. This is relevant form the dihedral angle of 10.42° between the two planes containing the atoms viz., O1O2N2C6C7 and O1O2Na1. But the chelate ring at Na2 deviate slightly from planarity with dihedral angle of 3.33° between the two planes that include the atoms O3O4N14C18C19 and O3O4Na2. The chelate bites at Na1 and Na2 respectively are 77.38(5)° and 69.80(7)°. In **2**, the chelate ring at Na2 having mode **III** has an envelope conformation with the dihedral angle of 13.24° between the planes that include the atoms O1O2N2C6C7 and O1O2Na2. The chelate bite angle is 71.56°. The dihedral angle between the two planes containing the atoms O1O2N2C6C7 and O1O2K1 in **3** is 4.07° while that in **4** is 17.48°. In **4** the chelate ring is twisted with the torsion angle of 6.74°. The chelate bite of the mode **I** in **3** and **4** respectively are 62.48 and 59.70°. The mode **II** is found only in compound **4** in which two K1 atoms are skewed with an angle of 56.22°.

4.4 Conclusion

In summary, four new hetero-bimetallic Co^{3+}–Na^{+} and Co^{3+}–K^{+} coordination polymers of composition $[Na(H_2O)Co(\mathbf{L1})(N_3)_3]_n$ (**1**), $[Na_2Co(\mathbf{L1})(N_3)_3(H_2O)_5][Co(\mathbf{L1})(N_3)_3]$ (**2**), $K[Co(\mathbf{L1})(NCS)_3]\cdot H_2O$ (**3**) and $K[Co(\mathbf{L1})_2][Co(NCS)_4]\cdot 0.5H_2O$ (**4**) have been synthesized. Determination of their molecular structures reveal the presence of (i) binding by **L1** in modes **I**, **II**, **III**; (ii) EE, EO bridging by azide group (in **1**, **2**); and (iii) bent (in **1**, **2**, **3**) and linear (in **1**, **4**) aquo bridges. Also present are Z and diamond shaped Co_2Na_2 clusters in **1**, a centrosymmetric double ladder like polymer based on Na_4 cluster in **2**, and a linear KOK core having paddle–wheel structure in **4**. The Na_4 cluster present in **2** has been constituted by a face-sharing between trigonal prism and octahedron as well as edge-sharing between two octahedra. The chelate bites by the carbonyl oxygen atoms at K^{+} are lower than those at Na^{+}.

4.5 References

1. B. Moulton, M.J. Zaworotko, Chem. Rev. 101 (2001) 1629–1658.
2. C. Janiak, Dalton Trans. (2003) 2781–2804.
3. J.J. Perry IV, J.A. Perman, M.J. Zaworotko, Chem. Soc. Rev. 38 (2009) 1400–1417.
4. J.Y. Lee, O.K. Farha, J. Roberts, K.A. Scheidt, S.T. Nguyen, J.T. Hupp, Chem. Soc. Rev. 38 (2009) 1450–1459.
5. A. Corma, H. García, F.X. Llabrés i Xamena, Chem. Rev. 110 (2010) 4606–4655.
6. J. Crassous, Chem. Soc. Rev. 38 (2009) 830–845.
7. L. Ma, C. Abney, W. Lin, Chem. Soc. Rev. 38 (2009) 1248–1256.
8. M.D. Allendorf, C.A. Bauer, R.K. Bhakta, R.J.T. Houk, Chem. Soc. Rev. 38 (2009) 1330–1352.
9. V. Martinez, A.B. Gaspar, M.C. Munoz, R. Ballesteros, N. Ortega-Villar, V.M. Ugalde-Saldivar, R. Moreno-Esparza, J.A. Real, Eur. J. Inorg. Chem. (2009) 303–310.
10. V. Martinez, A.B. Gaspar, M.C. Munoz, G.V. Bukin, G. Levchenko, J.A. Real, Chem. Eur. J. 15 (2009) 10960–10971.
11. X-M. Zhang, T. Jiang, H-S. Wu, M-H. Zeng, Inorg. Chem. 48 (2009) 4536–4541.
12. P-K. Chen, S.R. Batten, Y. Qi, J-M. Zheng, Cryst. Growth Des. 9 (2009) 2756–2761.

13. A. Muhammad, D.J. Craig, R. Bircher, J.A. Stride, Dalton Trans. 39 (2010) 4358–4362.
14. T. Uemura, N. Yanai, S. Kitagawa, Chem. Soc. Rev. 38 (2009) 1228–1236.
15. L.J. Murray, M. Dincâ, J. R. Long, Chem. Soc. Rev. 38 (2009) 1294–1314.
16. S.S. Han, J.L.M. Cortés, W.A. Goddard III, Chem. Soc. Rev. 38 (2009) 1460–1476.
17. J-R. Li, R.J. Kuppler, H-C. Zhou, Chem. Soc. Rev. 38 (2009) 1477–1504.
18. T. Kajiwara, T. Ito, Angew. Chem. Int. Ed. 39 (2000) 230–233.
19. H. Casellas, F. Costantino, A. Mandonnet, A. Caneschi, D. Gatteschi, Inorg.Chim. Acta 358 (2005) 177–185.
20. A. Bencini, F. Totti, Int. J. Quantum Chem. 101 (2005) 819–825.
21. T. Kajiwara, T. Ito, J. Chem. Soc., Dalton Trans. (1998) 3351–3352.
22. T. Kajiwara, T. Ito, Mol. Cryst. Liq. Cryst. 335 (1999) 73–80.
23. A. Kamiyama, T. Noguchi, T. Kajiwara, T. Ito, Inorg. Chem. 41 (2002) 507–512.
24. T. Kajiwara, R. Sensui, T. Noguch, A. Kamiyama, T. Ito, Inorg. Chim. Acta 337 (2002) 299–307.
25. T. Kajiwara, M. Nakano, Y. Kaneko, S. Takaishi, T. Ito, M. Yamashita, A.I. Kamiyama, H. Nojiri, Y. Ono, N. Kojima, J. Am. Chem. Soc. 127 (2005) 10150–10151.
26. Y. Kaneko, T. Kajiwara, H. Yamane, M. Yamashita, Polyhedron 26 (2007) 2074–2078.
27. T. Kajiwara, I. Watanabe, Y. Kaneko, S. Takaishi, M. Enomoto, N. Kojima, M. Yamashita, J. Am. Chem. Soc. 129 (2007) 12360–12361.
28. A. Kamiyama, T. Noguchi, T. Kajiwara, T. Ito, Angew. Chem., Int. Ed. 39 (2000) 3130–3132.
29. A. Kamiyama, T. Noguchi, T. Kajiwara, T. Ito, CrystEngComm. 5 (2003) 231–237.
30. M. Ferbinteanu, T. Kajiwara, K-Y. Choi, H. Nojiri, A. Nakamoto, N. Kojima, F. Cimpoesu, Y. Fujimura, S. Takaishi, M. Yamashita, J. Am. Chem. Soc. 128 (2006) 9008–9009.
31. F. Pointillart, K. Bernot, R. Sessoli, D. Gatteschi, Chem. Eur. J. 13 (2007) 1602–1609.
32. A.M. Madalan, K. Bernot, F. Pointillart, M. Andruh, A. Caneschi, Eur. J. Inorg. Chem. (2007) 5533–5540.

33. R. Sahu, S.K. Padhi, H.S. Jena, V. Manivannan, Inorg. Chim. Acta 363 (2010) 1448–1454.
34. K. Nakamoto, Infrared and Raman Spectra of Inorganic and Coordination Compounds. Part B, 5th ed., Wiley, New York, 1997.
35. F.A. Cotton, M.L. Goodgame, M. Goodgame, A. Sacoo, J. Am. Chem. Soc. 83 (1961) 4153–4161.
36. B.T. Collins, S.M. Fine, J.A. Potenza, P.P. Tsai, M. Greenblatt, Inorg. Chem. 28 (1989) 2444–2447.
37. Y. Kim, Y.W. Han, K. Seff, J. Phys. Chem. 97 (1993) 12663–12664.
38. G.J.T. Cooper, H. Abbas, P. Kögerler, D-L. Long, L. Cronin, Inorg. Chem. 43 (2004) 7266–7268.
39. L. Cañadillas-Delgado, Ó. Fabelo, C. Ruíz-Pérez, F.S. Delgado, M. Julve, M. Hernández-Molina, M. M. Laz, P. Lorenzo-Luis, Cryst. Growth Des. 6 (2006) 87–93.
40. H-X. Zhang, J. Zhang, S-T. Zheng, G-Y. Yang, Cryst. Growth Des. 5 (2005) 157–161.
41. R.D. Bergougnant, A.Y. Robin, K.M. Fromm, Cryst. Growth Des. 5 (2005) 1691–1694.
42. J. Kühnert, T. Rüffer, P. Ecorchard, B. Bräuer, Y. Lan, A.K. Powell, H. Lang, Dalton Trans. (2009) 4499–4508.

Chapter 5

Molecular Structures of Copper(II) Monochelates of Bis(2-quinolylcarbonyl)amide Ion

Abstract

Copper(II) monochelates of **L2** having the formulae [Cu(**L2**)(DMF)(NCO)] (**1**), [Cu(**L2**)(DMF)(NCS)] (**2**), [Cu(**L2**)(PhCOO)(H_2O)]·(CH_3OH) (**3**) and [Cu(**L2**)(dca)]$_n$ (**4**) {**L2** = bis(2-quinolylcarbonyl)amide ion} have been synthesized using respective coligands. Compounds **1**–**4** were characterized by single crystal X-ray diffraction, IR, UV-Vis, and EPR spectroscopic methods. Compounds **1**–**3** are mononuclear in nature, having *O*-coordinated cyanato ligand in **1** and *N*-coordinated thiocyanato ligand in **2**. Dicyanamide ion acts as a bridge between two copper centers that leads to one-dimensional coordination polymer in compound **4**. Also π···π interaction between the quinolinyl rings is present in **1**, **2** and **4**.

5.1 Introduction

In Chapter 2, it has been demonstrated that bis(2-quinolylcarbonyl)amide (**L2**) can be readily obtained from 2-aminomethylquinoline and copper(II) acetate [1]. Since **L2** is a new ligand, a study on its coordination chemistry with respect to copper monochelates with cyanate, thicyanate, benzoate, and dicyanamide ions as coligands, has been carried out and the results are discussed in this Chapter.

5.2 Experimental Section

The ligand **L2H** was prepared using the procedure reported in Chapter 2.

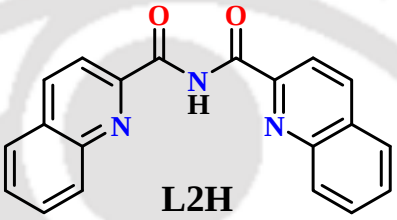

L2H

5.2.1 Syntheses

[Cu(L2)(OCN)(DMF)] (1): To [Cu(**L2**)(OAc)(H_2O)] (0.040 g, 0.086 mmol) dissolved in methanol (30 mL) was added solid KOCN (0.020 g, 0.246 mmol) and stirred for 6-8 h. The solvent was removed in a rotary evaporator and the solid was dissolved in minimum amount of DMF which was left undisturbed. The green crystals of **1** were collected after 2 weeks. Yield: 0.020 g, 46%. IR (KBr, cm^{-1}) **Fig. 1**.: 3445(b), 2235(s), 1709(s), 1618(s), 1592(m), 1509(w), 1459(s), 1372(s), 1340(s), 1258(m), 1216(w), 1201(w), 1154(s), 1117(s), 1013(m), 987(m), 968(m), 888(m), 846(m), 802(m), 773(s), 723(s), 637(m), 613(m), 513(m). Anal Calcd. for **1**: C 57.08, H 3.79, N 13.87. Found: C 57.00, H 3.72, N 13.81.

[Cu(L2)(NCS)(DMF)] (2): To a solution of $CuCl_2.2H_2O$ (0.021 g, 0.123 mmol) and KSCN (0.024 g, 0.246 mmol) in methanol (30 mL), solid **L2H** (0.040 g, 0.123 mmol) was added and stirred for 6 h. The solvent was removed in a rotary evaporator and the solid was dissolved in minimum amount of DMF which was left undisturbed. The green crystals of **2** were collected after 2 weeks. Yield: 0.026g, 40%. IR (KBr, cm^{-1}) **Fig. 1**.: 3459(b), 2081(s), 1713(s), 1641(s), 1595(s), 1565(m), 1512(m), 1460(s), 1434(m), 1418(w),

1370(s), 1344(s), 1268(w), 1216(w), 1202(w), 1150(w), 1105(m), 1052(w), 1013(w), 953(w), 888(w), 874(w), 849 (m), 799(m), 777(s),768(m), 737(m), 722(s), 663(m), 638(m), 611(w), 510(m). Calcd. for **2**: C 55.32, H 3.68, N 13.44. Found: C 55.17, H 3.61, N 13.37.

[Cu(L2)(PhCOO)(H_2O)]·(CH_3OH) (3): To **L2H** (0.42 g, 0.128 mmol) dissolved in methanol (30 mL) was added solid $Cu(PhCOO)_2·3H_2O$ (0.039 g, 0.128 mmol) and stirred for 8 h. The solution was left undisturbed, green crystals of **3** deposited after a week were collected and washed with ice-cold methanol. Yield: 0.029 g, 40%. IR (KBr, cm^{-1}) **Fig. 1**.: 3431(b), 1702(s), 1600(s), 1566(s), 1513(m), 1462(s), 1384(s), 1337(s), 1219(w), 1157(w), 1116(w), 1068(m), 1017(m), 965(w), 892(w),876(w), 848(m), 805(m), 776(s), 723(s), 711(m), 687(w), 663(w), 637(w), 610(w), 570(w), 495(w), 477(w), 465(w). Calcd. for **3**: C 59.94, H 4.13, N 7.49. Found: C 59.70, H 4.08, N 7.31.

$[Cu(L2)(DCA)]_n$ (4): To a solution of $Cu(NO_3)_2·3H_2O$ (0.025 g, 0.103 mmol) and $NaN(CN)_2$ (0.018 g, 0.206 mmol) in methanol (30 mL), solid **L2H** (0.035 g, 0.106 mmol) was added and stirred for 8 h. The solution was left undisturbed, green crystals of **4** deposited after a week were collected and washed with ice-cold methanol. Yield: 0.020g, 43%. IR (KBr, cm^{-1}) **Fig. 1**.: 3401(b), 2312(m), 2237(m), 2179(s), 1713(s), 1634(s), 1568(m), 1510(m), 1459(m), 1435(w), 1383(s), 1358(s),1342(s), 1263(m), 1215(w), 1154(w), 1113(w), 1027(m), 965(m), 900(w), 886(w), 848(m), 801(s), 772(s), 721(w), 669(w), 639(w), 601(w), 524(w), 500(m), 471(w), 394(w). Calcd. for **4**: C 57.96, H 2.65, N 18.43. Found: C 57.72, H 2.54, N 18.46.

5.3 Results and Discussion

5.3.1 Optical Spectra and Magnetism

The free ligand exhibits a strong *ν*(CO) peak at 1753 cm^{-1} which has been shifted to 1700–1720 cm^{-1} on binding to copper(II) ions in **1**–**4**. This shift in the *ν*(CO) has been used to infer the complexation of **L2** to the Cu(II) ion. In addition a single strong band at 2235 cm^{-1} observed in cyanato complex **1** is suggestive of presence of NCO^- coordinated to the

bivalent copper. Isothiocyanato complex exhibits a strong peak for the ν_{CN} at 2081 cm^{-1} while the dicyanamido complex exhibits multiple peaks for ν_{CN} at 2260, 2211 and 2152 cm^{-1} [2–4].

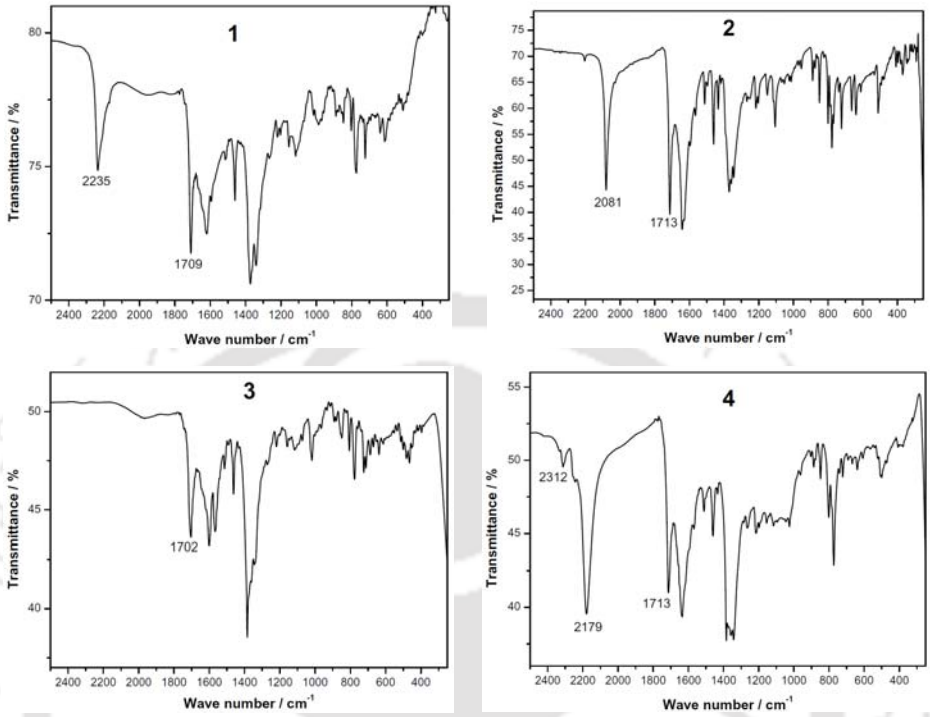

Fig. 1. IR spectra of **1–4**.

UV-Vis spectra of **1–4** have been recorded in DMF. Compounds **1**, **2** and **4** show two *d–d* transitions, one in the range 950–970 and another ~710 nm. These may be arising from the transitions $d_{x^2-y^2}$ to d_{z^2} and $d_{x^2-y^2}$ to d_{xy}, respectively [5]. However in **3** the later transition was observed ~680 nm while the lower-energy transition was not observed. In all the complexes, three intra-ligand transitions were observed in the range 265–330 nm. The λ_{max} and corresponding molar extinction coefficient values are listed in Table 1.

Table 1. UV-Vis and EPR data.

	λ_{max}, nm (ε, M^{-1} cm^{-1})[a]	EPR[a,b]			μ_{eff}[d]
		$g_\perp$	$g_\parallel$	$A_\parallel$[c]	
1	975(32), 707(131), 327(14470), 296 (22370), 266(37680)	2.058	2.251	126	2.20
2	980(30), 707 (125), 327 (19240), 300 (23375), 265 (32280)	2.028	2.224	101	2.60
3	650 (102), 330 (14340), 317 (18105), 295 (25760)	2.023	2.185	155	2.03
4	950(58), 714 (108), 330 (12980), 300 (16735), 266 (26520)	2.031	2.223	144	2.24/Cu

[a]DMF solution; [b]At 77 K; [c]In units of G; [d]In units of B.M. and at 298 K.

All the four complexes behave as one electron paramagnets and room temperature μ_{eff} values are higher than $\mu_{s.o.}$ values. At 77K, the EPR spectra (Fig. 2) of **1**–**4** are typically axial in nature with the $g_{\perp}$ and $g_{\parallel}$ values lying respectively in the range 2.02–2.06 and 2.18–2.25. The observed trend $g_{\parallel} > g_{\perp} > 2$ is consistent with the odd electron being in the $d_{x^2-y^2}$ orbital [6].

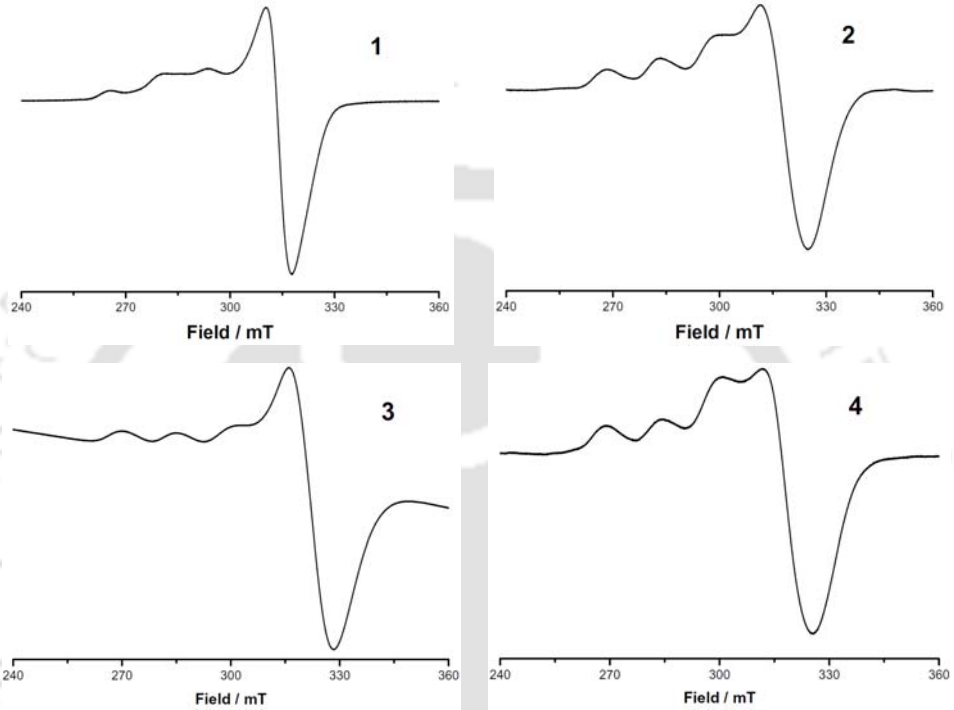

Fig. 2. EPR Spectra of **1**–**4** in DMF at 77 K

5.3.2 Molecular Structures

The molecular structures of **1**–**4** were determined and the crystallographic data are listed in Table 2. In all the four complexes, copper(II) center is penta-coordinated and is bound by the anionic ligand **L2** in meridional fashion and selected bond distances and angles are listed in Tables 3 and 4. The structural features are observed in copper(II) complexes of similar ligand **L1** having different coligands (bridging / unbridging) [7–18]. The trigonality parameter τ calculated is: 0.27 for **1**, 0.33 for **2**, 0.032 for **3**, and 0.62 for **4**, (τ = 0 and 1 for ideal square pyramid and trigonal bipyramid, respectively) [19].

In **1**, the fourth and fifth coordination sites were occupied by oxygen atom of the *O*CN$^-$ ion and by the oxygen atom of the DMF. Cyanato ion is an ambidentate ligand which

Table 2. Crystallographic Data for **1–4**.

	1	**2**	**3**	**4**
Formula	$C_{24}H_{19}N_5O_4Cu$	$C_{24}H_{19}N_5O_3SCu$	$C_{28}H_{23}N_3O_6Cu$	$C_{22}H_{12}N_6O_2Cu$
Formula weight	504.99	521.06	561.03	455.93
T, K	298(2)	298(2)	298(2)	298(2)
Cryst syst	Triclinic	Triclinic	Monoclinic	Orthorhombic
Space group	*P*-1	*P*-1	$P2_1/n$	*P*bcn
a, Å	9.7197(10)	9.8236(7)	9.5250(3)	13.3815(4)
b, Å	10.3961(11)	10.5101(7)	19.7035(5)	19.0112(6)
c, Å	11.9047(13)	11.9713(8)	13.8719(4)	7.5818(3)
α, deg	90.152(5)	83.657(5)	90.00	90.00
β, deg	112.458(5)	67.255(4)	104.714(2)	90.00
γ, deg	97.340(6)	81.325(5)	90.00	90.00
V, Å^3	1100.9(2)	1125.00(13)	2518.04(13)	1928.80(11)
Z	2	2	4	4
D_{calcd}, gcm^{-3}	1.523	1.024	1.477	1.570
μ, mm^{-1}	1.035	1.101	0.917	1.166
GOF[a] on F^2	1.093	1.301	1.049	0.926
R[I > 2σ(I)]	[b]R_1 = 0.0431 [c]wR_2 = 0.1462	[b]R_1 = 0.0318 [c]wR_2 = 0.0713	[b]R_1 = 0.0510 [c]wR_2 = 0.1364	[b]R_1 = 0.0346 [c]wR_2 = 0.1087
R indices (all data)	[b]R_1 = 0.0431 [c]wR_2 = 0.1462	[b]R_1 = 0.0319 [c]wR_2 = 0.0713	[b]R_1 = 0.0625 [c]wR_2 = 0.1438	[b]R_1 = 0.0497 [c]wR_2 = 0.1282

[a] GOF = $[\sum[w(F_0^2 - F_c^2)^2] / M - N]^{1/2}$ (M =number of reflections, N = number of parameters refined).
[b] $R_1 = \sum \| F_0 | - | Fc \| / \sum | F_0 |$.
[c] $wR_2 = [\sum[w(F_0^2 - F_c^2)^2] / \sum[w(F_0^2)^2]]^{1/2}$.

possibly can coordinate through the N-atom or through the O-atom. The common coordination occurs through the N-atom and in complex **1**, the rarer coordination through O-atom has been observed. As one can expect a bent geometry at the O-atom, the angle observed is 146.8(3)°. A perspective view of **1** is shown in Fig. 3. The Cu atom lies out of the plane formed by three nitrogen atoms of **L2** by 0.182 Å towards the cyanato O-atom. The Cu–N_P distances lie in the range 2.047(2)–2.055(3) Å, are longer by ~0.1 Å than the Cu–N_A distance 1.954(2) Å {N_P = pyridyl-N, N_A = amido-N and O_B = benzoate-O}. These values are similar to the copper(II) complexes of **L1** reported earlier [7–18]. The overall geometry around the copper(II) ion is distorted square pyramid, in which the angles formed at the O_2N_A trigonal plane are

Table 3.Bond distances (Å).

1		2		3		4	
Cu1–N1	2.051(3)	Cu1–N1	2.041(2)	Cu1–N1	2.100(5)	Cu1–N1	2.0375(18)
Cu1–N2	1.953(3)	Cu1–N2	1.939(2)	Cu1–N2	1.926(6)	Cu1–N1[a]	2.0375(18)
Cu1–N3	2.054(3)	Cu1–N3	2.042(2)	Cu1–N3	2.091(5)	Cu1–N2	1.945(3)
Cu1–O3	1.939(3)	Cu1–N4	2.016(2)	Cu1–O3	2.225(5)	Cu1–N5	2.0561(19)
Cu1–O4	2.312(3)	Cu1–O3	2.276(1)	Cu1–O4	1.932(4)	Cu1–N5[a]	2.056(2)[a]

[a] -x+1, y, -z+1/2

Table 4. Selected Bond Angles (º)

1		2	
N1–Cu1–N2	81.65(13)	N1–Cu1–N3	161.75(7)
N1–Cu1–N3	160.78(12)	N1–Cu1–O3	90.60(6)
N1–Cu1–O4	87.60(12)	N2–Cu1–N1	81.41(7)
N2–Cu1–N3	81.36(14)	N2–Cu1–N3	81.86(7)
N2–Cu1–O4	108.76(11)	N2–Cu1–N4	141.82(8)
N3–Cu1–O4	89.40(11)	N2–Cu1–O3	109.72(6)
O3–Cu1–N1	99.03(14)	N3–Cu1–O3	88.22(6)
O3–Cu1–N2	144.67(15)	N4–Cu1–N1	98.83(7)
O3–Cu1–N3	100.03(14)	N4–Cu1–N3	98.81(7)
O3–Cu1–O4	106.56(13)	N4–Cu1–O3	108.45(7)
3		**4**	
N1–Cu1–O3	92.2(3)	N1–Cu1–N5	93.39(7)
N2–Cu1–O4	160.3(2)	N1–Cu1–N5[a]	96.53(8)
N2–Cu1–O3	116.1(2)	N1[a]–Cu1–N5[a]	93.39(7)
N2–Cu1–N1	80.9(2)	N1[a]–Cu1–N5	96.53(8)
N2–Cu1–N3	81.2(2)	N1[a]–Cu1–N1	162.97(10)
N3–Cu1–N1	162.1(3)	N2–Cu1–N1	81.48(5)
N3–Cu1–O3	94.8(2)	N2–Cu1–N1[a]	81.48(5)
O4–Cu1–N1	98.5(2)	N2–Cu1–N5	125.71(6)
O4–Cu1–N3	98.6(2)	N2–Cu1–N5[a]	125.71(6)
O4–Cu1–O3	83.62(19)	N5–Cu1–N5[a]	108.59(12)

[a] -x+1, y, -z+1/2

106.5(1), 108.8(1) and 144.7(1)°. The *trans* angle N_P–Cu–N_P being 160.83(9)°.

Packing diagram shows the presence of π···π interaction between quinolinyl rings, distance between two centroids C1C2C3C4C5C6 and C1N1C6C7C8C9 being 3.72 Å with a shortest non-bonded contact of C1···C6 3.690(5) Å. An intermolecular dipolar interaction

between oxygen and carbon atoms of amide group is also present and the non-bonded contacts are O1···C11, 3.111(4) and O2···C10, 3.055(4) Å.

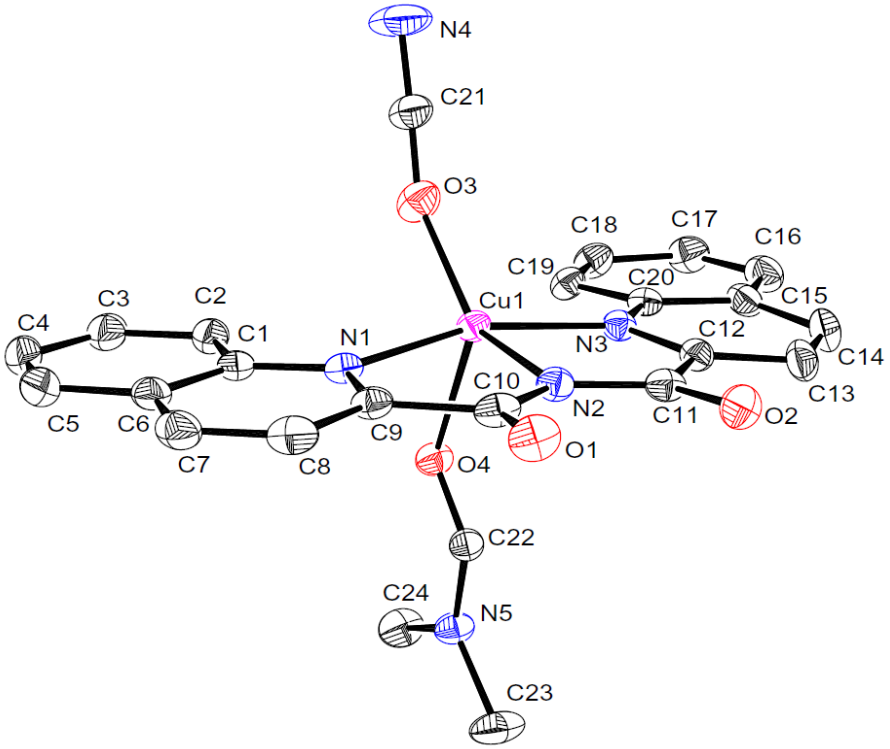

Fig. 3. ORTEP (20% probability ellipsoid) diagram of **1** and the hydrogen atoms are omitted for clarity.

Compound **2** crystallized in *P*–1 space group in which the fourth and fifth coordination sites are filled by nitrogen atom of *N*CS$^-$ ion and oxygen atom of DMF. Thiocyanato ion is an ambidentate ligand which possibly can coordinate through N- or S-atom. In this case coordination through N-atom has been observed but with a bending at N-atom is 162.5(2)°. A perspective view of **1** is shown in Fig. 4. The Cu atom lies out of the plane formed by three nitrogen atoms of **L2** by 0.152 Å and is towards thiocyanato N-atom. The Cu–N_P distances 2.042(2)Å, are longer by ~0.1 Å than the Cu–N_A distance 1.939(2) Å. The overall geometry around copper(II) ion is distorted square pyramid, in which angles formed in ONN_A trigonal plane are 108.55(7), 109.72(7) and 141.82(8)°. The *trans* angle N_p–Cu–N_p being 161.76(7)°. The packing diagram shows presence of π···π interaction between quinolinyl rings, distance between the two centroids C1N1C6C7C8C9 and C1N1C6C7C8C9 being 3.72 Å. An intermolecular dipolar interaction between oxygen and

carbon atom of amide group is also present and the non-bonded contacts are O1···C11, 3.096(2) and O2···C10, 3.008(2) Å.

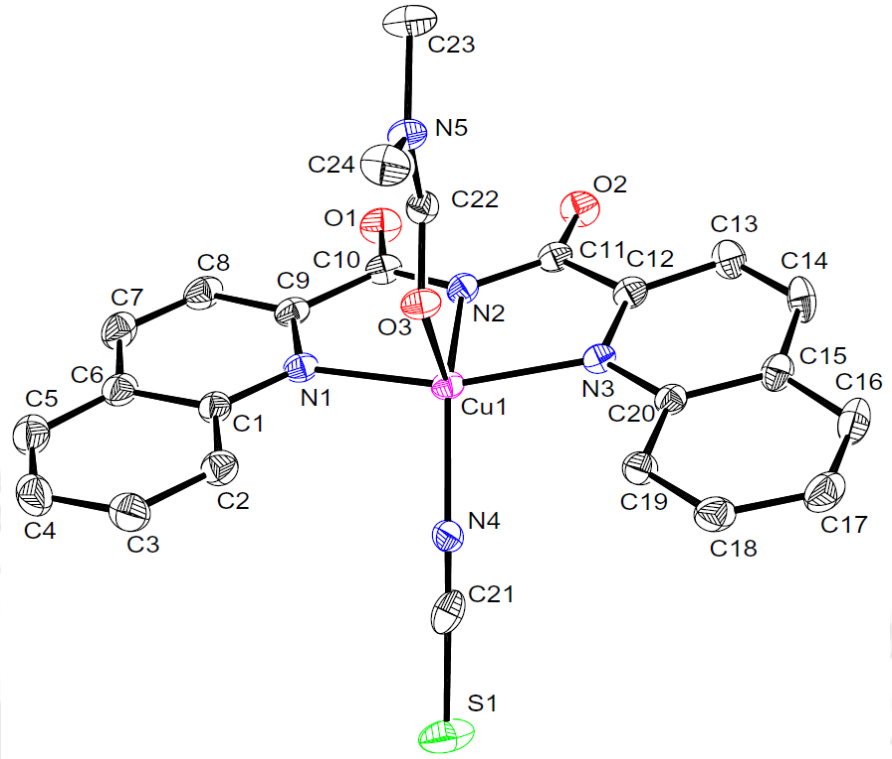

Fig. 4. ORTEP (20% probability ellipsoid) diagram of **2** and the hydrogen atoms are omitted for clarity.

Compound **3** crystallized in $P2_1/n$ space group in which the fourth and fifth coordination sites are occupied by oxygen atom of $PhCOO^-$ ion and by the oxygen atom of water molecule. The Cu atom lies out of the plane formed by three nitrogen atoms of **L2** by 0.024 Å and is towards O-atom of coordinated water molecule. The Cu–N_P distances lie in the range 2.093(7) – 2.105(7) Å, are longer by ~0.1 Å than the Cu–N_A distance 1.940(6) Å. The overall geometry around the copper(II) ion is distorted square pyramid, in which angles formed at O_2N_A trigonal plane are 160.3(2), 116.1(2) and 83.6(2)°. The *trans* angle N_p–Cu–N_p being 162.0(2)°. An intermolecular dipolar interaction between oxygen atoms of amide group and carbon atom of methanol is present and the non-bonded contacts are O1···C28, 3.03(1) and O2···C28, 2.95(1) Å. Other significant intermolecular contacts present are O3···O5, 2.691(6) and O3···C28, 2.74(1) Å.

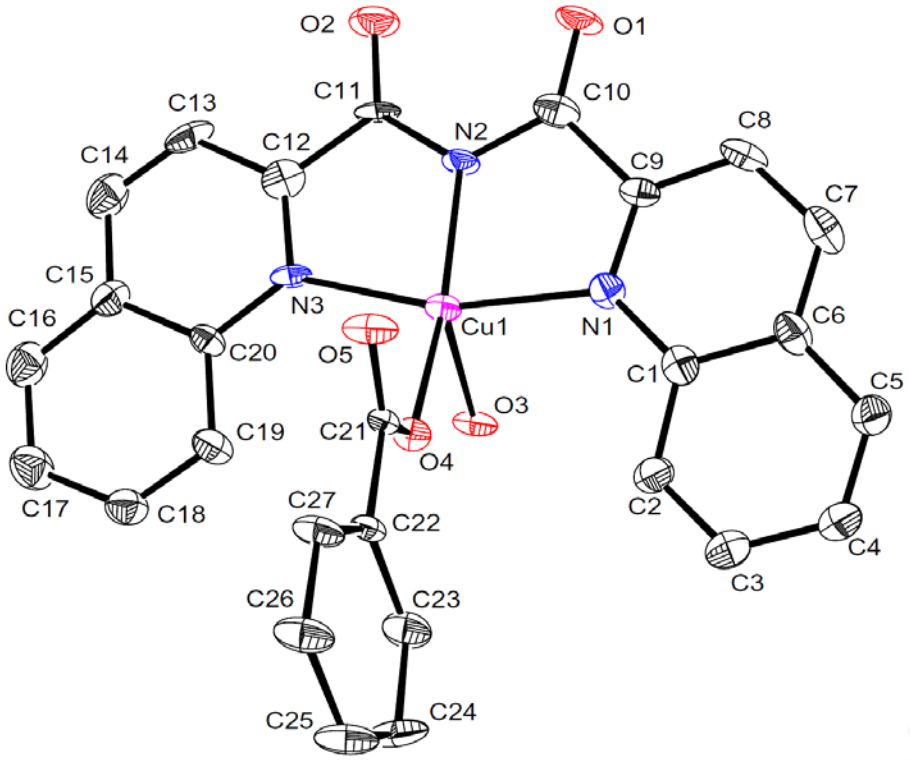

Fig. 5. ORTEP (20% probability ellipsoid) diagram of **3** and the hydrogen atoms are omitted for clarity.

Compound **4** crystallized in *P*bca space group in which the fourth and fifth coordination sites are filled by two nitrogen atoms of the *N*CNC*N*$^-$ ion. A ORTEP diagram of **4** is displayed in Fig 6. Dicyanamide is known to bridge two metal centers and such a bridging by dicyanamide is present in **4** which lead one-dimensional coordination polymer having the non-bonded Cu···Cu distance of 7.582(1) Å. A perspective view of the 1D polymer is shown in Fig 7. The Cu atom sits in the plane by three nitrogen atoms of **L2**. The Cu–N_P distances 2.037(2)Å, are longer by ~0.1 Å than the Cu–N_A distance 1.945(2) Å. The overall geometry around the copper(II) ion is distorted trigonal bipyramid, in which the angles formed at N_2N_A trigonal plane are 108.6(1), 125.7(1) and 125.7(1)°. The *trans* angle N_p–Cu–N_p being 162.97(8)°. The packing diagram shows presence of π···π interaction between quinolinyl rings and distance between two centroids C1N1C6C7C8C9 and C1N1C6C7C8C9 being 4.07 Å with a shortest non-bonded contact C7···C9, 3.395(4) Å. This π···π interaction occurs between quinolinyl rings of two adjacent chains. Other non-bonded distance between the two amide oxygen atoms is O1···O1, 2.892(3) Å.

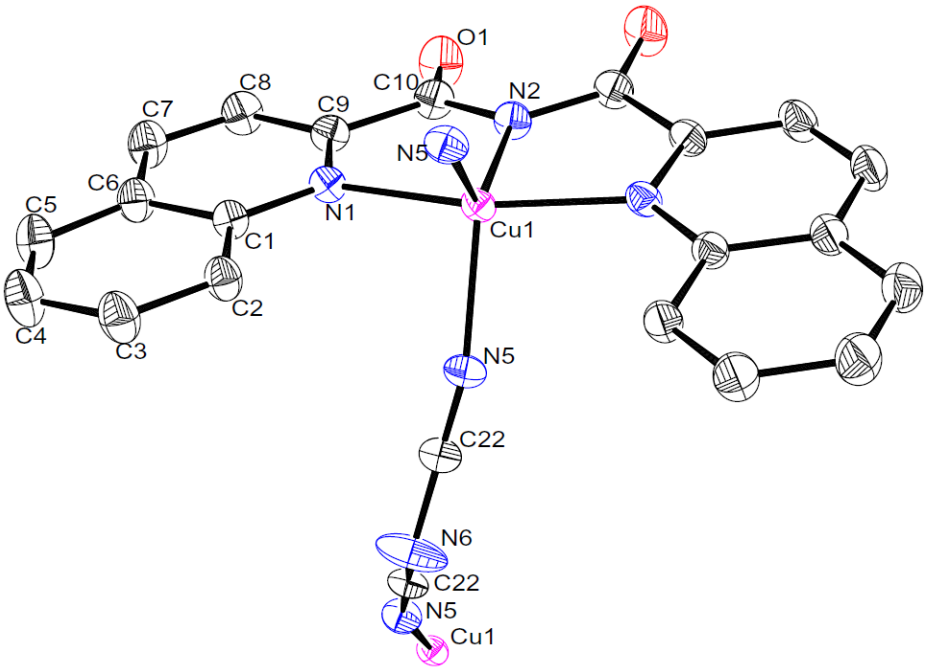

Fig. 6. ORTEP (20% probability ellipsoid) diagram of **4** and the hydrogen atoms are omitted for clarity.

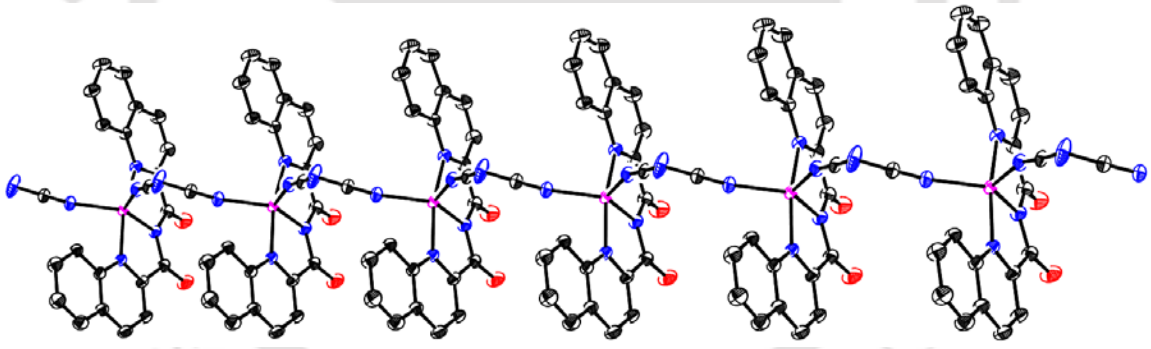

Fig. 7. ORTEP (20% probability ellipsoid) diagram of **4** showing the presence of dicyanamide linked chain.

5.4 Conclusion

Using cyanate, thiocyanate, benzoate and dicyanamide ions as co-ligands, copper(II) monochelates of **L2** have been synthesized. Determination of their molecular structures revealed that first three contain discrete mononuclear units and the last one contains a 1-D ladder-like coordination polymer. EPR spectra of **1**–**4** show axial spectrum with $g_{\|} > g_{\perp} > 2$ signifying that the odd electron being in $d_{x^2-y^2}$ orbital. Room temperature μ_{eff} values are consistent with the presence of one unpaired electron. The molecular structures of **1**–**4**

were established by single crystal X-ray diffraction studies and packing diagrams of all **1**, **2** and **4** show the presence of π···π interaction between the quinolyl rings.

5.5 References

1. R. Sahu, S.K. Padhi, H.S. Jena, V. Manivannan, Inorg. Chim. Acta 363 (2010) 1448–1454.
2. K. Nakamoto, Infrared and Raman Spectra of Inorganic and Coordination Compounds, fourth ed., Wiley, New York, 1986, p. 228.
3. S. Wocadlo, W. Massa, J.V. Folgado, Inorg. Chim. Acta 207 (1993) 199–206.
4. D. Marcos, J.V. Folgado, D. Beltran-Porter, M.T. Do Prado-Gambardella, S.H. Pulcinelli, R.H. De Almeida-Santos, Polyhedron 9 (1990) 2699–2704.
5. A.B.P. Lever, Inorganic Electronic Spectroscopy, Elsevier, Amsterdam, 1986.
6. R.S. Drago, Physical Methods for Chemists, 2nd ed., Saunders College Publishers, New York, 1992.
7. B. Vangdal, J. Carranza, F. Lloret, M. Julve, J. Sletten, J. Chem. Soc., Dalton Trans., (2002) 566–574.
8. D. Marcos, R. Martinez-Mañe, J-V. Folgado, A. Beltrán-Porter, D. Beltrán-Porter, A. Fuertes, Inorg. Chim. Acta, 159 (1989) 11–18.
9. M.L. Calatayud, I. Castro, J. Sletten, F. Lloret, M. Julve, Inorg. Chim. Acta 300–302 (2000) 846–854.
10. I. Castro, M.L. Calatayud, J. Sletten, F. Lloret, J. Cano, M. Julve, G. Seitz, K. Mann, Inorg. Chem. 38 (1999) 4680–4687.
11. H. Casellas, F. Costantino, A. Mandonnet, A. Caneschi, D. Gatteschi, Inorg.Chim. Acta 358 (2005) 177–185.
12. I. Castro, J. Faus, M. Julve, Y. Journaux, J. Sletten, J. Chem. Soc., Dalton Trans. (1991) 2533–2538.
13. J. Carranza, C. Brennan, J. Sletten, F. Lloret, M. Julve, J. Chem. Soc., Dalton Trans., (2002) 3164–3170.
14. J.V. Folgado, E. Martínez-Tamayo, A. Beltran-Porter, D. Beltrán-Porter, A. Fuertes, C. Miravitlles, Polyhedron 8 (1989) 1077–1083.

15. P. Halder, E. Zangrando, T.K. Paine, Polyhedron 29 (2010) 434–440.
16. D.C. de Castro Gomes, L.M. Toma, H.O. Stumpf, H. Adams, J.A. Thomas, F. Lloret, M. Julve, Polyhedron, 27 (2008) 559–573.
17. J.V. Folgado, E. Escriva, A. Beltrán-Porter, D. Beltrán-Porter, Transition Met. Chem. 12 (1987) 306–310.
18. J. Kohout, M. Hvastijova, J. Mrozinski, Journal of Molecular Structure, 116 (1984) 211–216.
19. A.W. Addison, T.N. Rao, J. Reedijk, J. van Rijn, G.C. Verschor, J. Chem. Soc. Dalton Trans. (1984) 1349–1356.

Chapter 6

A Novel Iron(III) Chloride Mediated Reduction of Bis(1-isoquinolylcarbonyl)amide to an Asymmetric Amide

Abstract

A iron(III) complex of formula [Fe(**L5**)Cl_2] (**1**) where **L5** = N-((1-isoquinolyl)(methoxy)methyl)isoquinoline-1-carboxamide ion has been isolated from the reaction of $FeCl_3$ with **1-L4H** (**1-L4H** = bis(1-isoquinolylcarbonyl)amide) in methanol. In this reaction, one carbonyl group of bis(1-isoquinolylcarbonyl)amide has been reduced to (methoxy)methyl group. A plausible mechanism for the conversion of **1-L4H** to **L5** has been proposed. Single crystal X-ray structure of **l** has been determined which confirmed this conversion and Fe(III) ion is surrounded by three nitrogen atoms of ligand and two chloride ions in a distorted trigonal bipyramidal fashion. The low temperature EPR spectrum of **1** consists a broad signal centered at g_{eff} = 4.27 and has a room temperature magnetic moment value of 5.60 B. M. which are consistent with presence of high-spin d^5 Fe(III) ion.

6.1 Introduction

Iron(III) chloride has been known to catalyze or assist several kind of organic reactions. This includes Friedel–Crafts [1,2], Michael addition [3–5], Ritter [6], alkylation of indoles with enamides [7,8], oxidation of thiols (RSH) to RSSR in the presence of butadiene [9], oxidation of alkanes by $[Os(N)O_3]^-$ [10], coupling of ArMgX with alkyl halides [11], synthesis of polysubstituted benzofurans (a component in synthesis of coumarins by Pechmann condensation) using di-*tert*-butyl peroxide, phenols and *β*-keto esters [12], oxygenation of cycloalkanones to oxo esters [13], oxidative coupling reactions of phenols [14], disproportionation of allylic alcohols [15], alkenylation simple arenes with aryl-substituted alkynes [16], synthesis of sulfonyl amidines [17] α-glycosidation [18], synthesis of indene derivatives [19], 1,4-addition of various thiols to α,β-unsaturated ketones [20], cyanohydrin esters preparation [21], protection of diols and carbonyls [22], formation of β-nitroalcohols [23] etc.

In this Chapter a facile reaction of **1-L4H** with $FeCl_3$ that led to formation of $[Fe(\mathbf{L5})Cl_2]$ under ambient conditions, wherein **L5** = N-((1-isoquinolyl)(methoxy)methyl)-isoquinoline-1-carboxamide ion, has been described.

6.2 Experimental Section

6.2.1 Synthesis

Bis(1-Isoquinolylcarbonyl)amide (1-L4H): Was prepared using the procedure reported in Chapter 3.

$[Fe(L5)Cl_2]$ (1): To methanolic solution (20 mL) of $FeCl_3$ (16.0 mg, 0.1 mmol) solid **1-L4H** (33.0 mg, 0.1 mmol) was added and stirred for 8 h. The reaction mixture was left undisturbed and after 4 days red crystals of **1** were isolated. For **1**, Yield: 30.0 mg, 64%. IR (KBr, cm^{-1}) **Fig. 1**.: 3438(b), 1719(s), 1651(s), 1618(s), 1588(m), 1500(w), 1449(m), 1432(w), 1394(w), 1382(w), 1356(m), 1331(m), 1289(s), 1255(s), 1190(m), 1152(s), 1092(s), 1054(s), 1017(s), 903(w), 878(w), 867(w), 824(s),750(s), 672(w), 654(w), 628(w), 609(m), 572(w), 507(w), 489(w), 473(m), 415(w), 386(s), 356(s). Calcd. for **1**: C 53.77, H 3.44, N 8.96. Found: C 53.57, H 3.40, N 8.89. [λ_{max}, nm (ε, $M^{-1}cm^{-1}$), MeOH

solution]: 370 (9425), 335 (15180), 325 (15570). EPR (DMF solution, 77 K): g_{eff} = 4.27; μ_{eff} (polycrystalline, 25 ºC) = 5.60 B. M.

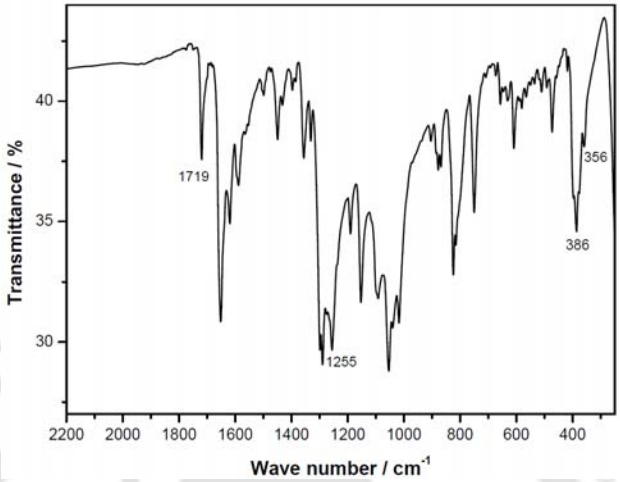

Fig. 1. IR spectrum of **1**.

6.3 Results and Discussion

6.3.1 Synthesis

On stirring **1-L4H** with anhydrous $FeCl_3$ in methanol a yellowish red solution was obtained, which on standing afforded red crystals of **1**. The molecular structure of **1** has been determined (*vide infra*) and the composition [Fe(**L5**)Cl_2] has been formulated wherein **L5** = N-((1-isoquinolyl)(methoxy)methyl)isoquinoline-1-carboxamide ion (as shown below). It is relevant to note that **L1H** has been reported to react with $FeCl_3$ resulting in the formation of [Fe(**L1**)$Cl_2(H_2O)$] and [Fe(**L1**)$_2$]$^+$ ion [24].

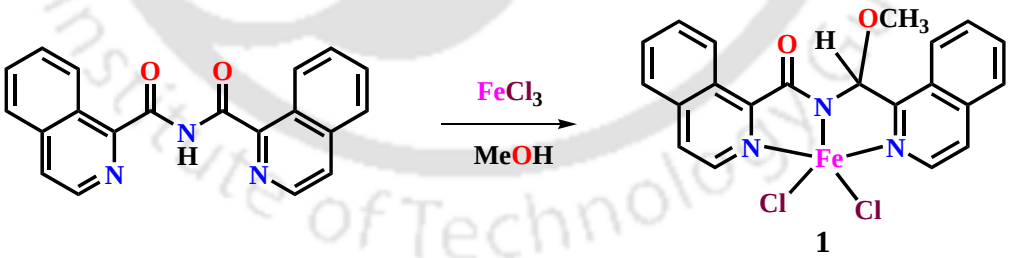

1

During the course of reaction, one carbonyl group of bis(1-isoquinolylcarbonyl) amide has been reduced to (methoxy)methyl group. A plausible mechanism for this conversion has been proposed in Scheme 1. First step is formation of simple monochelate of **1-L4** (**1-L4** = bis(1-isoquinolylcarbonyl)amide ion) having the composition [Fe(**1-L4**)Cl_3]$^-$ (**I**). Compound **I** having a hexa-coordinated iron(III) formed from $FeCl_3$ and **1-L4H** will release a proton which will attach to one of the carbonyl oxygen atoms as in **II**. This will

polarize the carbonyl group, which will become susceptible to nucleophilic attack by CH_3OH molecule and a concomitant proton shift will lead to intermediate **III**. Elimination of a water molecule from **III** will yield cation **IV**, which could undergo a homolytic cleavage at one of the Fe(III)–Cl bonds. This will release a Cl· atom and intermediate **V** containing five-coordinated iron(II) center. Iron(II) could transfer one electron to the electrophilic carbon to generate a radical intermediate **VI**, containing five-coordinated iron(III) center. This radical could abstract a H· atom from MeOH leading to the final product **1**. It can also be noted that further experimental studies are required by using different alcohols and deuterated methanols (like CD_3OD, CD_3OH and CH_3OD) in order to gain insights into the possible mechanism for this conversion.

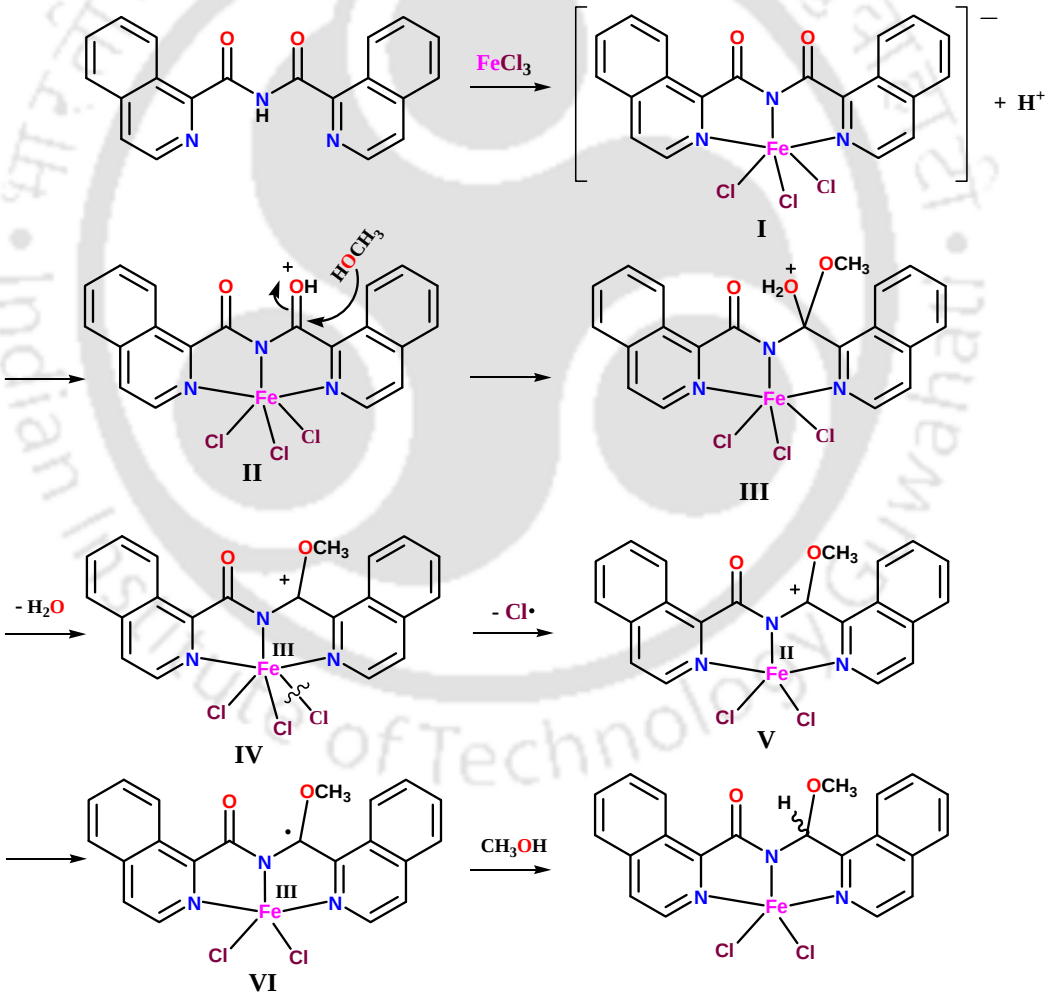

Scheme 1. A plausible mechanism for the formation of **1** from **1-L4H**.

6.2.2 Optical Spectra and Magnetism

The IR spectrum of ligand **1-L4H** shows ν_{CO} around 1745 cm^{-1} and in its coordination complexes {in $[Cu(\mathbf{1\text{-}L4})(H_2O)_2]ClO_4$ and $[Ni(\mathbf{1\text{-}L4})_2]$} ν_{CO} peak is observed in the range 1690–1710 cm^{-1}. Compound **1** shows a characteristic 1719 cm^{-1} peak for ν_{CO}. In addition a strong peak for ν_{C-O} at ~1250 cm^{-1} and ν_{Fe-Cl} peaks at ~386 and 356 cm^{-1} were notable. Methanol solutions of **1** show allowed transitions in the UV region and the peak at 370 nm tails into visible region, accounting for red/yellow color of compound. Since in the case of high-spin d^5 complexes, *d-d* transitions are both Laporte and spin forbidden, such transitions are not observed in **1** [24]. The room temperature magnetic moment of polycrystalline samples of **1** has the value of 5.60 B. M. which is less than the spin-only value of 5.92 B.M. At temperature of 77 K, EPR spectrum of **1** (DMF solutions) shows a broad signal centered at g_{eff} = 4.27. These features are consistent with the presence of high-spin d^5 iron(III) center [24].

6.2.3 Molecular Structure

The molecular structure of **1** has been determined by single crystal X-ray diffraction method and its ORTEP diagram is displayed in Fig 2. The crystallographic data and selected bond parameters are is listed in Table 1 and 2, respectively. The compound crystallized in $P2_1/n$ space group and the trivalent iron is penta-coordinated. The geometry around Fe(III) can be best described as distorted trigonal bipyramidal containing a N_ACl_2 (N_A = amide–N; N_P = pyridyl–N) distorted trigonal plane having angles Cl1–Fe1–N2, 120.70(9); Cl2–Fe1–N2, 127.38(9) and Cl1–Fe1–Cl2, 111.91(5)°. As a result of severe distortion in the axial N1–Fe1–N3 angle (153.6(1)°), the calculated τ value of 0.44 is less significant in inferring the geometry [25]. The Fe–N_A bond is shorter than the two Fe–N_P bonds by an average of 0.176(3) Å, which can be ascribed to geometrical constraints of ligand framework. Such a trend in which the central bond of a end-cap tridentate chelating ligand bearing geometrical constraints, being shorter than the other two, has also been observed in Fe^{II} complexes of bis(imino)pyridines having the coordination environment $Fe^{II}N_3Cl_2$ [26, 27]. However such discrepancy was not observed in complexes having flexible tripodal ligand framework [28]. Overall the Fe^{III}–N distances observed here are

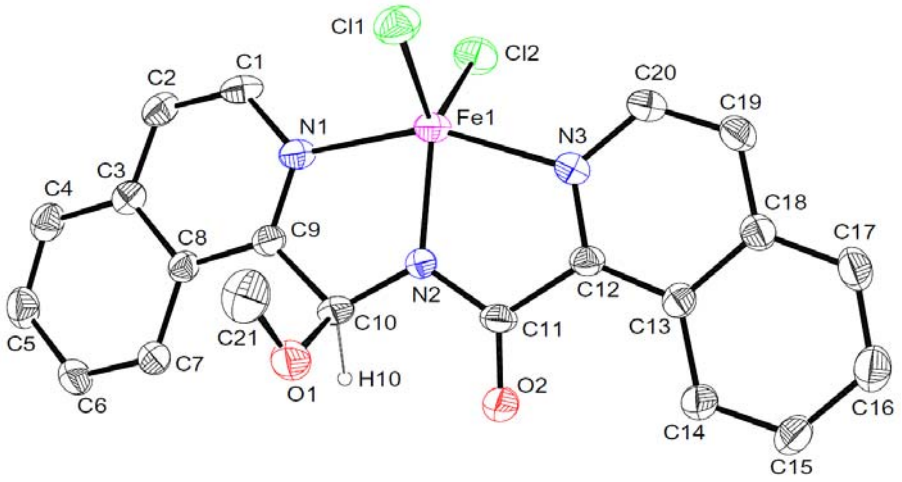

Fig. 2. ORTEP (30% probability ellipsoids diagram of **1**, hydrogen atoms except H10 were omitted for clarity.

shorter than reported Fe^{II}–N values. Two Fe^{III}–Cl bonds having a length of 2.210(2) and 2.212(1) Å are shorter than that found (lying in the range 2.266(2)–2.312(2) Å) in closely related five-coordinated bivalent iron complex having a similar $Fe^{II}N_3Cl_2$ coordination environment reported earlier [28,29]. In Table 3 a list of Fe–N and Fe–Cl bond distances are given for comparison.

The methyl of methoxy group is uniquely projected towards the metal center having the non-bonded contacts Fe1···C21, 3.997(5) Å and Cl1···C21, 4.213(5) Å. In the packing diagram, π···π interaction is present having the following cg···cg (cg = centroid) contacts: N1C2C3C8C9 with N3C12C13C18C19C20, 3.84 Å; N1C2C3C8C9 with C13–C18, 3.89 Å; C4–C8 with C13–C18, 3.94 Å; C4–C8 with N3C12C13C18C19C20, 3.95 Å. These π···π interactions and an intermolecular short contact (C4···C12, 3.378(6) Å) lead to a chain composed of molecules having a same configuration for the asymmetric carbon. An intermolecular contact C7···O2, 3.251(6) Å, is present between the chains which link two chains containing opposite chiral carbon atoms in head-to-head fashion to double stranded chains. Within a double strand, isoquinolyl rings are tilted such that inter-strand angle between planes of two isoquinolyl rings is 38.18° and between two planes of chelated ring Fe1N1C9C10N2C11C12N3 is 48.54°. A perspective view of packing diagram and that of a double stranded chain are shown in Fig. 3 and 4, respectively.

Table 1. Crystallographic Data for **1**

Formula	$C_{21}H_{16}N_3O_2Cl_2Fe$
Formula weight	469.12
T, K	296(2)
Crystal system	Monoclinic
Space group	$P2_1/n$
a, Å	14.4079(10)
b, Å	9.0517(5)
c, Å	15.6056(10)
α, deg	90
β, deg	104.923(4)
γ, deg	90
V, Å^3	1966.6(2)
Z	4
D_{calcd}, gcm^{-3}	1.584
μ, mm^{-1}	1.062
GOF[a] on F^2	1.001
R[I > 2σ(I)]	[b]R_1 = 0.0577; [c]wR_2 = 0.1078
Rindices (all data)	[b]R_1 = 0.1321; [c]wR_2 = 0.1654

[a] GOF = $[\sum[w(F_0^2 - F_c^2)^2] / M - N]^{1/2}$ (M = number of reflections, N = number of parameters refined). [b] $R_1 = \sum \| F_0 | - | Fc \| / \sum | F_0 |$. [c] $wR_2 = [\sum[w(F_0^2 - F_c^2)^2] / \sum[w(F_0^2)^2]]^{1/2}$.

Table 2. Selected bond distances (Å) and angles (°)

Fe1–N1	2.123(3)	N2– Fe1–N1	77.56(14)
Fe1–N2	1.951(3)	N2– Fe1–N3	76.84(13)
Fe1–N3	2.131(3)	N1– Fe1–N3	153.67(14)
Fe1–Cl1	2.210(2)	N2– Fe1–Cl1	120.71(10)
Fe1–Cl2	2.212(1)	N1– Fe1–Cl1	99.11(10)
O1–C10	1.441(5)	N3– Fe1–Cl1	99.15(10)
O1–C21	1.474(5)	N2– Fe1–Cl2	127.37(10)
O2–C11	1.222(4)	N1– Fe1–Cl2	95.27(10)
C10–N2	1.431(5)	N3– Fe1–Cl2	95.33(10)
C11–N2	1.355(6)	Cl1– Fe1–Cl2	111.92(5)
		C10–O1–C21	114.6(4)
		C11–N2–C10	116.9(3)
		N2–C10–O1	113.2(3)
		O2–C11–N2	125.3(4)
		C12–C11–O2	122.1(4)
		N2–C10–C9	109.1(4)
		C12–C11–N2	112.5(4)

Table 3. Comparison of bond distances

	Fe–N_C	Fe–N_E		Fe–Cl		
1	1.951(3)	2.123(3)	2.131(3)	2.210(2)	2.212(1)	this work
2	2.091(4)	2.222(4)	2.225(5)	2.263(2)	2.317(2)	ref 26
3	2.088(4)	2.238(4)	2.250(4)	2.311(2)	2.266(2)	ref 27
4	2.110(6)	2.271(6)	2.266(5)	2.312(2)	2.278(2)	ref 27
5	2.229(8)	2.188(6)	2.246(7)	2.303(2)	2.298(2)	ref 28
6	2.186(4)	2.213(3)	2.258(3)	2.333(1)	2.290(1)	ref 28

N_C, N_E are central, terminal nitrogen atoms of ligand;

2 = [2,6-bis-[1-(2,6-diisopropylphenylimino)ethyl]pyridine]$Fe^{II}Cl_2$;

3 = (2,6-diacetylpyridinebis(2,6-diisopropylanil))$Fe^{II}Cl_2$;

4 = (2,6-diacetylpyridinebis(2,4,6-trimethylanil))$Fe^{II}Cl_2$;

5 = [bis(2-bromo-6-pyridylmethyl)(2-pyridylmethyl)amine]$Fe^{II}Cl_2$;

6 = [bis(2-phenyl-6-pyridylmethyl)(2-pyridylmethyl)amine]$Fe^{II}Cl_2$.

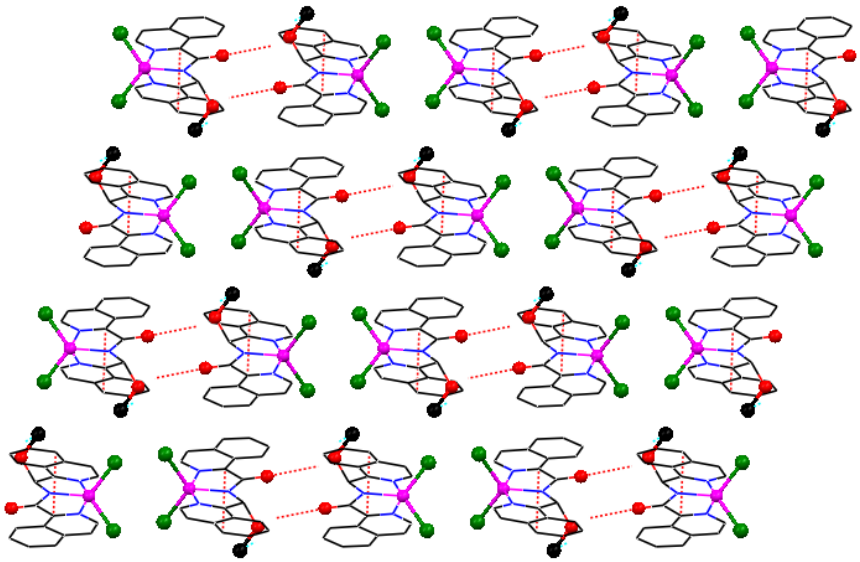

Fig. 3. Packing diagram on viewing down *b*-axis.

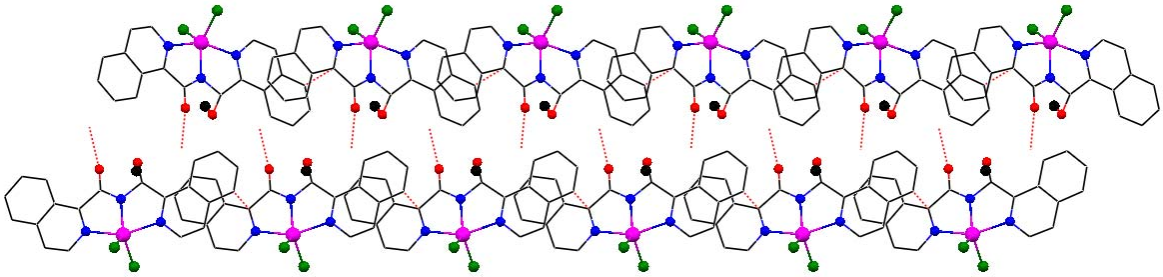

Fig. 4. Double stranded chain.

6.4 Conclusion

The ligand **1-L4H** reacted readily with anhydrous $FeCl_3$ in methanol yielding red crystals of composition [Fe(**L5**)Cl_2] in which **L5** is N-((1-isoquinolyl)(methoxy)methyl)-isoquinoline-1-carboxamide ion. During the course of the reaction, one carbonyl group of bis(1-isoquinolylcarbonyl) amide has been reduced to (methoxy)methyl group and plausible mechanism for this conversion is proposed. The molecular structure of the complex has been determined by single crystal X-ray diffraction method. The geometry around Fe(III) can be best described as distorted trigonal bipyramidal containing a distorted trigonal plane as well as axial bonds. The Fe(III) ligand distances are shorter than that reported values of Fe(II) complexes. Packing diagram shows the presence of π···π

interactions and an intermolecular short contact lead to a chain composed of molecules having a same configuration for the asymmetric carbon. Another intermolecular contact links two chains containing opposite chiral carbon atom in head-to-head fashion to double stranded chains.

6.5 References

1. P. Thirupathi, S.S. Kim, J. Org. Chem. 75 (2010) 5240–5249.
2. S. Csihony, H. Mehdi, Z. Homonnay, A. Vértes, Ö. Farkas, I.T. Horváth, J. Chem. Soc., Dalton Trans. (2002) 680–685.
3. M. Kidwai, N.K. Mishra, V. Bansal, A. Kumar, S. Mozumdar, Tetrahedron Lett. 50 (2009) 1355–1358.
4. J. Christoffers, Chem. Commun. (1997) 943–944.
5. H. Li, X. Xu, J. Yang, X. Xie, H. Huang, Y. Li, Tetrahedron Lett. 52 (2011) 530–533.
6. B.M. Trost, P.L. Ornstein, J. Org. Chem. 48 (1983) 1133–1135.
7. T. Niu, L. Huang, T. Wu, Y. Zhang, Org. Biomol. Chem., 9 (2011) 273–277.
8. R. Li, S.R. Wang, W. Lu, Org. Lett. 9 (2007) 2219–2222.
9. B.E.L. Jenner, R.V. Lindsey, Jr., J. Am. Chem. Soc. 83 (1960) 1911–1915.
10. S-M. Yiu, Z-B. Wu, C-K. Mak, T-C. Lau, J. Am. Chem. Soc. 126 (2004) 14921–14929.
11. D. Noda, Y. Sunada, T. Hatakeyama, M. Nakamura, H. Nagashima, J. Am. Chem. Soc. 131 (2009) 6078–6079.
12. D.A. Stoyanovsky, R. Clancy, A.I. Cederbaum, J. Am. Chem. Soc. 121 (1999) 5093–5094.
13. B.M. Trost, P.L. Ornstein, J. Org. Chem. 48 (1983) 1133–1135.
14. F. Toda, K. Tanaka, S. Iwata, J. Org. Chem. 54 (1989) 3007–3009.
15. J. Wang, W. Huang, Z. Zhang, X. Xiang, R. Liu, X. Zhou, J. Org. Chem. 74 (2009) 3299–3304.
16. R. Li, S.R. Wang, W. Lu, Org. Lett. 9 (2007) 2219–2222.
17. S. Wang, Z. Wang, X. Zheng, Chem. Commun. (2009) 7372–7374.
18. S.K. Chatterjee, P. Nuhn, Chem. Commun. (1998) 1729–1730.

19. C-R. Liu, F-L. Yang, Y-Z. Jin, X-T. Ma, D-J. Cheng, N. Li, S.-K. Tian, Org. Lett. 12 (2010) 3832–3835.
20. C-M. Chu, W-J. Huang, C. Lu, P. Wu, J-T. Liu, C-F Yao, Tetrahedron Lett. 47 (2006) 7375–7380.
21. K. Iwanami, M. Aoyagi, T. Oriyama, Tetrahedron Lett. 46 (2005) 7487–7490.
22. I. Karamé, M. Alamé, A. Kanj, G.N. Baydoun, H. Hazimeh, M. Masri, L. Christ, C. R. Chimie (2011) doi:10.1016/j.crci.2010.12.001
23. M.N. Elinson, A.I. Ilovaisky, V.M. Merkulova, F. Barba, B. Batanero, Tetrahedron 64 (2008) 5915–5919.
24. S. Wocadlo, W. Massa, J-V. Folgado, Inorg. Chim. Acta. 207 (1993) 199–206.
25. A.W. Addison, T.N. Rao, J. Reedijk, J. van Rijn, G.C. Verschor, J. Chem. Soc. Dalton Trans. (1984) 1349–1356.
26. B. L. Small, M. Brookhart, A.M.A. Bennett, J. Am. Chem. Soc. 120 (1998) 4049–4050.
27. G.J.P. Britovsek, M. Bruce, V.C. Gibson, B.S. Kimberley, P.J. Maddox, S. Mastroianni, S.J. McTavish, C. Redshaw, G.A. Solan, S. Strömberg, A.J.P. White, D.J. Williams, J. Am. Chem. Soc. 121 (1999) 8728–8740.
28. D. Mandon, A. Machkour, S. Goetz, R. Welter, Inorg. Chem. 41 (2002) 5364–5372.

Publications

9. Syntheses and Molecular Structures of Co^{3+}–Na^{+} and Co^{3+}–K^{+} Coordination Polymers Constructed Using Mono- and Bis-Chelated Cobalt(III) Complexes of Bis(2-pyridylcarbonyl)amide Ion
   R. Sahu, V. Manivannan, Inorg. Chim. Acta 363 (2010) 4008–4016.

8. Conversion of 2-(Aminomethyl) Substituted Pyridine and Quinoline to Their Dicarbonyldiimides Using Copper(II) Acetate
   R. Sahu, S. K. Padhi, H. S. Jena, V. Manivannan, Inorg. Chim. Acta 363 (2010) 1448–1454.

7. Protonated 4′-(2-Pyridyl)-2,2′:6′,2″-Terpyridine and Its Fe(II) Bischelates: Syntheses and Molecular Structures
   S. K. Padhi, R. Sahu, D. Saha, V. Manivannan, Inorg. Chim. Acta 367 (2011) 0000.

6. Syntheses and Structures of Cobalt(III) Alcoholate Complexes Formed by Addition of a Water Molecule Across 2-Pyridyl Substituted Imine Function
   S. K. Padhi, R. Sahu, V. Manivannan, Inorg. Chim. Acta 367 (2011) 57–63.

5. Water–Chloride 2D–Network in 4′-(2-Pyridyl)-2,2′:6′,2″-Terpyridine Bis-chelates of M(II) {M = Fe, Ni, Ru}
   S. K. Padhi, R. Sahu, V. Manivannan, Polyhedron 29 (2010) 709-714.

4. Novel Synthesis of 2,4-Bis(2-pyridyl)-5-(pyridyl)imidazoles and Formation of N-(3-(Pyridyl)imidazo[1,5-*a*]pyridine)picolinamidines: Nitrogen–Rich Ligands
   V. K. Fulwa, R. Sahu, H. S. Jena, V. Manivannan, Tetrahedron Lett. 50 (2009) 6264–6267.

3. Ni(II) Complexes of 4′-(2-Pyridyl)-2,2′:6′,2′′-Terpyridine: Structure of Mono- and Bis-chelates Containing Anion···π Interactions
   S. K. Padhi, R. Sahu, V. Manivannan, Polyhedron *27* (2008) 2221–2225.

2. Synthesis, Structure, Optical and Magnetic Properties of $[CrL(X)_3]$, {L = 4′-(2-Pyridyl)-2,2′:6′,2′′-Terpyridine; X = Cl^-, N_3^-, NCS^-}
   S. K. Padhi, D. Saha, R. Sahu, J. Subramanian, V. Manivannan, Polyhedron *27* (2008) 1714–1720.

1. Synthesis, Structure, Thermal Studies on Zn(II), Cd(II) Complexes of N-(2-Pyridyl methyl)pyridine-2-carbaldimine and N-(2-Pyridylmethyl)pyridine-2-methylketimine.
   S. K. Padhi, R. Sahu, V. Manivannan, Polyhedron *27* (2008) 805–811.